JAGIELLONIAN UNIVERSITY

MARTA DERECKA

TO BE OR NOT TO BE FAT: A NOVEL ROLE OF JAK/STAT PATHWAY IN BROWN FAT DEVELOPMENT AND PREVENTING OBESITY

Virginia Commonwealth University
Department of Biochemistry and Molecular Biology
Richmond, VA, USA

Promoters:
Andrew Larner, M.D., Ph.D.
Joanna Cichy, Ph.D.

Kraków, 2011

To my beloved parents,

for their constant support, motivation

and great faith in my success.

Moim kochanym rodzicom,

w podziękowaniu za ich nieustanne wsparcie, motywację

oraz ogromną wiarę w mój sukces.

ACKNOWLEDGMENTS

This thesis is the result of almost five years of work, therefore it is my great pleasure to thank the many people who made it possible.

I would like to express my deep and sincere gratitude to my thesis advisors Dr. Andrew C. Larner and Dr hab. Joanna Cichy for their support and guidance during writing this dissertation. I am greatly indebted to Dr. Andrew Larner for the opportunity of joining his laboratory and teaching me how to be a scientist with an open mind. His constant help, encouragement and most of all patience made my Ph.D. journey easier and much more fun. This thesis would not have been possible without his support. I am very grateful to Dr hab. Joanna Cichy for her valuable suggestions during writing this thesis and for her tremendous help in guiding me through the defense path. I would like to extend my appreciation to my thesis reviewers- Prof. Jadwiga Bryła and Prof. Alicja Józkowicz for their time spent reading this dissertation and helpful commentary.

I am also grateful to the faculty, staff and students of the Department of Biochemistry and Molecular Biology, Virginia Commonwealth University and the Department of Immunology, Lerner Research Institute, Cleveland Clinic Foundation for creating a professional and friendly environment during my dissertation work.

I owe my sincere gratitude to Dr. Tomasz Kordula for his tremendous help, countless hours spent analyzing data, even the most bizarre ones and great intellectual contribution to the project.

It is a pleasure to acknowledge my colleagues I have been working with: Dr. Joanna Wegrzyn, Dr. Magdalena Szelag, Dr. Yong-Joon Chwae, Dr. Qifang Zhang, Dr. Agnieszka Gornicka, Dr. Catherine Koebel, Dr. Maciej Kmieciak, Dr. Karol Szczepanek, Jennifer Sisler, Vidisha Raje and Samantha Umali for creating great working environment and all the help I got from them. I warmly thank especially my friends Karol, Misiek, Aga and Larner girls- Magda, Jenny and Vidi for providing support, help and laughter, when I needed it the most.

I would like to also express my deepest appreciation to my dearest friends: Dominika Dańda, Paulina Kulig and Patrycja Fejdych for their great friendship and being there when I laughed and when I cried. I hope they know how lucky I am to have them in my life.

My special thank you goes to Marcin, the special someone who came into my life and made it sunny and colourful. Thank you for believing in me no mater what, for your enthusiasm and endless patience.

Finally, I cannot find the words to express how grateful I am to my family, especially my parents Danuta and Czesław and my brother Bartosz. This work would be simply impossible without them. I am thankful for their endless support, encouragement, unconditional love and faith in all my decisions. My parents thought me how to be strong and independent, for which I am grateful the most. It is thanks to them that I can present this thesis

TABLE OF CONTENTS

ABBREVIATIONS

ADP - adenosine diphosphate

Akt - serine-threonine protein Akt kinase

AMPK - AMP-activated protein kinase

AOX - acyl-CoA oxidase

aP2 - adipocyte protein 2

AR - adrenergic receptor

ATP - adenosine triphosphate

BAT - brown adipose tissue

BMI - body mass index

BMPs - bone morphogenetic proteins

BSA - bovine serum albumine

C/EBP - CCAAT/enhancer binding protein

CA - constitutively active

CBP - CREB binding domain

CC - coiled-coiled

Cidea - cell death-inducing DFFA-like effector a

CMV - cytomegalovirus

CNS - central nervous system

CoA - coenzyme A

Cox8b - cytochrome c oxidase subunit 8b

CREB - cAMP response element binding

CS - citrate synthase

CT - computed tomography

CtBPs - C-terminal binding proteins

DBD - DNA binding domain

DEPC - diethyl pyrocarbonate

Dex - dexamethason

Dio2 - type 2 deiodinase

DNA - desoxyribonucleic acid

Elovl3 - elongation of very long chain fatty acids protein 3

EM - electron microscopy

EPO - erythropoietin

ERR - estrogen-related receptor

ETC - electron transport chain

$FADH_2$ - flavin adenine dinucleotide

FAS - fatty acid synthase

FERM - band-4.1, ezrin, radixin, meosin

FFA - free fatty acids

GAS - gamma interferon activated sequence

G-CSF - granulocyte-colony stimulating factor

GFP - green fluorescent protein

GH - growth hormone

GLUT4 - glucose transporter 4

GSK3 - glycogen synthase kinase 3

GTP - guanosine triphosphate

HDL - high density lipoprotein

HIES - hyper IgE syndrome

HL - hormone sensitive lipase

HP1 - heterochromatin protein 1

HRP - horse radish peroxidase

IBMX - isobutylmethylxanthine

IFN - interferon

IL - interleukin

IRES - internal ribosome entry site

IRS - insulin receptor substrate

ISRE - interferon stimulated response element

Jak - Janus kinase

JH - Jak homology

KD - kinase-dead

LCAD - long chain acyl-CoA dehydrogenase

LD - linker domain

LDL - low density lipoprotein

LIF - leukemia inhibitory factor

MAPK - mitogen-activated protein kinase

MCK - muscle creatine kinase

MEFs - mouse embryonic fibroblasts

Mfn - mitofusin

mRNA - messenger ribonucleic acid

MSC - mesenchymal/mesodermal stem cells

MSCV - murine stem cell virus

Myg - myogenin

NADH - nicotinamide adenine dinucleotide

OPA1 - optic atrophy protein 1

OSM - oncostatin M

PCR - polymerase chain reaction

PEPCK - phosphoenolpyruvate carboxykinase

PET - positron emission tomography

PGC - peroxisome proliferator-activated receptor gamma coactivator

PKA - protein kinase A

PMSF - phenylmethanesulfonyl fluoride

PPAR - peroxisome proliferator-activated receptor

PRDM16 - PRD1-BF-RIZ1 homologus domain-containing protein 16

PRL - prolactin

RER - respiratory exchange rate

ROS - reactive oxygen species

RXR - retinoid X receptor

SCID - severe combined immunodeficiency

SDS - sodium dodecyl sulfate

SH2 - Src homology 2

shRNA - short hairpin ribonucleic acid

SIRT - sirtuin

SNPs - single-nucleotide polymorphisms

SNS - sympathetic nervous system

Stat - signal transducer and activator of transcription

T3 - triiodothyronine

TAD - transactivation domain

TBS - Tris buffered saline

TG - triglyceride

TGF - transforming growth factor

TLR - toll-like receptor

TNFα - tumor necrosis factor α

TPO - thrombopoietin

Tyk2 - tyrosine kinase 2

TZDs - thiazolidinediones

UCP - uncoupling protein

VSV-G - vesicular stomatitis virus- gene

WAT - white adipose tissue

WT - wild type

YFP - yellow fluorescent protein

ABSTRACT

Obesity is defined as abnormal or excessive fat accumulation that presents a significant risk to health and is a major risk factor for a number of chronic diseases such as diabetes, cardiovascular disorders and cancer.

Janus kinases (Jaks) and signal transducers and activators of transcription (Stats) have emerged as critical regulators of numerous fundamental biological processes and are important in the etiology of various disease conditions. The Jak/Stat pathway is a primary mediator of leptin signaling, which has been implicated in obesity. We found that mice lacking Tyk2, one of the Jak's, become spontaneously obese. We discovered that expression of a variety of mRNAs that regulate fatty acid and glucose homeostasis are altered in liver, skeletal muscle and adipose tissue of Tyk2- null mice, which is consistent with metabolic syndrome. Proper energy balance prevents the development of obesity and is dependent on energy expenditure. Brown adipose tissue (BAT) dissipates chemical energy in the form of heat in response to excess of calories and constitutes a natural defense mechanism against hypothermia and obesity. Our data suggest that differentiation and function of BAT is defective in mice that do not express Tyk2, which might explain the obese phenotype in these animals. Using an in vitro differentiation model of brown preadipocytes isolated from mice with a Tyk2 deletion, we were able to restore the differentiation by expression of either wild type or kinase inactive Tyk2 (Tyk2KD), as well as constitutively active form of Stat3 (Stat3CA). Recent data provided evidence that PRDM16 is the master regulator controlling the brown fat/skeletal muscle switch from a common progenitors. Consistent with severe decrease in PRDM16 expression, we observed up-regulation of muscle-specific mRNAs in Tyk2- null cells. Remarkably, differentiation of Tyk2 -/- preadipocytes cannot be rescued by PRDM16. These data suggest that Tyk2 is key player in brown preadipocytes differentiation acting upstream of PRDM16 or in parallel with it. Interestingly, we also found that the absence of Tyk2 results in epigenetic changes in the promoters of BAT- specific genes such as UCP1 (uncoupling protein 1) and Cidea (cell death-inducing DFFA-like effector a), abrogating their expression. Consistent with our in vitro data, BAT- specific expression of the Stat3CA transgene restores BAT differentiation in mice. Animals expressing Stat3CA in

BAT exhibit significantly reduced body weight and improved insulin sensitivity in comparison to control mice, which demonstrate that the obese phenotype of Tyk2 -/- mice is most likely a result of defects in BAT differentiation occurring in these animals.

The above observations present a novel role of Jak/Stat pathway in development of BAT and the control of obesity. The fact that kinase inactive Tyk2 also restores brown adipocytes differentiation reinforces the innovative concept that the actions of this kinase are not mediated by its well described activation in cytokine activation of the Jak/Stat cascade.

CHAPTER I

INTRODUCTION

1.2 Jak/Stat signaling pathway

Janus family tyrosine kinases (Jaks) and signal transducers and activators of transcription (Stats) were first discovered as mediators of interferon (IFN) induced gene expression (162, 228, 274). Over the years, it became clear that Jaks and Stats mediate signal transduction of wide array of cytokines and growth factors (105, 131, 132). The Jak/Stat pathway is involved in cell growth, survival, development and differentiation of multiple tissues, from flies to humans (7, 90, 95). Mutations leading to aberrant regulation of Jak/Stat signaling can cause malignant transformation, inflammatory diseases and erythrocytosis.

The binding of a ligand to its cell surface receptor activates one of associated Jaks, leading to the tyrosine phosphorylation of specific residues in the cytoplasmic domain of the receptor. These phosphorylated tyrosines provide a docking site for Stat proteins via their Src homology (SH2) domain. Subsequently, recruited Stats are tyrosine phosphorylated by activated Jak kinases (74, 106). Activated Stats dissociate from the receptor complex, form homo- or heterodimers and translocate to the nucleus, where they bind to specific DNA sequences: interferon stimulated response elements (ISREs) or gamma interferon activation sequence (GAS), in the promoter regions of their target genes (57, 60, 182).

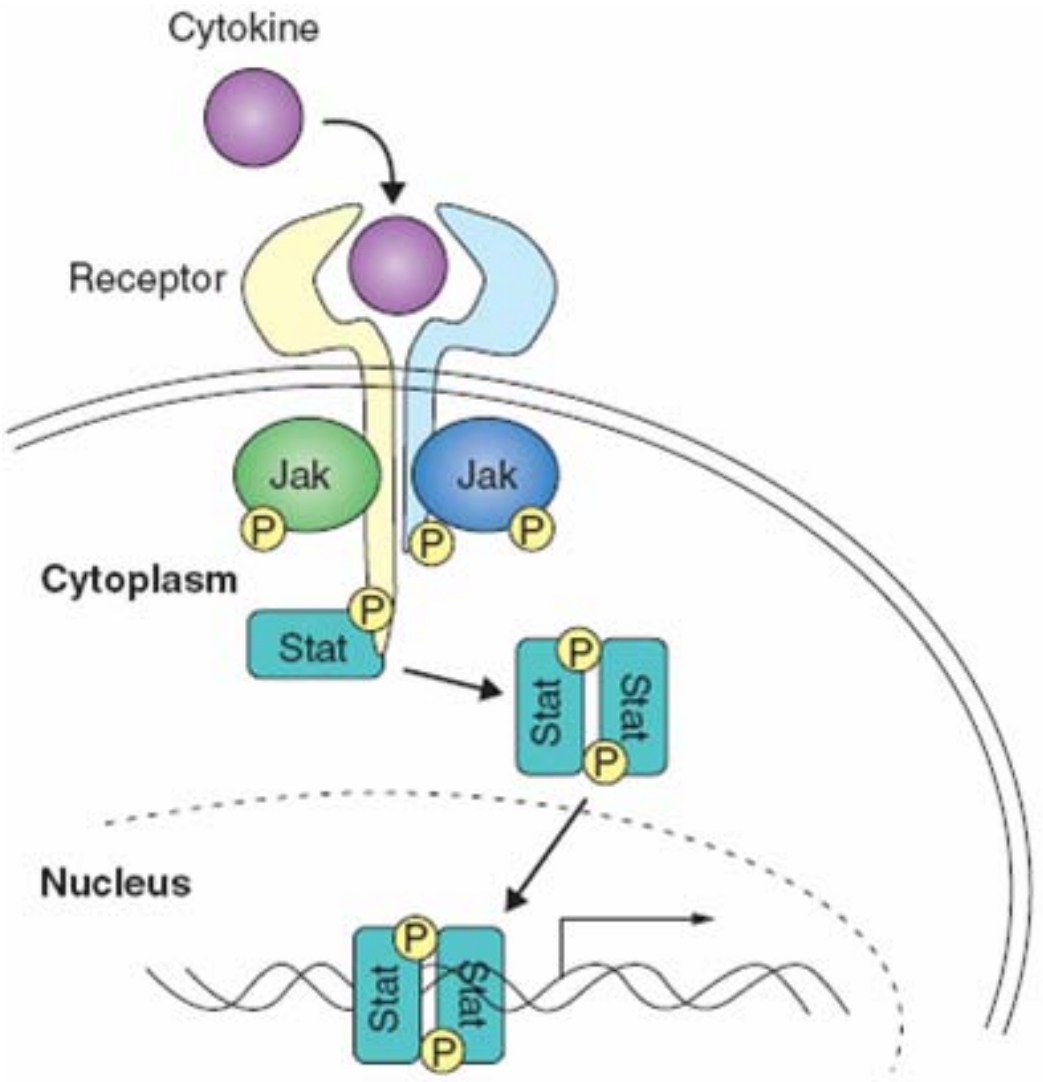

Figure 1.1 Overview of canonical Jak/Stat signaling pathway (282).

1.2 Jak family of protein tyrosine kinases

In mammals, there are four members of the non- receptor Janus kinase family including Jak1, Jak2, Jak3 and tyrosine kinase 2 (Tyk2) (98, 198). Jaks are relatively large proteins containing over 1000 amino acids with molecular weights between 120 and 140 kDa. Based on sequence similarities between Jak family members seven Jak homology (JH) domains have been described. The catalytically active kinase domain (JH1) is located at the carboxyl- terminus. Adjacent to the JH1 domain is a catalytically

inactive pseudokinase or kinase- like domain (JH2), which has a kinase domain fold but lacks crucial residues for catalytic activity and for nucleotide binding. This tandem architecture of kinase domains is a unique feature of Jaks, among other protein tyrosine kinases, and gives them their name derived from the Roman mythological, two- faced God Janus (183, 282). The precise function of the JH2 domain is still unclear. However, published results show that this region is definitively required to modulate (39, 208, 209, 290), or even retain the kinase activity (260). The JH2 domain appears to be also involved in the association with other signaling proteins. It has been described as a potential docking site for Stats (80). The amino- terminus of Jaks contains a SH2- like domain (JH3, JH4 and part of JH5), and a FERM (Band- 4.1, ezrin, radixin, moesin) homology domain (JH5- JH7). The FERM domain is 300 amino acids long and is essential for binding of Jaks to their receptors (40, 300). In addition, the FERM domain has been also reported to regulate catalytic activity of Jaks (301). Interestingly the N-terminal region in Jaks appears to be important in regulating cell- surface expression of the receptors (104, 259), as well as trafficking of IFNα/β receptor subunit 1 (IFNAR1) to the plasma membrane (85, 196).

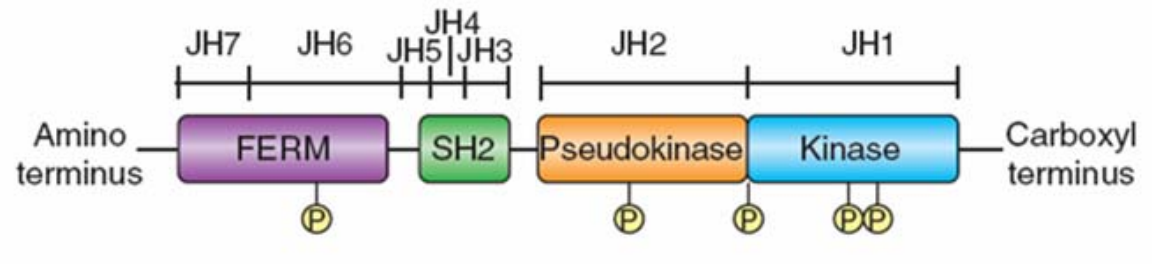

Figure 1.2 A schematic representation of the primary structure of Jaks (282).

In mammals Jak1, Jak2 and Tyk2 are ubiquitously expressed, whereas the expression of Jak3 is predominantly limited to the cells of hematopoietic origin (121, 151, 165, 219), although, expression of Jak3 was also reported in endothelium and vascular smooth muscles (248, 261). A large number of cytokines and growth factors mediate Jak/Stat activation. Animals with targeted disruption of each Jak kinase gene have illustrated their essential and specific functions in growth and development.

Jak1 plays fundamental role in the signaling of IFNs, interleukin- 2 (IL-2), IL- 4, IL- 7, IL- 9, IL- 15, IL- 21, oncostatin M (OSM), leukemia inhibitory factor (LIF) and granulocyte colony- stimulating factor (G- CSF)(164, 171). Jak1 knockout mice show perinatal lethality due to neurological defects that prevent them from suckling (204). They are small at birth and have impaired lymphoid development (8).

Jak2 is essential for the hormone- like cytokines such as growth hormone (GH), prolactin (PRL), erythropoietin (EPO), thrombopoietin (TPO), IFNγ and family of cytokines that signal through the IL- 23, as well as gp130 receptor. Jak2- null mice are embryonic lethal due to failure in definitive erythropoiesis (167, 175).

Interestingly, Jak3 deficiency was first identified in humans with severe combined immunodeficiency (SCID) (148, 207). Mice lacking Jak3 also exhibit SCID phenotype. Additionally, they show severe impairment in development of B-cells, T-cell, NK cells and defects in response to IL-2/ IL-4 family of cytokines (170, 179, 244).

1.3 Tyrosine kinase 2 (Tyk2)

Tyk2 was the first Jak family member identified to be essential for type I interferon signaling and was the prototype of a new protein kinase gene subfamily (75, 128). Whereas type I IFNs absolutely require Tyk2 and Jak1, IFNγ signaling depends on the Jak1 and Jak2. A combination of Tyk2 and Jak2 is needed for the differentiation of IFNγ- producing Th1 cells from the naive Th cells (162, 274). Generation of the Th1 cells is driven mainly by lineage– specific IL- 12, which signals through Tyk2 and Stat4 (1, 13). Moreover, the Tyk2- associated IL-12β1 chain is also used by IL- 23 signaling,

which promotes Th17 cells (43, 176). Interestingly, Tyk2 along with Jak2 have been also reported to play a role in early lineage decision of mouse embryonic stem cells (mESCs) to various differentiated cell types, possibly as early as in germ layer specification (47). Since numerous cytokines, involved mainly in pro- inflammatory immune response, engage Tyk2 in their pathways, any mutations leading to loss of function of this kinase were expected to lead to striking immunological phenotypes. Tyk2- null mice are viable and fertile. Stat3 activation by the type I IFNs (IFNα/β) is absent but activation of Stat1 and Stat2 is only slightly reduced. Mice lacking Tyk2 are more susceptible for viral or bacterial infections due to impaired Th1 lineage development and inability to produce IFNγ by T cells (118, 220, 223). Additionally, Tyk2 seems to regulate Toll- like receptors (TLR)- mediated signals in dendritic cells (DC). Activation of Tyk2- null DCs by TLR9 or TLR4 results in decreased production of IL- 12 and IL- 23, which can contribute to weak Th1 and Th17 differentiation in case of infection (3, 246). Due to greatly diminished IL- 12 effect on its targets, Tyk2 knockout mice exhibit reduced levels of IL-18 receptors. Since IL- 12 and IL- 18 cooperation is required to activate natural killer cells (NK), NK- dependent innate immune response is abrogated in the absence of Tyk2 (224). According to the published data, Tyk2 deficient mice demonstrate enhanced Th2 responses, caused by lack of suppressive signals derived from IL- 12 or IFNs. Consequently, Th2- driven conditions like allergic lung inflammation was accelerated in Tyk2- null animals (218).

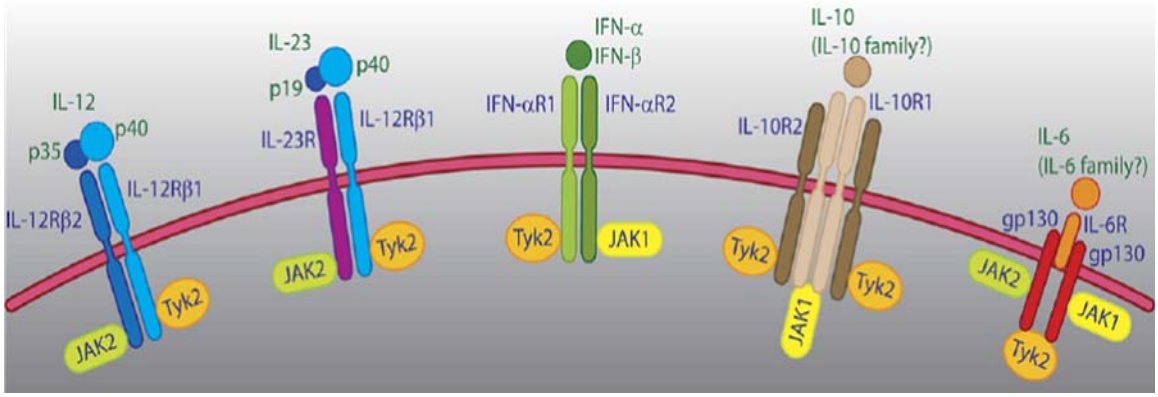

Figure 1.3 Representation of Tyk2- dependent cytokine signaling (273).

Only a single patient with Tyk2 deficiency has been identified so far (154). Described patient presented very similar defects in cytokine signaling, as observed previously in the mouse model. In addition to the susceptibility to atypical and opportunistic viral, fungal and mycobacterial infections, the patient suffered from severe atopic dermatitis and hyper- IgE syndrome (HIES). In general, the patient with Tyk2 deficiency showed broader and more profound immunodeficiency than it would be expected form studies of Tyk2- null mice. Nevertheless, experiments performed on the human cells lacking Tyk2 supported clinical observations. The discrepancy between human and murine in vitro models can be partially explained by the fact that IFNα-induced phosphorylation of key signaling molecules, such as Jak1 and Stat1, was completely abolished in the Tyk2 -/- human cells, whereas the effects were partial in mouse cells. Additionally, human Tyk2 deficiency results in reduced expression of IFNAR1 in the plasma membrane (273). Furthermore, in contrast to the human cells, IL-6 signaling in the mouse is Tyk2- independent (273).

1.4 Signals transducers and activators of transcription (Stats)

The signal transducers and activators of transcription (Stats) are a family of proteins that regulate many processes such as cell growth, cell survival, proliferation, differentiation and response to stress. Thus, dysregulation of these transcription factors leads very often to increased tumor formation and metastasis. (24, 291).

Seven Stat proteins have been identified in mammalian cells: Stat 1, 2, 3, 4, 5A, 5B and 6 (57, 134). The Stat genes are localized as clusters on chromosomes, which suggests that they arose through duplication of a common ancestral gene (51). Differential splicing of primary transcripts results in the generation of a β isoform for Stat 1, 3, 4 and 5 (27, 201, 212, 270). The shorter β versions of Stat proteins often function as a negative regulators and are capable of mediating the expression of different set of genes, than the full length Stats (157, 178, 211).

Consistent with the evolutionary sequence homology, Stats share structurally and functionally conserved domains. This includes an N- terminal regulatory domain (NTD),

a coiled- coiled domain (CC), a DNA- binding domain (DBD), a SH2 domain (SH2), a linker domain (LD), and a C- terminal transactivation domain (TAD).

The N- terminal domain, comprising approximately 130 amino acids, has been described to be involved in receptor recognition, oligomerization of Stat dimmers, interaction with co- activators like CBP/p300 and nuclear translocation (136, 163, 234, 296). In addition, it has been shown in Stat1 that the NTD plays the role in phosphorylation and dephosphorylation of Tyr701 (160, 229).

The coiled- coiled domain contain four α- helices, which form a large predominantly hydrophilic surface that is available for specific interactions with other helical proteins (17, 41). Interacting proteins include p48/IRF9, N- myc and c- Jun transcription factor (50, 103, 299, 303). Studied have also implicated the CC domain in receptor binding, tyrosine phosphorylation and nuclear export (18, 298).

The DNA- binding domain, located approximately between amino acids 320 and 490, comprises of several β- barrels with immunoglobulin fold, which resembles the DBD of NF- κB or p53 transcription factors (41).

The linker domain, situated between amino acids 490 and 580, connects the DNA- binding domain with the SH2 domain. Although the LD domain is highly conserved among all Stats, its function is still not clear (124). Mutational analysis revealed that linker domain influences stability of DNA binding and ability to induce gene expression by Stat1, after IFN treatment (285). Recent studies suggest also that LD domain of Stat3 can serve as a place of interaction with a subunit of electron transport chain- GRIM19, in the inner mitochondrial membrane (147).

The SH2 domain, which follows from residues 580 to 680, is the most highly conserved Stat domain. Differences in the SH2 domains of different Stats determines the selectivity of Stat binding to various cytokine receptors (106). The SH2 domain structure consists of anti- parallel β- sheets flanked by two α- helices, which form a pocket. An absolutely conserved arginine, which is required for interaction with phosphate, lies at the base of the structural pocket (124). The ability of the SH2 domain to recognize specific phosphotyrosine motifs plays an essential role in the Stat signaling. The SH2 domain is

responsible for binding of Stats with the tyrosine phosphorylated cytokine receptors, association with activated Jaks and Stat homo- or heterodimerization (14, 97, 227, 228). Conserved in all Stat proteins is a tyrosine residue at the C- terminus, which is phosphorylated by Jaks or other tyrosine kinases and plays an essential role in the transcriptional function of Stats (134, 199).

Despite the fact that C- terminal transactivation domain is poorly conserved among Stats, it is fundamental for enhancing transcriptional efficiency of Stat proteins by promoting the association of Stats with other members of transcriptional machinery (21, 91). In addition to the crucial tyrosine residue, almost all Stat proteins contain also a serine residue within TAD domain. Its phosphorylation appears to play a role in full activation of transcription by Stats (20, 184, 275, 277). It has been suggested that serine phosphorylation may alter its affinity for other transcriptional regulators like MCM5, BRCA1 or CBP/p300 (174, 181, 297).

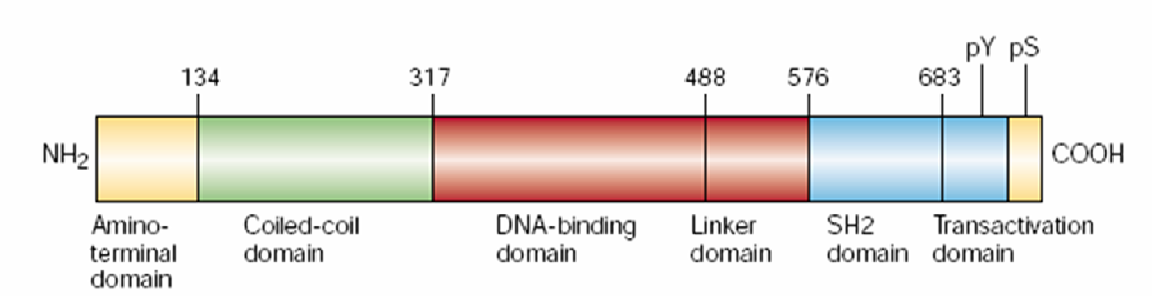

Figure 1.4 A schematic representation of Stats structure (134). Aminoterminal (N-terminal) domain (NTD), coiled-coil domain (CC), DNA-binding domain (DBD), linker domain (LD), transactivation (C-terminal) domain (TAD), phosphorylated tyrosine (pY), phosphorylated serine (pS).

Despite the great advance in understanding the Jak/Stat signaling in normal development and pathogenesis, the details in molecular mechanisms of this pathway remain incomplete. In the canonical mode, Stats phosphorylation seems to be a crucial event in order to initiate the transcription of the target genes. Lately an increasing amount of evidence has challenged this paradigm. Over the past couple of years, it has been found that Stat1, Stat3 and Stat6 also can act without tyrosine phosphorylation (36, 53, 288). Moreover, ligand- dependent increase in the concentration of unphosphorylated Stats (U- Stat) drive the expression of genes that are distinct from those activated by phosphorylated Stats. U- Stat1 can bind to DNA as monomers, recognizing only one half of a palindromic GAS element. However, in vitro experiments showed that U- Stat1 can also form dimmers through interaction of their N- terminal domains of each monomer and bind to the full GAS sequence. Interestingly, there is evidence that U- Stats can play a role in pathological conditions. The abnormally high levels of U- Stat3 were reported in many tumors, which along with well described constitutive activation of Stat3 can contribute to enhanced tumorigenesis (289). Furthermore, studies in Drosophila have demonstrated a non- canonical Jak/Stat mode, which affects cellular epigenetic status (135, 284). According to the published data, a portion of the fly U- Stat pool is located in the nucleus, where is associated with heterochromatin protein 1 (HP1). This association between U- Stat and HP1 is essential for maintaining HP1 localization and heterochromatin stability (221, 222). More importantly, consistent with the findings in Drosophila, nuclear localization of unphosphorylated mammalian Stat3 and Stat5 has also been reported (109, 142, 264). However, their involvement in regulation of chromatin status is still under investigation.

So far all Stat genes have been targeted and disrupted in mouse models. The phenotypes of these mutant mice revealed distinctive functions for the particular Stat proteins.

Stat protein	Phenotype of null mice
Stat1	Viable and fertile, defective IFNs signaling, increased susceptibility to viral infections and tumors, impaired growth control (65, 152)
Stat2	Viable and fertile, impaired response to IFNα/β (177)
Stat3	Embryonic lethality, multiple defects in adult tissues, impaired cell survival, impaired response to pathogens (4, 235-237)
Stat4	Viable and fertile, impaired Th1 differentiation due to loss of IL- 12 signaling (117, 243)
Stat5A	Viable and fertile, defective mammary gland development as a result of impaired prolactin signaling (143)
Stat5B	Viable and fertile, impaired growth due to loss of growth hormone responsiveness (253)
Stat5A/B	Early postnatal lethality due to impaired erythropoiesis, defective T- cell proliferation and NK- cell differentiation (158, 241)
Stat6	Viable and fertile, defective IL- 4 and IL- 13 signaling resulting in impaired T- cell development toward Th2 cells (116, 225)

Table 1.1 Phenotypes of Stat deficient mice.

1.5 Stat3 in metabolism

Since general knockout of Stat3 is embryonic lethal, Cre/loxP system was used to investigate the Stat3 function in the physiology of particular tissues. Many of Stat3 conditional knockout mice appeared to have metabolic problems and develop obesity. Stat3 function in central nervous system (CNS) has been described in a number of reports. It is expressed during embryonic development in order to control glial and

neuron differentiation. In adults, Stat3 has been implicated in the regulation of energy balance through the impact on leptin signaling. Although leptin can activate Stat3, Stat5 and Stat6 in vitro, only Stat3 activation was reported in the mouse hypothalamus upon leptin administration (56, 88, 255). In order to further investigate the role of Stat3 in energy homeostasis, mice with targeted deletion in the brain were generated. Surprisingly, mice with neural-specific Stat3 deletion were born without obvious development abnormalities but prone to neonatal lethality. Animals that survived the neonatal period appeared to be hyperphagic due to impaired leptin signaling in the hypothalamus. Consequently, mutant mice developed obesity and diabetes (16, 83). They also exhibit infertility and reduced linear growth. Additionally, Stat3 deficient mice became hypothermic after cold exposure or fasting (83). Acquired data showed that CNS knockout of Stat3 recapitulates the well described phenotype of ob/ob (leptin deficient mice) and db/db (leptin receptor deficient mice) obese models. Interestingly, mice expressing a constitutively active version of Stat3 in the hypothalamus are lean and resistant to diet- induced obesity, as a result of increased locomotor activity (153). Stats have been also implicated in in vitro model of 3T3-L1 differentiation. Stat3 is abundantly expressed in preadipocytes, as well as mature adipocytes and highly activated during their proliferation (62, 233). To determine the role of Stat3 in adipose tissue in vivo, the mice with adipocyte- specific knock down of Stat3 were created. Studies performed on these animals showed that mutant mice weighed more than their littermate controls. Higher body weight of the knockout mice was caused by the increased adiposity associated with adipocyte hypertrophy, hyperphagia or reduced energy expenditure (34). It is well established that Stat3 is one of the most important signaling molecule used by the IL- 6 family of cytokines, specifically in the liver. Interestingly, the serum concentration of IL-6 is increased in a patient with altered metabolic states like obesity (262). Moreover, IL-6 was also suggested as one of the modulators of gluoconeogenic genes expression (44). These observations led to the generation of mice with liver- specific deficiency of Stat3. It appeared that Stat3 plays an essential role in glucose homeostasis. Mice with targeted disruption of Stat3 displayed insulin resistance associated with increased expression of gluconeogenic genes (108). Conversely, expression of constitutively active Stat3 in the

liver markedly reduced blood glucose level, plasma insulin concentration and hepatic gluconeogenic gene expression.

1.6 Metabolic syndrome and obesity

Metabolic syndrome (syndrome X) is a constellation of physiological and biochemical abnormalities including abdominal obesity, high fasting glucose level, insulin resistance, dyslipidemia, atherosclerosis, hypertension, type 2 diabetes and low-grade inflammation. This clustering of features lead to many dangerous complications like cardiovascular disease, fatty liver, sleep apnea, gallstones, polycystic ovary syndrome in women and hypogonadism in men or even some types of cancer (96). Complex pathogenesis of metabolic syndrome causes a lot of diagnostic and therapeutic problems. Visceral obesity for example results in excessive release of free fatty acids, adipokines and proinflammatory cytokines, which contribute to insulin resistance and hyperlipidemia. In the setting of insulin resistance, the vasodilatory effect of insulin and VEGF production are diminished, which leads to endothelial dysfunction and hypertension. The increased flux of free fatty acids to the liver results in lower level of high-density lipoproteins (HDL) called a "good" cholesterol, and higher level of low-density lipoproteins (LDL)- "bad" cholesterol. This altered balance of the HDL and LDL helps a plaque to build up in artery walls, causing higher blood pressure and even coronary heart disease (22, 272).

Body weight and composition are determined by the genetic, environmental and psychosocial factors. Obesity is defined as a state of excessive fat accumulation, which develops when food intake exceeds energy expenditure. The incidence of obesity is fast growing problem that is reaching epidemic proportions worldwide. Weight gain during adult life or even during childhood and adolescence seems to contribute to type 2 diabetes and cardiovascular risk, even within the normal body mass index (BMI) range (232). Two types of obesity are distinguished, based on the classification of fat depots in the body. Subcutaneous or pear- shape obesity is characterized by fat accumulation in the thigh and hips. Visceral or apple- shape obesity is related with intraabdominal fat storage. Individuals with a central/abdominal deposition of adipose tissue are more subjected to insulin resistance, stroke, congestive hear failure, cardiovascular death and certain types

of cancer (257, 268). Fat cells secrete many hormones and adipokines such as leptin, adiponectin or resistin, which regulate overall metabolism. Leptin is bioactive substance that controls mainly food intake and energy expenditure through its action in the brain. Visceral adiposity is also associated with low- grade but chronic inflammation caused by production of proinflammatory cytokines like IL- 6, Il-1 or TNFα, which promote apoptosis, changes in vasoregulatory responses, increase leukocyte adhesion to the endothelium that facilitate thrombus formation by inducing procoagulant activity (256).

1.7 Diabetes

Diabetes mellitus is a metabolic disorder characterized by hyperglycemia caused by insufficiency of secretion or receptor insensitivity to endogenous insulin. Altered carbohydrate metabolism is usually a consequence of hereditary and environmental factors. Early in the course of diabetes, intracellular hyperglycemia causes abnormalities in blood flow and increase vascular permeability. These changes lead to ischemia and hypoxia in the retina, kidney problems and degeneration in peripheral nerves. That is why diabetes is a leading cause of blindness, end- stage renal disease and variety of neuropathies. Diabetes is also associated with accelerated atherosclerosis and macrovascular disease affecting arteries that supply the heart, brain and lower limbs. These alterations increase the risk of myocardial infarction, stroke and amputation (25). Diabetes mellitus has been classified in two forms: type 1 and type 2.

Type 1 diabetes, which accounts for about 10% of all cases, is characterized by destruction of the insulin- producing β- cell in the pancreas, which results in insulin deficiency. About 90% of childhood- onset diabetes id diagnosed as type 1 and called juvenile diabetes. The major cause of type 1 diabetes is autoimmune response, which seems to be due to a combination of genetic predisposition and environmental factors. The largest contribution to the genetic susceptibility comes from the genes located in the major histocompatibility complex (MHC). Polymorphism of the gene PTPN22 encoding a tyrosine phosphatase that affects T cell receptor signaling, also influences diabetes risk (110). Destruction of insulin producing cells is an autoimmune event. Chronic

inflammation in pancreas with the infiltration of T and B cells, macrophages and dendritic cells result in recognition of β cell autoantigens and eventual destruction of pancreatic islets by the T cells (2).

Type 2 diabetes, the more prevalent form of diabetes, is considered a heterogeneous disorder due to multiple factors that account for the clinical phenotype. According to calculated data, there are 150 million people with type 2 diabetes worldwide, and this number will rise to 300 million in 2025. About an equal number are though to be prediabetic, having early symptoms but not yet the full manifestation of the disease. Insulin resistance in offspring of parents with type 2 diabetes is a strong predictor of the disease later in life. In the U.S., 30% of all new cases are children with diabetes type 2. Despite the fact that genetics plays also the role in this type of diabetes, it is well established now that environmental factors have a bigger impact in most of the cases (64, 168). Overfeeding and lack of physical activity cause weight gain and finally obesity with related insulin resistance in adipose tissue, muscle and liver. Insulin resistance is a condition, where insulin becomes less effective with time in promoting proper glucose disposal especially in the muscle tissue and inhibiting gluconeogenesis in the liver. As a result of high blood glucose level, pancreatic β cells increase insulin secretion, causing hyperinsulinemia. Glucotoxicity, lipotoxicity, proinflammatory cytokines and high leptin levels occurring in obese patients contribute to the accelerated apoptosis of β cells and eventually to loss of β cell mass. Consequently, production of insulin is drastically diminished to the point that there is not enough of this hormone to drive glucose uptake (26, 267). An autoimmune component had also been implicated in the pathophysiology of type 2 diabetes. Systemic inflammation in patients with type 2 diabetes is considered to be a non- specific consequence of metabolic stress. Under this condition, overwhelmed β cells can start expressing immunogenic proteins not displayed normally, which results in the induction of autoimmune response to these new antigens. Alternatively, usually hidden inside of the cells autoantigens, such as CD38, could be presented to the immune system following β cell apoptosis. Anti- CD38 autoantibodies have been detected in patients with both types of diabetes (150, 187). Untreated type 2 diabetes, similarly to type 1, causes changes in vascular system, cardiac and kidney problems, peripheral nerves damage, affecting quality of life and longevity.

Although the primary cause of type 2 diabetes is still unknown, it is evident that insulin resistance in skeletal muscle and liver plays a role in its pathogenesis. Skeletal muscle is the major site for disposal of ingested glucose. Following a meal, approximately one third of ingested carbohydrates is taken up by the liver and the rest by peripheral tissues, primarily skeletal muscles via insulin- dependent mechanism. In insulin resistance states, such as obesity or diabetes, glucose uptake and metabolism in skeletal muscles are markedly impaired (61). The exact mechanism that leads to the development of insulin resistance is not yet fully understood. However, an increased intramyocellar fat content and fatty acid metabolites have been implicated in the progress of insulin resistance in muscles. Recent studies showed that defects in mitochondrial oxidative phosphorylation contribute to the accumulation of triglycerides in myocytes (133, 202). Fatty acids transported into the muscle tissue are normally oxidized during exercise or fasting period in order to retain glucose for use by the central nervous system. Conversely, during the fed state skeletal muscles shift from fat to glucose metabolism in response to insulin. In insulin resistant individuals the ability of insulin to inhibit lipolysis is diminished, leading to chronic elevation in the plasma free fatty acids (FFA) level. Increased plasma concentration of FFA severely reduces glucose transport into the muscle through the insulin- dependant glucose transporter 4 (GLUT4). Interestingly, insulin resistance in skeletal muscle is manifested long before hyperglycemia occurs. Therefore, healthy offspring of diabetic parents have a significant decrease in insulin-stimulated total body and muscle glucose disposal, similarly to the diabetic parents (120).

The liver is responsible for maintenance of physiologic glucose level in the blood. A large fraction of glucose absorbed by the liver is converted into glycogen and stored. However, when the liver is saturated with glycogen, any additional glucose is transferred to fatty acids synthesis, which are esterified later into triglycerides to be exported to white adipose tissue. Under the condition of nutrient deprivation, liver provides a constant supply of glucose for the central nervous system. Hepatic glycogen breakdown, as well as de novo synthesis of glucose from precursors such as lactate, amino acids and glycerol in the process of gluconeogenesis, are the sources of glucose. Patients with type 2 diabetes exhibit increased hepatic glucose production due to impaired gluconeogenesis.

Overproduction of glucose along with a high level of fatty acids drive the secretion of insulin from the pancreas, eventually causing peripheral insulin resistance (129, 190).

Fluctuation in insulin sensitivity occurs during the normal life cycle, with insulin resistance being observed during puberty and pregnancy. Insulin resistance during normal pregnancy usually begins in the third trimester and is a result of maternal adiposity, as well as insulin- desensitizing effects of hormones released by the placenta. Gestational diabetes mellitus in a condition diagnosed in pregnant women with markedly high blood glucose level. This type of diabetes occurs in about 2-5% of pregnancies and resembles type 2 diabetes. Over 20% of affected women develop type 2 diabetes later in life. Uncontrolled gestational obesity can harm both: the mother and the fetus. Risks to the baby include high birth weight, muscle malformations, cardiac and central nervous system abnormalities, respiratory distress syndrome or even perinatal death. Offspring of mothers with gestational diabetes present higher susceptibility to childhood obesity and following type 2 diabetes later in life (19, 33).

1.8 Mitochondria in metabolic syndrome

Mitochondria are the organelles that use highly reducing metabolites and coenzymes to carry out oxidative phosphorylation (OXPHOS) to generate ATP, which is indispensable for the maintenance of physiological functions of cells. Therefore, mitochondrial dysfunction can cause pathological changes in the organism. It is well established that mitochondrial defects contribute to many disorders, particularly age-related. Abundant evidence supports the importance of mitochondria damage in development of type 2 diabetes. Substantial amount of clinical data showed that mitochondrial dysfunction, including the reduction in mitochondrial density and OXPHOS efficiency is associated with diabetes (101, 122). Genetic analysis of skeletal muscle samples form diabetic patients revealed higher frequency of large- scale deletions in mitochondrial DNA (mtDNA), when compared to control individuals (138). Moreover, expression profiles of muscle tissue in diabetic subjects showed reduced levels of the master regulators of mitochondrial biogenesis- PGC1α and nuclear respiratory factor 1

(NRF1), as well as their downstream targets (156, 180). Consequently, proteins needed to form the electron transport chain (ETC) and encoded by these genes may be insufficient to execute OXPHOS in case of diabetic patients. It has been reported that activity of both mitochondria oxidative enzymes and complex I of the ETC are decreased in muscles of obese diabetic patients (266) and insulin- resistance offspring of diabetic parents (185). The ATP insufficiency coming from mitochondrial dysfunction may impair the regulation of potassium and calcium channels, which inhibits the exocytosis of insulin form pancreatic β- islet cells (149). Furthermore, defective OXPHOS cause overproduction of reactive oxygen species (ROS), which may damage most of the intracellular components. Oxidative stress can activate multiple signaling pathways, including p38 MAPK and JNK, which may affect components of insulin signaling such as the insulin receptor and the family of insulin receptor substrates (IRS). This in turn can inactivate PI3 kinase and abrogate the translocation of GLUT4 to the plasma membrane. It was shown that mouse C2C12 myotubes treated with respiratory inhibitors display reduction in insulin- stimulated glucose uptake due to inactivation of AKT and IRS-1 in insulin signaling (69, 139). Additionally, mitochondria malfunction can be associated with diminished activity of enzymes involved in β- oxidation of fatty acids, which causes intracellular lipid accumulation. Reduced oxidative metabolism of lipids was confirmed in skeletal muscle of type 2 diabetic patients (84). Similar defects were observed in fatty liver disease. It has been shown that a decrease in carnitine palmitoyl transferase (CPT) activity, which transports long- chain acyl- CoA into mitochondria, or deficiency of long-chain acyl- CoA dehydrogenase (LCAD), an β- oxidation enzyme, leads to the high lipid content and following insulin resistance in hepatocytes, which causes the liver steatosis in the long term (295). Interestingly, adiponectin signaling has been recently implicated in regulation of mitochondrial bioenergetics. In animal models of type 2 diabetes, the activation of 5'- AMP- activated protein kinase (AMPK) by adiponectin, increases muscle and hepatic fat oxidation and improves insulin sensitivity (48, 283). Moreover, numerous abnormalities in mitochondria structure like smaller size, poorly defined cristae and derangement of mitochondrial network, have been found in skeletal muscle of obese individuals (122). Importantly, results from the current studies demonstrate that mitochondrial defects are found in the prediabetic state, suggesting that mitochondrial

dysfunction may be primary event leading to the development of type 2 diabetes (185, 186). Due to overwhelming predominance of type 2 diabetes in industrialized countries, environmental pollutants and toxins have been postulated as additional factors in the development of this disease. Organic compounds, added to many herbicides, insecticides, rodenticides, industrial products and wastes, are resistant to any kind of degradation. Thus, they are present for a long time in our habitat and accumulate in the organisms.

1.9 Adipogenesis

It is generally accepted that adipose tissue is derived from mesoderm. Mesenchymal / mesodermal stem cells (MSCs), which reside in the vascular stroma of adipose tissue, are capable of differentiating into adipocytes. The exact number of intermediate stages between MSC and mature adipocyte is still not clear. However, it is believed that MSCs give rise first to a common early progenitors (adipoblasts), which later on turn into committed preadipocytes that can differentiate into mature adipocytes, when given appropriate stimuli. In vitro adipogenesis follows a highly ordered and temporal sequence composed of four events: growth arrest, mitotic clonal expansion, early differentiation and terminal differentiation (173). The entire differentiation process is orchestrated by particular inducers, such as insulin, insulin- like growth factors- 1 (IGF-1), glucocorticoids, triiodothyronine and cAMP, which regulate the expression of key transcription factors like CCAAT/enhancer binding proteins (C/EBPs) and peroxisome proliferators-activated receptors (PPARs) (87, 205). The initial step of growth arrest is achieved after contact inhibition of proliferating preadipocytes. At this stage rapid phosphorylation of cAMP- response element binding (CREB) occurs, which activates C/EBPβ, causing sequential expression of other essential factors. The growth arrest is followed by one or two additional rounds of cell division known as clonal expansion. This step coincidences with the phosphorylation of C/EBPβ by family of mitogen-activated protein kinases (MAPKs). Fully activated C/EBPβ induces the expression of PPARγ and C/EBPα, key adipogenic transcription factors, which can subsequently regulate each other's expression. These two factors activate de novo or enhance expression of most of the genes during early and terminal differentiation.

Throughout this process, lipid droplets begin to appear in the cytoplasm, and over time they become large and merge into one or a few major droplets, which is a characteristic of white adippocytes (23, 280).

1.10 Brown adipose tissue

Adipose tissue has a pivotal role in the regulation of energy balance. Two types of adipose tissue can be distinguished histologically and functionally: white adipose tissue (WAT) and brown adipose tissue (BAT). WAT accumulates excess energy mainly in the form of triacylglycerol and also functions as an endocrine organ, secreting adipokines and proinflammatory cytokines. BAT on the other hand is specialized in dissipating energy in the form of heat.

Brown adipose tissue is a unique organ that exists only in mammals. It is probably the outcome of a single evolutionary adaptation, occurring very early during the development of mammals. Acquisition of BAT gave mammals an evolutionary advantage of surviving and being active during periods of cold, surviving the cold stress of birth and promoting the survival on diets low in essential macronutrients. Development of BAT occurs late in embryonic life (29). In rodents BAT is present throughout life. Major depots are located primarily in the interscapular region and the axillae, whereas minor amounts exists near the thymus and in the dorsal midline region of the thorax and abdomen. Interestingly, brown adipocyte-like cells are also found interspersed in WAT of adult animals that have been acclimated to cold or chronically treated with selective β_3-adrenergic agonists. The activity of BAT in non- hibernating animals is strictly related to the environmental temperature with cold exposure inducing its action. In neonates and hibernating animals, BAT serves as important regulator of the body temperature via non-shivering thermogenesis. In the human infants, BAT is situated as axillary, cervical, perirenal and periadrenal depots and also surrounding the great vessels. At birth, the total weight of BAT is around 150-250 g, which accounts for 2-5% of total body weight and it disappears rapidly within the first years after birth (12, 278).

Characteristics	WAT	BAT
Function	Energy storage, lipolysis and lipogenesis, secretion of adipokines and growth factors,	Heat production, thermogenesis, lower fat storage capacity and low secretory activity,
Macroscopic features	Subcutaneous, abdominal, perirenal, inguinal and gonadal location White colour, adequate vascularization (++), mainly sympathetic innervation (++), tissue organized as small lobules of densely packed cells,	Interscapular, paravertebral, axillary and perirenal location, Brown colour, extraordinary vascularization (++++), sympathetic innervation (++++), lobular organization with gland-like structure,
Microscopic features	Unilocular adipocytes with one single large lipid droplet that occupies 90% of the cell volume, variable shape and size of adipocytes (25-200 μm) Few, small and elongated mitochondria, High presence of other cell types (fibroblasts and immune cells),	Multilocilar adipocytes with abundant small lipid droplets, mainly polygonal and small adipocytes (15-60 μm), Abundant, large and round mitochondria, Low presence of other cell types,
Molecular features	Lack of UCP1 (-) and Cidea (-) expression, Low UCP2 (++), PGC1α (+), PRDM16 (+), Dio2 (+), cytochrome c (+), β_3-AR (+), β_1-AR (++), $\alpha_{1/2}$-AR (+) expression, High leptin (+++) and RIP140 (+++) expression,	Low leptin (present at birth), RIP140, UCP2 (+),β_1-AR (++), $\alpha_{1/2}$-AR (+) expression, High UCP1 (++++),β_3-AR (+++), β_1-AR (+), $\alpha_{1/2}$-AR (+), PGC1α (+++), PRDM16 (+++), Cidea (+++), Elovl3 (+++), Dio2 (+++), cytochrome c (+++) expression,

Table 1.2 Summary of WAT and BAT characteristics (modified from (79).

The main function of brown adipose tissue is energy expenditure, which changes markedly in response to environmental temperature. Oxygen consumption is increased up to fourfold after acute and chronic cold exposure. A part of acute response is due to shivering carried by the muscle tissue. However, with adaptation, shivering stops and increasing adaptive thermogenesis in BAT becomes prominent. Temperature information that is detected by the cutaneous and core body thermoreceptors is transmitted to the regulatory center located in the hypothalamus, which leads to the activation of efferent pathways controlling energy dissipation. The main effector component of this response is the sympathetic nervous system (SNS), which heavily innervates BAT (145, 159). Catecholamines, such as norepinephrine, released from the SNS trigger nonshivering thermogenesis in BAT. Activation of G protein- coupled β_3- adrenergic receptor stimulates membrane- bound adenylyl cyclase, which increases intracellular levels of cAMP. The further signaling pathway is mediated via cAMP- dependent protein kinase A (PKA), which leads to the increased lipolysis. The stimulation of lipolysis is composed of two processes: activation of hormone- sensitive lipase (HL) and deactivation of perilipin by its phosphorylation. Perilipin protects the triglycerides against HL. Activated PKA phosphorylates perilipin causing its dissociation from the triglyceride droplets that become freely exposed to the attack by HL. Released in this process free fatty acids serve as a substrate for thermogenesis. Free fatty acids are converted to acyl- CoA and then transported to the mitochondria via the carnitine shuttle. Once inside the mitochondrial matrix, fatty acids undergo β- oxidation, during which molecules of acetyl- CoA are repeatedly cleaved from the fatty acid. Acetyl- CoA enters later on citric acid cycle (TCA), leading to the formation of reduced electron carries, such as nicotinamide and flavin adenine dinucleotides (NADH and FADH), which are then oxidized by the electron transport chain in the inner mitochondrial membrane. This results in a pumping out of protons from the matrix to the intermembrane space and creation of proton- motive force that allows most of the cell types to produce ATP. However, in brown adipocytes electron transport is uncoupled from the ATP synthase by the UCP1 therefore potential energy is lost in the form of heat. Apart from lipolysis initiation, PKA activates p38 MAPK pathway, which is responsible for the expression of key thermogenic factors like PGC1α, UCP1 and type 2 deiodinase (Dio2). Additionally, PKA phosphorylates the

CREB transcription factor that also activates UCP1 expression. All specific evolutionary adjustments of brown adipocytes, such as huge UCP1 concentration, high expression of β- oxidation enzymes and low level of ATP synthase allow for extremely efficient adaptive thermogenesis (29, 49, 145). Interestingly, the brain can also affect energy expenditure by the hypothalamic- pituitary- thyroid axis. In BAT of human newborns and small mammals, activation of thyroid hormone by Dio2 has been known to play a role in adaptive thermogenesis during cold exposure. It has been also reported that changes in thyroid hormone are reflected in parallel changes in energy expenditure. More importantly, even small fluctuations in hormone level can have significant effects. The exact mechanisms by which thyroid hormone accelerates energy expenditure are poorly understood (5, 230).

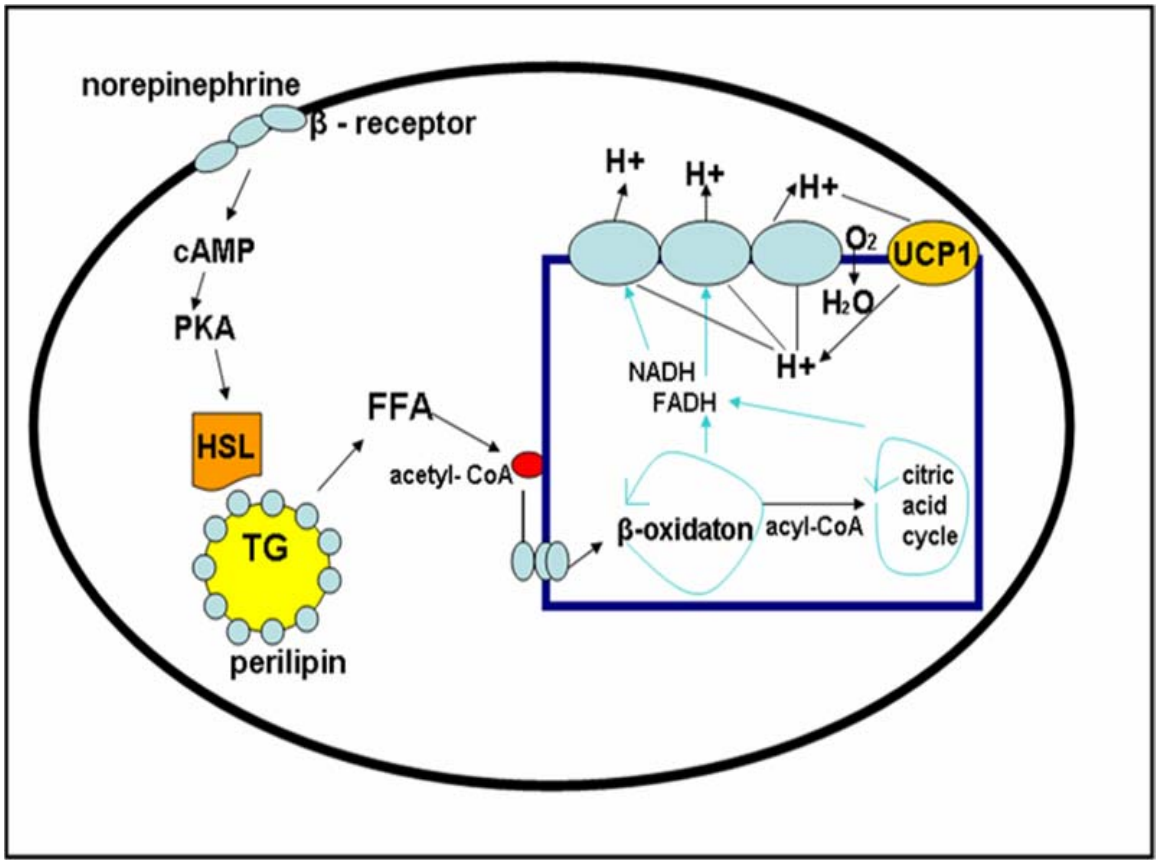

Figure 1.5 Norepinephrine- stimulated thermogenesis in BAT (29).

1.11 Brown adipose tissue and obesity

There is compelling evidence, coming from studies on rodent models, that brown adipose tissue has anti- obesity function. Earliest reports showed that surgical excision or denervation of interscapular BAT caused increase in the amount of WAT (99). Furthermore, mice with genetically ablated BAT exhibit an obese phenotype at the age of 16 days. This degree of pathology is comparable to that seen in the in most commonly used mouse models of obesity like ob/ob or db/db mice. Transgenic mice with BAT ablation display also insulin resistance, hyperglycemia and hyperlipidemia (146). Moreover, UCP1 deficient animals also develop obesity and demonstrate abolished diet-induced thermogenesis, when kept at thermoneutral temperature (73). Importantly, transgenic mice expressing UCP1 from the aP2 promoter are resistant to genetic and diet-induced weight gain. Also, targeted disruption of other BAT- specific protein such as Cidea (cell-death-inducing DFF45-like effector A), which inhibits the uncoupling activity of UCP1, results in a lean phenotype and resistance to diet- induced obesity (302). Finally, in most rodent models susceptibility to obesity correlates with diminished function of BAT, whereas resistance to weight gain is associated with up regulated BAT function or the recruitment of brown adipocyte- like cells in WAT (79, 127). Additionally, small amounts of brown adipose tissue can be found interspersed between skeletal muscle in mice and humans. These diffuse brown adipocytes have been suggested to help protect some strains of mice from obesity (6, 52).

It was believed that BAT regresses with age and is completely lost by the time we reach adulthood. However, the ability to produce BAT in adulthood has been noticed in patients with catecholamine- secreting tumors such as pheochromocytomas and paragangliomas, in whom distinct BAT depots were found (81). According to mathematical estimates as little as 50 g of maximally activated BAT could account for up to 20% of daily energy expenditure in an adult human, equivalent to 20 kg of body weight over the course of a year (66). It has been also calculated that affecting energy balance by as little as 50-100 kcal/day could prevent weight gain in most of the population. Since any action that causes negative energy balance in overweight and obese patients is effective in their weight loss, even small stimulation of BAT would be

beneficial for these patients. These observations and calculations encouraged clinicians to investigate a potential BAT occurrence in healthy humans. Scanning with a combination of PET (positron emission tomography) and CT (computed tomography) with the analogue ^{18}F- FDG (^{18}F- fluorodeoxyglucose) as a tracer showed depots of BAT in healthy humans. Immunohistological and molecular analysis of biopsy specimens of depots identified as BAT by PET/CT scans confirmed that the observed tissue indeed corresponds to BAT (54, 166). It appeared that in individuals under ambient conditions (22 °C), active BAT is detectable only in 3% of men and 7% of women. However, in individuals subjected to a 2 hour cold exposure, the incidence of detectable active BAT in lean subjects increases up to 96% (210, 258). More importantly, BAT activity is lower in overweight and obese subjects than in lean ones. BMI (body mass index) and body fat content showed an inverse correlation with amount of BAT and resting metabolic rate a positive correlation with BAT activity. Furthermore, glucose tolerance in people with obesity but high levels of UCP1 is better than that in people with obesity and low levels of UCP1. Insulin levels also seem to be inversely associated with the activity of BAT in lean individuals. Interestingly, a correlation between amount and activity of BAT and thyroid hormone level was found in case of a single patient with severe insulin resistance due to mutation in insulin receptor gene. Prolonged treatment of this patient with synthetic thyroid hormone resulted in dramatic improvement in insulin sensitivity, paralleled by enhanced BAT volume and activity. It suggests a possible role of BAT in non-insulin-dependent glucose disposal (231). All the clinical and laboratory data suggest that upregulation of BAT function can contribute to a lean and metabolically correct phenotype in humans. These findings suggest that manipulation of BAT function as a potential therapeutic target for treatment of obesity. Transplantation and/or stimulation of already existing BAT or recruitment of new brown adipocytes might be used as a therapeutic approach to increase energy expenditure in order to improve overall metabolism (79, 250, 265).

1.12 Transcriptional control of BAT development

Despite the differences in physiological functions of BAT and WAT, both cell types share a similar transcriptional cascade that controls adipogenesis process. Previous studies using white adipose tissue models identified PPARs and C/EBPs as key transcription factors that orchestrate fat cell differentiation and maintain the stable differentiated state of adipocytes.

The C/EBPs are a family of basic- leucine zipper transcription factors, which comprise of six members: C/EBPα, C/EBPβ, C/EBPδ, C/EBPγ, C/EBPε and C/EBPζ, encoded by separate genes. The number of isoforms present in the tissues can be even higher due to differential splicing and alternative use of the promoters. They are widely expressed and target a variety of the genes. Nevertheless, only C/EBPα, C/EBPβ and C/EBPδ play important role in adipocyte differentiation (280).

The expression of C/EBPα is induced relatively late during differentiation of preadipocyte cell lines due to its anti- mitotic activity. Premature appearance of C/EBPα prevents preadipocytes from entering the mitotic clonal expansion phase during adipogenesis. C/EBPα has been implicated in transcriptional regulation of several genes critical for adipose tissue function like adipose protein 2 (aP2), GLUT4, acetyl-CoA carboxylase and stearyl-CoA desaturase 1 (55). Ectopic expression of this C/EBP family member can induce the adipogenic program in many fibroblastic cell lines (78). Overexpression of C/EBPα in regular preadipocyte cell lines accelerates differentiation, whereas knock down greatly inhibits lipid accumulation. Mice that carry a homozygous deletion of C/EBPα die from hypoglycemia within several hours after birth. Consistently with in vitro results, C/EBPα- null animals show markedly reduced triglyceride content in WAT and BAT (271). Moreover, further analysis of BAT from embryos and neonates revealed decreased and/or delayed expression of PPARγ, PPARα, UCP1, PGC1α, attenuated Dio2 function and defective mitochondrial biogenesis (32). Since a C/EBPα liver transgene can rescue BAT and not WAT phenotype, it suggests that altered BAT is secondary to severe metabolic derangement. Accordingly, postnatal ablation of C/EBPα affects only WAT and not BAT (99, 286).

C/EBPβ and C/EBPδ are induced early during differentiation of preadipocytes upon hormonal stimulation, which is followed by the induction of PPARγ and C/EBPα. However, newly expressed C/EBPs lack DNA binding activity until they undergo phosphorylation occurring several hours later, resulting in full activation of these transcription factors. During differentiation program C/EBPβ is sequentially phosphorylated, first by MAP kinase on Thr188 and then much later by GSK-3β on Thr179 and Ser184 (173, 239). C/EBPβ is most abundantly expressed in BAT, liver and WAT. Two C/EBPβ isoforms are generated from a single mRNA: the 35-38 kDa full-length LAP (liver enriched transcriptional activatory protein) and truncated 20 kDa LIP (liver enriched transcriptional inhibitory protein) (173, 205). Interestingly, C/EBPβ was identified as one of the first transcription factors involved in the regulation of UCP1 expression. Therefore it was proposed to play a role in BAT development. Mice with targeted disruption of C/EBPβ are born at expected ratio, but around 35% of knockout animals die shortly after birth due to sever hypoglycemia. The surviving mice have a compromised immune system, decreased gluconeogenesis in liver and lipolysis in WAT during fasting or diabetic state. Expectedly, mice lacking C/EBPβ display reduction in lipid accumulation and UCP1 expression in BAT, whereas WAT remains unaltered. When exposed to cold, C/EBPβ deficient mice did not maintain their body temperature. Although, the induction of UCP1 and PGC1α expression in response to cold was not impaired in BAT of C/EBPβ- null mice, suggesting that defective thermoregulation is a result of reduced lipid metabolism. Surprisingly, primary brown adipocytes lacking C/EBPβ appeared to differentiate normally in vitro (31, 238). Remarkably, recent studies have shown that overexpression of C/EBPβ in white 3T3-L1 preadipocytes can reprogram them to brown adipocyte pattern of gene expression (119).

PPARs belong to ligand- activated nuclear receptor superfamily. There are three types of PPARs encoded by separate genes: PPARα, PPARβ/δ and PPARγ. All members of PPAR family consist of a ligand- independent transactivation domain, DNA binding domain and a ligand binding and dimerization domain. Upon ligand binding PPARs undergo conformational changes that allow them to heterodimerize with a retinoid X receptor (RXR) prior to binding DNA at the peroxisome proliferators response element (PPRE) in the promoter of target genes. This transcriptional heterodimers require

interactions with co-activators and co-repressors for transcriptional specificity. PPARs are also subjected to posttranslational modifications such as phosphorylation and sumoylation, which regulate their activity (173).

PPARγ is the central regulator of adipose differentiation in vitro and is required for the formation of both WAT and BAT in vivo. It exists in three isoforms: PPARγ$_1$, PPARγ$_2$ and PPARγ$_3$, which are transcribed from the same gene through alternative splicing and promoter use (304). All isoforms are expressed in tissue- dependent manner. PPARγ$_1$ is expressed in variety of tissues and cell types, whereas PPARγ$_3$ has been detected mainly in adipose tissue, large intestine and macrophages. PPARγ$_2$ appeared to be the adipose- specific isoform. PPARγ is induced during differentiation in order to activate a number of genes involved in fatty acid binding, uptake and storage such as aP2, lipoprotein lipase (LPL), acyl-CoA synthase and phosphoenolpyruvate carboxykinase (PEPCK). PPARγ is also described as an insulin sensitizer through activation of GLUT4 expression and enhancing glucose uptake. In addition, PPARγ seems to regulate survival of mature adipocytes (107). The importance of this transcription factor in adipogenesis has been demonstrated in cell culture and animal models. PPARγ knockout mice die in utero due to dysfunctional placenta. Embryos that survive thanks to tetraploid rescue are deficient in BAT (15). 3T3-L1 preadipocytes lacking PPARγ expression are not capable of differentiating into mature adipocytes (200). Moreover, overexpression of PPARγ in non- adipogenic mouse fibroblasts stimulates fat accumulation (247). PPARγ natural ligands including fatty, fatty acid derivatives and prostaglandins have significant impact on both brown and white adipose tissue function. Therefore, high- affinity synthetic ligands such as TZDs (thialidinediones) are currently used to manage type 2 diabetes. TZDs promote white and brown adipogenesis in vitro and can induce expression of UCP1 in BAT and WAT depots in vivo (99, 263).

The major function of PPARα is regulation of fat breakdown through induction of the expression of β- oxidation enzymes, such as acyl- CoA oxidase (AOX) and long acyl- CoA dehydrogenase (LCAD). In general, PPARα is abundantly expressed in tissues that have high level of fatty acids catabolism like liver, heart or muscles. As a consequence of this pattern, its expression in BAT is much higher than in WAT.

Although, PPARα deficient mice have morphologically normal BAT with appropriate UCP1 level and no defects in cold response (99, 292).

PPARγ co-activator 1α (PGC1α) war first cloned as PPARγ- interacting protein (195). There are three members of PGC family: PGC1α, PGC1β and PGC1-related coactivator (PRC). PGC1α and PGC1β are enriched in tissues with high oxidative capacity like BAT, slow twitch muscle fibers, heart, brain and liver. PGC1α activity is adjusted through posttranslational modifications. Phosphorylation by the p38 MAPK and methylation carried by PRMT (protein arginine methyltransferase 1) increase stability and transcriptional activity of PGC1α (193, 242). PGC1α was also shown to be activated by deacetylation via sirtuin 1 (203). Over the years, PGC1α has been repeatedly proven as a major regulator of mitochondrial biogenesis and oxidative metabolic pathways. It induces transcription of NRFs (nuclear respiratory factors) and co- activates NRF-1, which regulates the expression of mitochondrial transcription factor A (Tfam). In turn, Tfam is crucial for replication, maintenance and transcription of mitochondrial DNA (279). PGC1α is potently induced in response to cold exposure via the PKA-CREB pathway. Additionally, it strongly co- activates PPARγ and TRβ on the UCP1 promoter. In compliance with that, overexpression of PGC1α in white fat cells enhances mitochondrial number and UCP1 levels (195, 279). Consequently, mice devoid of PGC1α show poor UCP1 expression and cold sensitivity. In addition, BAT displays altered morphology, with abundant accumulation of large lipid droplets seen usually in WAT (141). Importantly, differentiation of brown preadipocytes lacking PGC1α remains unchanged. Nevertheless, induction of the genes involved in thermoregulation is impaired (254). Notably, it has been shown that some molecules like well known co- repressor RIP140 can antagonize PGC1α function on its target gene promoters. Forced expression of RIP140 in adipose tissue or skeletal muscles ablates mitochondrial biogenesis and oxidative metabolism. Conversely, deficiency of RIP140 leads to increased appearance of brown fat cells in WAT and elevated UCP1 expression in cell culture (45, 192).

Despite similarities in the signaling pathways responsible for triglyceride metabolism in both BAT and WAT, recent studies showed that they have distinct developmental origins. Elegant lineage tracking experiments indicated that BAT, dermis

and skeletal muscles are derived from a population of Engrailed-1 (En-1)- expressing cells in the dermamyotome (10). Moreover, microarray experiments revealed that only BAT precursors share many genes and microRNAs with Myf5 positive muscle progenitor (245, 269), which was independently confirmed by in vivo fate mapping in mice (215). Furthermore, even the BAT mitochondrial proteome analysis showed a large overlap with proteins from muscle mitochondria, not from WAT (76). Interestingly, the pockets of brown fat cells spread within WAT are not derived from Myf5- expressing cell lineage (215, 281). Genome- wide survey identified a PRD1-BF-1-RIZ1 homologous domain-containing protein 16 (PRDM16), as one of transcriptional regulators whose expression was strongly correlated with BAT phenotype in vivo and in cell culture system (217). PRDM16, a 140 kDa protein was first described at a chromosomal break point in human myeloid leukemia (169). It contains ZF1 domain at the N- terminus (seven repeats of C2H2 zinc- finger domain) and very similar ZF2 domain at the C-terminus (three repeats of C2H2 zinc- finger domain), which are responsible for the DNA binding and a putative SET domain, a conserved sequence among histone lysine methyltransferases. Despite the fact that PRDM16 has been shown to bind directly to a specific DNA sequence, a mutation in the protein that abrogates DNA binding does not alter its ability to induce proper phenotype of BAT. This observation suggests that PRDM16 functions rather through protein-protein interactions then direct DNA binding. Ectopic expression of PRDM16 in mouse fibroblast, white adipocytes or muscle precursors results in induction of entire program of brown fat differentiation, including activation of thermogenic genes like UCP1, PGC1α and Dio2, mitochondrial genes, and other BAT- specific markers such as Cidea and Elovl3 (long-chain fatty acid elongase3). This is achieved through co-activation of PGC1α, PGC1β, PPARγ and PPARα transcriptional activity by PRDM16 via direct physical interactions. At the same time, PRDM16 inhibits white fat genes such as resistin or angiotensinogen through association with C-terminal binding proteins (CtBP1 and CtBP2), well known co- repressors (114, 217). Moreover, coincidently with the induction of BAT genes, some of the muscle- selective markers become suppressed by PRDM16. The suppression includes MyoD, myogenin (Myg), myosin heavy chain (MyHC) or muscle creatine kinase (MCK). Finally, depletion of PRDM16 from cultured brown fat preadipocytes almost completely ablates their ability to acquire correct BAT

characteristics. Surprisingly, loss of PRDM16 does not interfere with fat accumulation in cell culture system. More importantly, PRDM16 knockdown in brown fat precursors promotes skeletal muscle differentiation. Consistent with the in vitro data, BAT from PRDM16- null embryos displays an altered morphology with reduced expression of thermogenic genes and upregulated expression of muscle- specific markers. These results demonstrated that PRDM16 is an essential determinant of the brown fat lineage during embryonic development. Notably, recent studies established that PRDM16 in complex with an active form of C/EBPβ control the conversion of myoblastic precursors to brown adipocytes, and is sufficient to induce fully functional BAT program in nonadipogenic cells like embryonic fibroblast or skin fibroblasts from mouse and man. In fact, C/EBPβ deficiency significantly suppresses the ability of PRDM16 to drive the brown fat differentiation in myoblasts. Indeed, BAT from PRDM16 knockout and C/EBPβ knockout mice exhibit similar phenotypes, with blunted BAT- selective and elevated muscle- specific gene expression (113, 215). Interestingly, it has been also indicated that PRDM16 can robustly induce the emergence of brow- like adipocytes in subcutaneous WAT, which causes rise in energy expenditure, limited weight gain and improved glucose tolerance in mice fed high- fat diet (216). So far, the signaling molecules that control PRDM16 expression during development remain unknown. Bone morphogenic proteins (BMPs), which belong to TGF-β superfamily, have been suggested to induce BAT differentiation. In particular BMP7, which has been shown to promote the in vitro differentiation of committed brown preadipocytes and multipotent fibroblasts, with the induction of PRDM16, UCP1 and PGC1α expression. Moreover, BMP7- null embryos display diminished amounts of BAT that lack UCP1 expression, although, the exact mechanism that mediates this effects are still not clear (252).

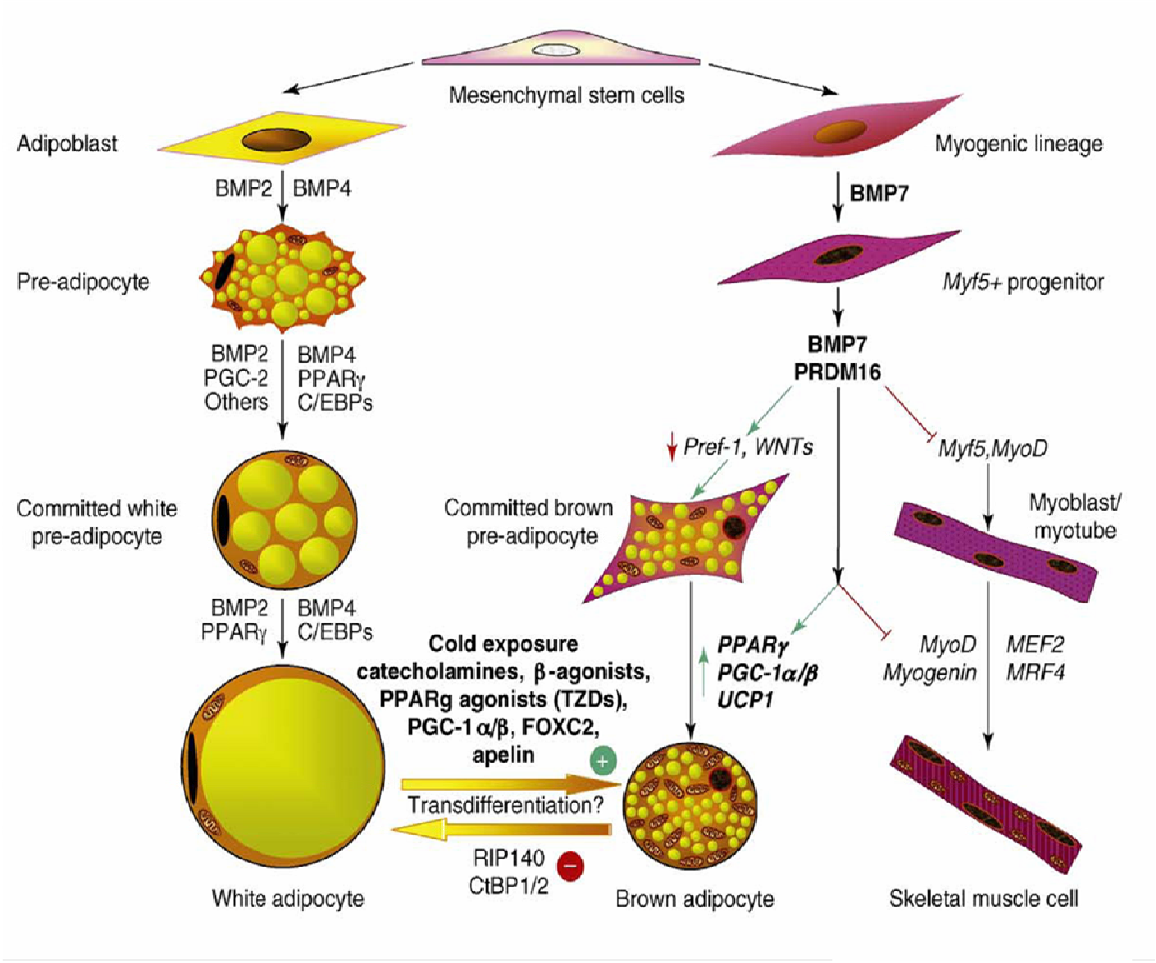

Figure 1.6 Model of BAT and WAT development from mesenchymal stem cells (79).

It has long been recognized that respiration and mitochondrial ATP synthesis are tightly coupled. The mitochondrial respiratory chain, carrying electrons is composed of four complexes and ATP synthase (complex V). Nutrients metabolized in specific pathways generate fixed amount of NADH and $FADH_2$. Oxidation of these substrates results in protons being pumped out of the mitochondrial matrix to the intermembrane space by complex I, III and IV. Then the proton gradient generated by the ETC is consumed by complex V, which catalyzes ATP synthesis. However, like any biological system, the coupling between substrate oxidation and ATP formation is not 100% efficient. According to Mitchell's theory, any proton leak not connected with ATP production can provoke uncoupling of respiration and thermogenesis. A well known

example of such a situation is presence of uncoupling proteins (UCPs) (145). UCPs are members of a large family of nuclear- encoded carrier proteins located in the inner mitochondrial membrane. The main function of UCPs is dissipation of energy, coming from proton leakage that results in the production of heat. There are three subtypes of UCPs: UCP1, UCP2 and UCP3. They all share over 50% homology in amino acid sequence, but differ with respect to tissue distribution. The UCP's triplicated structure consists of six transmembrane domains linked by hydrophilic segments. Each domain has two hydrophobic α- helices connected by the long hydrophilic loop, oriented toward the mitochondrial matrix (206). Original studies performed on isolated brown fat mitochondria showed very high rates of respiration under condition, when mitochondria from other tissues had lower respiratory rate. These conditions include presence of substrates for oxidation but absence of ADP, which indicated that BAT mitochondria are highly uncoupled. A rapid respiration without ATP production represents by definition a powerful thermogenic process. UCP1 (thermogenin) was identified later on as the protein responsible for this phenomenon (28, 125). Induction of UCP1 is caused by the rising amounts of intracellular cAMP that increase free fatty acids levels, which is thought to stimulate UCP1 activity. The exact molecular mechanism of this stimulation is still not clear. The hypothetical model assumes that either fatty acid carboxyl groups serve as H^+ donors to the UCP1 proton translocation channel or UCP1 transports free fatty acid anions not protons, from matrix to outside. Once in the intermembrane space, the FFA become re- protonated and then flip- flop back across the inner membrane, creating protonophore cycle (29). Since adaptive thermogenesis is considered to be related with overall metabolic control, UCP1 knockout mice were created to prove this assumption. As predicted, UCP1- null mice are susceptible to cold. However, it was very surprising that the UCP1 deficient mice failed to demonstrate an obese phenotype (67, 127). These results suggested the existence of alternative thermogenic response to diet, which is UCP1- independent. Such as alternative adaptive thermogenesis has been proposed to be localized in muscles, particularly in relation to obesity (130, 144, 145, 166). An important variable that should be considered is the fact that animals housed in normal conditions, approximately 22° C, are constantly exposed to thermal stress. To maintain their body temperature, they have to elevate their metabolism and food intake

about 50-60%. Therefore, this chronic thermal stress can significantly affect the outcome of any metabolic studies. Thus, the UCP1 knockout mice were examined again at the thermoneutral temperature of 30° C. Remarkably, animals with ablated UCP1 became obese even on regular chow diet. In addition, the obesogenic effect of high fat diet was accelerated in knockout mice due to the inability to recruit diet- induced thermogenesis (73). Moreover, it has been shown that mice with UCP1 transgene expressed in WAT or muscles are resistant to genetic and diet- induced obesity (126, 127). Interestingly, several single nucleotide polymorphisms (SNPs) in the UCP1 promoter have been reported to associate with obesity, diabetes and lipid- related disorders (112).

UCP2 and UCP3 (UCP1 homologues) are also capable of uncoupling process. Although, the evidence that they can regulate energy metabolism, in the way to prevent obesity, is not extensive. UCP2 is commonly expressed in almost all kind of tissues. It has been suggested to attenuate the production of reactive oxygen species (ROS) and regulate the ATP/ADP ratio. More recently, UCP2 was also shown to affect insulin secretion by the β- cells (9, 35). In contrast to UCP2, UCP3 is expressed predominantly in skeletal muscle and the exact function o this protein remains to be investigated. However, UCP3 has been implicated in regulation of ROS formation, mitochondrial fatty acid transport and regulation of glucose metabolism in muscle tissue (213). Interestingly, there are reports indicating that UCP3 expression is upregulated in response to cold exposure and overfeeding (92, 140, 214).

The main function of fatty acids (FA) is energy storage and building of membranes in the cell. Fatty acids have also been described as the signaling molecules, modulating the activity of nuclear receptors. The majority of FA synthesis inside of the cell is carried out by the cytosolic fatty acid synthase (FAS), which produce medium- to long- chain FA (up to C16). The products of FAS can be further elongated by membrane-bound enzymes located in the endoplasmatic reticulum (ER). These enzymes belong to the Elovl (elongation of very long- chain fatty acids) gene family that perform the first step in the elongation process. Elovl3 was identified during the search for specific molecules that are enriched in BAT. It is involved in the esterification of saturated and monounsaturated FA in the C20-C24 range. Expression of Elovl3 is controlled by PPARα

and SREBP-1 (sterol regulatory element-binding protein-1). Besides BAT, Elovl3 transcripts were found in less extend in liver and skin. Importantly, Elovl3 mRNA level appeared to be increased by over 200- fold in BAT of mice exposed to cold. Moreover, augmented expression of Elovl3 was also observed during embryonic development, reaching the maximum level just after birth. These results demonstrate that Elovl3 appearance is strongly correlated with recruitment of BAT (111, 276).

The cell death-inducing DFF45-like effector proteins (CIDE) have a distinct tissue expression pattern. One of the members Cidea has been identified as BAT-selective marker. Cidea has been shown to be regulated by key adipogenic transcription factors such as PPARγ and PPARα, as well as ERRα (estrogen-related receptor α) and NRF-1, with co-activation by PGC1α (93). Remarkably, Cidea knockout mice exhibit a profound lean phenotype and resistance to diet- induced obesity/diabetes. They also show higher metabolic rate and core body temperature, as well as elevated lipolysis in BAT, when subjected to the cold treatment. All the above features are the result of direct repressive action of Cidea on UCP1 activity (302).

RESEARCH AIMS

Jak kinases and Stat transcription factors are well recognized key players in a variety of innate and adaptive immune responses. The role of Jak/ Stat pathway has been reported to be a primary target of leptin action and to a lesser degree insulin signaling (102, 255). Interestingly, it was recently shown that Stat3 knock down in adipose tissue causes obesity in mice (34). According to the data obtain previously in our laboratory, Tyk2 deficient mice become obese and diabetic with age. Tyk2 knockout animals also exhibit decreased expression of brown fat- specific genes. Brown adipose tissue is pointed lately as a new target for obesity treatment. Nevertheless, participation of the Jak/Stat pathway in BAT development has not been investigated.

Specific aims:

1. To confirm an obese phenotype of Tyk2 deficient mice on different genetic backgrounds.
2. To identify the role of Tyk2 and Stat3 in differentiation of immortalized preadipocyte cell lines.
3. To determine whether Stat3 restores the function of brown adipose tissue in Tyk2 -/- mice and reverses their obese phenotype.

CHAPTER II

MATERIALS AND METHODS

2.1. Mice

All the mice were bred and maintained in MCV/VCU animal facility according to Institutional Animal Care and Use Committee (IACUC) regulations. Tyk2 deficient mice (C57Bl/6 and BALB/c background) were kindly provided by Dr. Ana Gamero from the Department of Biochemistry, Temple University School of Medicine, Philadelphia, USA. Tyk2 -/- were generated by Dr. Kazuya Shimoda and colleagues from the Department of Internal Medicine, Kyushu University, Fukuoka, Japan (223). The disruption of Tyk2 expression was performed by electroporation of embryonic stem cells with targeting vector that carried a neomycin resistance cassette design to replace the first coding exon of Tyk2 gene.

Mice carrying a transgene encoding a constitutively active form of the Stat3 protein (Stat3CA) including an upstream loxP- flanked stop sequence in the ubiquitously expressed Rosa26 locus were a kind gift of Dr. Klaus Rajewsky from the CBR Institute for Biomedical Research, Harvard Medical School, Boston, USA. The Tyk2 -/- mice expressing the constitutively active Stat3 only in BAT (brown adipose tissue) or WAT (white adipose tissue) were obtained by crossing Stat3CA transgenic animals with mice expressing the Cre recombinase under control of the aP2 promoter, which is specific for adipose tissue. Both transgenic lines (Stat3CA and aP2-Cre) were bred into Tyk2 -/- mice before final crossings. Only animals from the same mixed- background strain generation were compared. The specificity of transgene expression was confirmed by qPCR as described below.

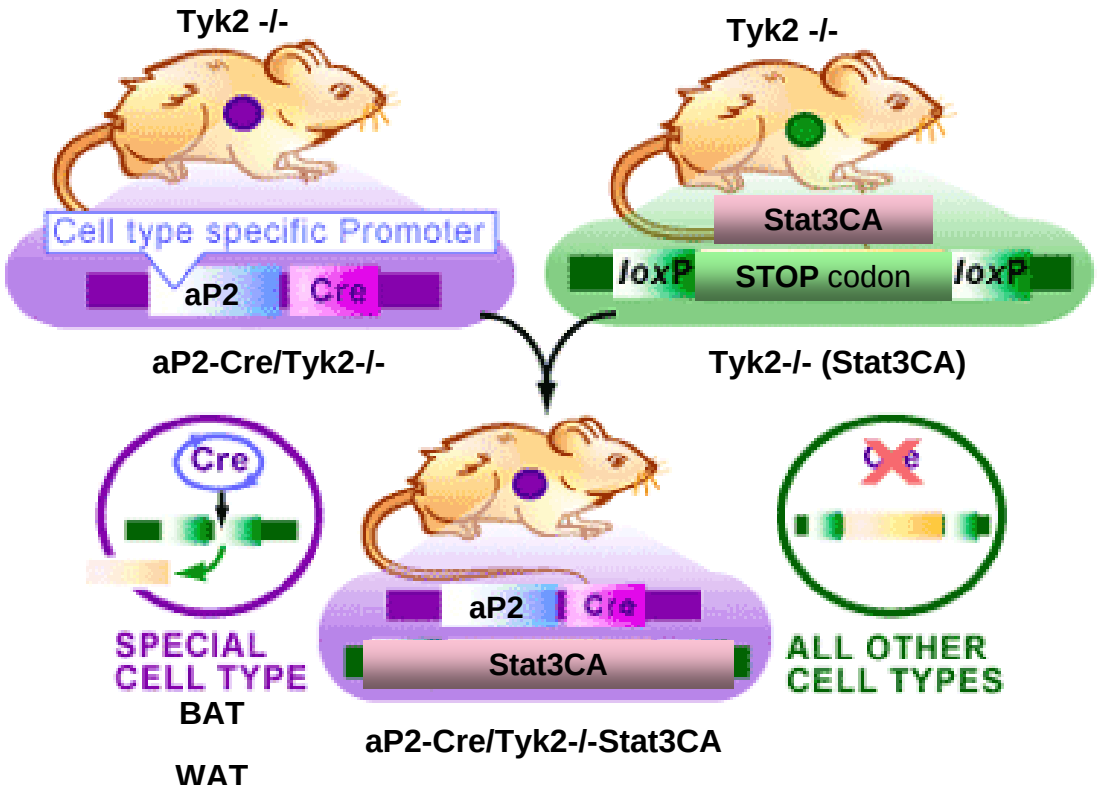

Figure 2.1 Generation of Tyk2 -/- mice with fat tissue- specific Stat3CA expression.

2.2 Isolation of DNA and genotyping

Modified HotSHOT genomic DNA isolation protocol was used for genotyping (251). In brief, tail snips were incubated in 75 µl of alkaline lysis buffer (25 mM NaOH/0.2 mM EDTA) at 95 ^{o}C for 45 min. After chilling the samples on ice, 75 µl of neutralization buffer (40 mM Tris-HCl) was added to the tubes followed by vortexing and centrifugation at 16,000 x g for 5 min at RT. 100 µl of the sample containing approximately 100 ng/µl of DNA was then transferred to the new tube and stored at -20 ^{o}C. Alleles of interest were detected by PCR using the appropriate primers listed below. PCR genotyping reaction contained 2 µl of DNA sample (about 200 ng), 1 µl 5 µM forward primer, 1 µl 5µM reverse primer, 12.5 µl of 2x GoTaq Hot Start Green Master Mix (Promega, Madison, WI) including 400 µM of each dNTP's, 4 mM $MgCl_2$ and GoTaq Hot Start Polymerase (final volume of the reaction- 25 µl). Amplification of wild type Tyk2 allele and neomycin cassette was performed using the following conditions:

stage 1: 95 ^{o}C/ 4 min/ 1 cycle; stage 2: 95 ^{o}C/ 45 sec/ 60 ^{o}C/ 45 sec/ 72 ^{o}C/ 1 min/ 35 cycles; stage 3: 72 ^{o}C/ 5 min/ 1 cycle. PCR products were resolved in 1% agarose/TBE gel supplemented with EtBr (ethidium bromide) to visualize the 800 bp specific bands under UV light. Amplification of constitutively active Stat3 (Stat3CA) allele and Cre recombinase transgene was performed using the following conditions: stage 1: 95 ^{o}C/ 3 min/ 1 cycle; stage 2: 95 ^{o}C/ 30 sec/ 55 ^{o}C/ 30 sec/ 73 ^{o}C/ 30 sec/ 35 cycles; stage 3: 73 ^{o}C/ 5 min/ 1 cycle. PCR products were resolved in 1% agarose/TBE gel with EtBr to visualize the 350 bp specific bands under UV light.

Gene	Primer sequence
Tyk2	(F) 5'- TGGACAAAATGGAGTGAGTGTAAG -3' (R) 5'- CTGGGTCATGGCTGGAAAAGCCCA -3'
Neo	(F) 5'- GATCGGCCATTGAACAAGATG -3' (R) 5'- CGCCAAGTCCTTCAGCAATAT -3'
Stat3CA	(F) 5'- GGATTGTACCTGCATCCTGGTG -3' (R) 5'- GCCCTTGTCATCGTCGTCCTTG -3'
Cre	(F) 5'- CCAGCTAAACATGCTTCATCGTCGTC -3' (R) 5'- ATTCTCCCACCGTCAGTACGTGAG -3'

Table 2.1 PCR primer sequences used for genotyping.

2.3 Dietary studies

Five-week-old mice were household four or five per cage and maintained on a fixed 12 hours light/dark cycle. The animals were fed regular chow diet (Teklad F6 S664, Harlan Tekland, Madison, WT) or high-fat diet (D12330, Research Diets, New Brunswick, NJ). The chow diet contained 27% kcal protein, 17% kcal fat and 57% kcal carbohydrate. The high-fat diet contained 20% kcal protein, 60% kcal fat and 20% kcal carbohydrate. The mice were kept on the diets for 12 weeks. They had free access to water and food. Food intake was measured weekly as grams of consumed food per kilogram body weight over a 24 h period.

2.4 Glucose tolerance test (GTT)

Mice were fasted overnight (16 h) and than 2 mg/g glucose was injected intraperitoneally. Blood glucose levels were measured using One-Touch Ultra glucose meter (LifeScan, Milpitas, CA) at 0, 15, 30, 60 and 120 min after glucose administration.

2.5 Metabolic cage studies

Metabolic cage studies of 2 month- old Tyk2 WT and Tyk2 -/- mice on C57Bl/6 background were performed by Dr. Susanna Keller from the Department of Cell Biology, University of Virginia, Charlottesville, USA. Analysis was performed using Comprehensive Laboratory Animals Monitoring System (CLAMS) from Colombus Instruments. Mice were housed individually and monitored in metabolic cages for 72 h (acclimation run), with ad libitum feeding. Animals were then given about 10 days to recover before second run and data analysis. The respiratory exchange ratio (RER) is the ratio between the carbon dioxide production and oxygen consumption measured by the CLAMS equipment. Higher RER indicates burning of more carbohydrates for energy production (or less fat). Heat production is calculated as calorific value based on the observed RER and oxygen consumption.

2.6 Insulin and leptin measurements

Mice were fed chow diet for 6 months and then fasted overnight. Blood samples were taken from the tail vein and centrifuged at 16,000 x g for 5 min at RT. Plasma was assayed for insulin using a Ultra sensitive mouse insulin ELISA kit (Crystal Chem Inc, Downers Grove, IL), and leptin using a Mouse Leptin ELISA Kit (Crystal Chem Inc, Downers Grove, IL).

2.7 Brown adipose tissue histology

Brown adipose tissues from overnight fasted mice were fixed in 10% formalin (Sigma, St. Louis, MO) at 4 ^{o}C. The tissues were stained with hematoxylin and eosin at the Pathology Research Service Facility (VCU Medical Center, Richmond, VA).

2.8 Electron microscopy

Skeletal muscle, heart and brown adipose tissues from fasted mice were fixed in 2% paraformaldehyde- 2% glutaraldehyde in 0.1 M cacodylate buffer. The tissue samples were processed and analyzed at the Microscopy Core Facility at the Department of Anatomy and Neurobiology (VCU Medical Center, Richmond, VA).

2.9 Reagents and antibodies

All chemical and reagents were purchased from Sigma-Aldrich, Saint Louis, MO, or indicated otherwise. Mouse monoclonal anti- Stat3 and phospho- Stat3 (Tyr 705), rabbit polyclonal anti- C/EBPβ and phospho- C/EBPβ (Thr 188), as well as rabbit polyclonal phospho- Stat1 (Tyr 701) and PPAR- gamma specific antibodies were purchased form Cell Signaling, Danvers, MA, and were used at a final dilution of 1:1000. Mouse monoclonal alpha- tubulin antibodies were purchased from Sigma- Aldrich and used at a final 1:10,000 dilution. Rabbit polyclonal anti- UCP-1 antibodies were purchased from Abcam, Cambridge, MA and were used at a final dilution of 1:5,000. Rabbit Tyk2 antisera was a kind gift of Dr. Birgit Strobl from the Department for Biomedical Sciences, University of Veterinary Medicine, Vienna, Austria. PRDM16 specific rabbit polyclonal antibodies were a kind gift of Dr. Patrick Seale from the Department of Cell and Developmental Biology, University of Pennsylvania, School of Medicine, Philadelphia, USA. Recombinant murine IFNβ was kindly provided by Dr. Darren Baker from Biogen Idec Inc, Cambridge, MA, USA. Cells were stimulated with 1000 U/ml of murine interferon in complete medium.

2.10 Cell isolation and culture

Brown preadipocytes were isolated as described by Fasshauer, Khan et al.(70, 71). Briefly, interscapular brown adipose tissue was isolated from newborn Tyk2 WT and Tyk2 -/- mice (SV129 background), minced and subjected to collagenase A digestion (1.5 mg/ml in isolation buffer containing 123 mM NaCl, 5 mM KCl, 1.3 mM $CaCl_2$, 5 mM glucose, 100 mM HEPES and 4% BSA) for 40 min at 37 °C. The digested tissue was filtered through 100 μm nylon screen (Labcor Products, Inc., Gaithersburg, MD). Collected cells were centrifuged at 200 x g at RT for 5 min and then resuspended in 1 ml

of primary culture medium (Dulbecco's modified Eagle medium, 450 mg/dl glucose (DMEM, Gibco, Carlsbad, CA) containing 20% FBS, 20 mM HEPES and 1% Penicillin-Streptomycin), transferred into 12 well plates and grown in humidified atmosphere of 5% CO_2 and 95% O_2 at 37 °C. The medium was changed every day. After 3 days of culture, cells were immortalized by infection with puromycin resistance retroviral vector pBabe encoding SV40 Large T antigen. 24 h after infection cells were transferred into 10 cm dishes and maintained in primary culture media for next 24 h and then subjected to selection with puromycin (Sigma, St. Louis, MO) at the concentration of 2 μg/ml in DMEM with 20% FBS for one week. After puromycin selection cells were maintained in medium directed against mycoplasma infection (BM Cyclin, Boehringer Mannheim) for 3 weeks.

For differentiation, brown preadipocytes were grown to 100% confluence in the differentiation medium: DMEM containing 450 mg/ml glucose, 10% FBS, 20 nM insulin and 1 nM triiodothyronine. Fully confluent cells were incubated for 48 h in the differentiation medium supplemented with 0.5 mM isobutylmethylxanthine (IMBX), 0.5 μM dexamethasone and 0.125 mM indomethacin (induction medium). After 48 h of induction, cells were maintained in differentiation medium for 5 days until exhibiting massive accumulation of multilocular fat droplets.

2.11 Transfection and infection

293T cells, used as packaging cells, were grown in complete DMEM medium containing 10% FBS and 1% penicillin-streptomycin. Cells were transfected in 10 cm dishes using Fugene reagent (Roche Diagnostics, Indianapolis, IN) according to the manufacturer's instructions. Briefly, 500 μl serum-free media was incubated for 15 min at RT with 15 μl of Fugene reagent, 5 μg of helper vector and 5 μg of empty vector (MSCV-IRES-GFP) or MSCV- based vectors encoding wild type Tyk2 (Tyk2WT), kinase dead Tyk2 (Tyk2KD), constitutively active Stat3 (Stat3CA). The transfection mix was added to 50-60% confluent 293T cells. The virus-containing medium was collected 48 h after transfection, centrifuged for 10 min at 500 x g and filtered through 0.45 μm filter. Filtered medium was incubated with 8 μg/ml polybrene (Chemicon Int., Temecula,CA) for 10 min at RT and then added to the preadipocytes to be infected. Cells were incubated

with the virus for 24 h, after which the medium was replaced. 7 days following infection, entire GFP-positive cell population was sorted by FACS to 100% purity and culture further for the experiments. Retrovirus containing SV40 Large T antigen was created according to the described protocol.

Adenoviral vector for PRDM16 expression (pAdTrack-CMV-PRDM16-GFP) was a kind gift of Dr. Patrick Seale from the Department of Cell and Developmental Biology, University of Pennsylvania, School of Medicine, Philadelphia, USA. Adenoviruses were produced by Virus Vector Shared Resource Facility at VCU Massey Cancer Center, Richmond, VA. Brown preadipocytes were grown to 100% confluence and than incubated with PRDM16-GFP-expressing adenovirus or GFP-expressing control adenovirus (moi = 500) for 6 h in DMEM with 10% FBS. The medium was then replaced and the cells were induced to differentiate. GFP expressed from the adenoviral vectors was used to monitor infection efficiency, which was typically over 70%.

Lentiviral vector expressing shRNA targeting Stat3 or non- target control shRNA (pFLRu-shtat3-YFP) and helper vectors (CMV-VSV-G encoding viral envelope proteins and packaging pHR'8.2 deltaR plasmid) were a kind gift of Dr Barry Sleckman from the Department of Pathology and Immunology, Washington University, School of Medicine, ST. Louis, USA. Lentiviruses were prepared in accordance with the protocol for MSCV-based retroviruses described above.

2.12 Oil Red O staining

Oil Red O staining protocol was used to test for lipid accumulation in fully differentiated cells. Briefly, all plates with cells were rinsed once with PBS and then fixed with buffered formalin for 1 h at RT. Fresh Oil Red O working solution was prepared by adding 6 ml of the stock solution (0.5 g Oil Red O in 100 ml of 2-propanol) to 4 ml of dH_2O, mixed and filtered through Whatman filter paper. Following fixation the cells were incubated for 1h at RT with Oil Red O stain. Then plates were carefully rinsed several times with dH_2O and air- dried to collect images.

2.13 Isolation of total RNA and cDNA synthesis

To prepare RNA, cells were washed with PBS and lysed directly in a 6-well plate with 1 ml of TRI Reagent (Molecular Research, Cincinnati, OH). Lysates were transferred to 1.5 ml tubes, 200 µl of chloroform was added and tubes were vortexed thoroughly and centrifuged at 12,000 x g for 15 min at 4 °C. The upper aqueous phase was transferred to a fresh tubes and RNA was precipitated for 15 min at RT with 500 µl of 100% 2-propanol. The samples were centrifuged at 12,000 x g for 25 min at 4 °C. The pellets were washed once with ice-cold 75% ethanol, air-dried and resuspended with DEPC-treated water. Isolated RNA samples were treated with DNase (Promega, Madison, WI) for 30 min at 37 °C, followed by adding a STOP solution and 10 min incubation at 65 °C. The concentration and purity of RNA samples was determined spectrophotometricaly by measuring absorbance at 260 nm and the 260 nm/280 nm absorbance ratio. RNA from tissue snips was prepared using the above protocol. Excised tissues were minced and immersed in 1 ml of TRI Reagent followed by incubation with shaking for 1 h at 4 °C. Further isolation was proceeded as described.

2 µg of total RNA from respective samples was reverse transcribed using the Tetro cDNA Synthesis Kit (Bioline, Taunton, MA). In brief, RNA sample was mixed with 1 µl of random hexamers, 1 µl of 10 mM dNTP's and DEPC-treated water in the final volume of 10 µl and then incubated for 1 min at 95 °C. The reaction mixture was chilled down on ice and combined with 10 µl of cDNA synthesis mix containing: 4 µl of 5x RT buffer, 1 µl of RNase inhibitor, 50 units of reverse transcriptase and DEPC-treated water. Samples were incubated for 50 min at 42 °C (cDNA synthesis step) followed by 15 min at 70 °C (termination step). RNA in newly synthesized cDNA samples was eliminated by the incubation of the reaction mixture with 1 µl of RNase H (Invitrogen, Carlsbad, CA) for 30 min at 37 °C.

2.14 Quantitative PCR

The mRNA levels of gene of interest were analyzed by real-time PCR using SensiMix SYBR and Fluorescein Kit (Bioline, Taunton, MA) according to manufacturer's instruction. The reaction mixtures were prepared as follows: for

measuring 18S rRNA (internal control)- 12.5 µl of SYBR and Fluorescein mix, 1 µl of 5 µM forward primer, 1 µl of 5 µM reverse primer, 1 µl of cDNA (final concentration 5 ng/µl), 9.5 µl of H_2O (total volume 25 µl); for measuring of mRNA level of any other gene- 12.5 µl of SYBR and Fluorescein mix, 2.5 µl of 5 µM forward primer, 2.5 µl of 5 µM reverse primer, 5 µl of cDNA (final concentration 5 ng/µl), 2.5 µl of H_2O (total volume 25 µl). All the samples were assayed in duplicates and analyzed using CFX96 Real- Time PCR Detection System (Bio-Rad, Hercules, CA) using the following amplification conditions: 1 cycle of 95 °C for 10 min, 40 cycles of 95 °C for 15 sec and 60 °C for 1 min. The results were analyzed according to ΔCt method using a reference gene (variation of Livak method). Briefly, to calculate relative expression, the gene of interest (target) expression was first normalized to a reference gene (18S rRNA): expression = $2^{[Ct(18S\ rRNA)-Ct(target)]}$. This applied to each sample of all experimental groups of cells or mice. The results obtained for wild-type cells or mice (calibrators) were set as 1 (ratio = $2^{[Ct(18S\ rRNA)-Ct(target)]}$ of calibrator/mean of calibrators' $2^{[Ct(18S\ rRNA)-Ct(target)]}$'s). The differences in expression of target genes in cells or mice were calculated as ratios of particular sample's $2^{[Ct(18S\ rRNA)-Ct(target)]}$ to the mean of calibrators' $2^{[Ct(18S\ rRNA)-Ct(target)]}$'s.

Gene	Primer sequence
PRDM16	(F) 5'- CAGCACGGTGAAGCCATTC -3' (R) 5'- GCGTGCATCCGCTTGTG -3'
UCP1	(F) 5'- CTGGGCTTAACGGGTCCTC -3' (R) 5'- CTGGGCTAGGTAGTGCCAGTG -3'
Cidea	(F) 5'- TGCTCTTCTGTATCGCCCAGT -3' (R) 5'- GCCGTGTTAAGGAATCTGCTG -3'
Elovl3	(F) 5'- TCCGCGTTCTCATGTAGGTCT -3' (R) 5'- GGACCTGATGCAACCCTATGA -3'
Cox8b	(F) 5'- GAACCATGAAGCCAACGACT -3' (R) 5'- GCGAAGTTCACAGTGGTTCC -3'
CS	(F) 5'- TTTGGCTGCTGGTAACTGG -3' (R) 5'- ATGGTGACCACATGAGAAGGCAG -3'

PGC1α	(F) 5'- CCCTGCCATTGTTAAGACC -3' (R) 5'- TGCTGCTGTTCCTGTTTTC -3'
PPARα	(F) 5'- GCGTACGGCAATGGCTTTAT -3' (R) 5'- GAACGGCTTCCTCAGGTTCTT -3'
PPARγ	(F) 5'- GTGCCAGTTTCGATCCGTAGA -3' (R) 5'- GGCCAGCATCGTGTAGATGA -3'
C/EBPα	(F) 5'- GATAAAGCCAAACAACGCAAC -3' (R) 5'- CTAGAGATCCAGCGACCCGA -3'
C/EBPβ	(F) 5'- AAGAGCCGCGACAAGGC -3' (R) 5'- GTCAGCTCCAGCACCTTGTG -3'
aP2	(F) 5'- ACACCGAGATTTCCTTCAAACTG -3' (R) 5'- ACACCGAGATTTCCTTCAAACTG -3'
MCK	(F) 5'- GCAAGCACCCCAAGTTTGA -3' (R) 5'- ACCTGTGCCGCGCTTCT -3'
Myg	(F) 5'- AGCGCAGGCTCAAGAAAGTGAATG -3' (R) 5'CTGTAGGCGCTCAATGTACTGGAT -3'
MyoD	(F) 5'- CGCCACTCCGGGACATAG -3' (R) 5'- GAAGTCGTCTGCTGTCTCAAAGG -3'
18S rRNA	(F) 5'- CCATCCAATCGGTAGTAGCG -3' (R) 5'- GTAACCCGTTGAACCCCATT -3'

Table 2.2 Real- time quantitative PCR primer sequences.

2.15 Preparation of whole cell extracts

Cells were harvested by centrifugation at 500 x g for 5 min at 4 °C, rinsed once with ice- cold PBS. Cell pellets were lysed in cold whole extraction buffer (20 mM HEPES, 300 mM NaCl, 10 mM KCl, 1 mM $MgCl_2$**,** 20% glycerol, 1% Triton X-100) with added protease and phosphatase inhibitor cocktails (Roche, Indianapolis, IN) for 30 min at 4 °C. Cell debris was removed from the lysates by centrifugation at 20,000 x g for

20 min at 4 °C. The protein concentration in the supernatants was determined using Bio-Rad protein assay (Bio-Rad, Hercules, CA).

2.16 Western blot analysis

Equal amounts of protein were mixed 1:1 with 2X Laemmli Sample Buffer (Bio-Rad, Hercules, CA) containing 1 mM β-mercaptoethanol and incubated at 95 °C for 5 min. Protein were separated using SDS-PAGE electrophoresis with appropriated acrylamide percentage of resolving gel (depending on the molecular size of the protein of intrest) in 1X Laemmli Running Buffer. After separation, gels were transferred to Immobilon-P PVDF (polyvinyldifluoridine) membrane (Milipore) using a Bio-Rad semi-dry transfer apparatus. The blots were then incubated for 1 h at RT with 5% non fat dry milk (Bio-Rad) in TBS-Tween20 buffer (10 mM Tris, pH 7.5, 150 mM NaCl, and 0.1% Tween20) and then incubated overnight at 4 ^{o}C with the indicated primary antibodies prepared in 5% BSA in TBS-Tween buffer. Following primary antibodies incubation, the blots were washed 3 times each for 15 min with TBS-Tween buffer and then incubated for 1h with a 1:10,000 dilution of anti-mouse or anti-rabbit IgG $F(ab)_2$ fragments conjugated with HRP (horse radish peroxidase) in 5% non fat dry milk in TBS-Tween buffer. Blots were then washed 3 times 15 min with TBS-Tween and developed using Amersham ECL Plus Western Blotting Detection Reagents (GE Healthcare Life Sciences, Piscataway, NJ).

2.17 Bisulfite sequencing

1.5 ug of genomic DNA was converted using EZ DNA methylation kit (Zymo Research, Orange, CA) according to the supplier's instructions. The treated DNA was amplified by PCR using the bisulfite- specific primers listed in the Table 2.3. The amplification conditions for the 830 bp (Cidea promoter) and 730 bp (UCP1 promoter) DNA fragments were as follow: stage 1: 95 ^{o}C/ 3 min/ 1 cycle; stage 2: 95 ^{o}C/ 1 min/ 55 ^{o}C/ 1 min/ 73 ^{o}C/ 1 min/ 40 cycles; stage 3: 73 ^{o}C/ 5 min/ 1 cycle. PCR products were cloned into pCR2.1- TOPO vector (Invitrogen, Carlsbad, CA), and 8-15 clones were picked out and sequenced for each sample.

Promoter	Primer sequence
Cidea	(F) 5'- GTTTAGTTATTAATGGGTGGTACTATT -3' (R) 5'- AAAACACTCCACTAAACACCTATAAC -3'
UCP1	(F) 5'- GAAAGGGATATTTAGAATTGAAAGGAG -3' (R) 5'- CTACCAACAAACTAAAACTCCGAC -3'

Table. 2.3 Bisulfite- specific primers sequences.

2.18 Statistical analysis

Results are presented as the mean ± SE. Statistical comparison was performed using two-tailed Student's t-test. While interpreting the data results, a p value less than 0.05 was considered as statistically significant and annotated by *.

CHAPTER III

RESULTS

3.1 Tyk2 deficient mice develop spontaneous obesity and metabolic syndrome

Results obtained previously in our laboratory showed that Tyk2- knockout mice on the SV129 background become spontaneously obese and develop many symptoms of the metabolic syndrome (94). Mice lacking Tyk2 presented also impaired glucose tolerance and insulin resistance, which are the major factors in the pathogenesis of type 2 diabetes. Also, the changes in the expression of many genes involved in the regulation of glucose and fat metabolism, increased leptin level along with altered expression of the neuropeptides in hypothalamus, contribute to the development of the metabolic syndrome (155). Due to the genetic differences in the susceptibility for obesity between mouse strains, we examined the obese phenotype in Tyk2 deficient animals using two, phenotypically opposite, congenic strains of mice. Mice on a C57Bl/6 background are described in the literature as an obesity- prone strain, whereas BALB/c are resistant to diet- induced obesity (72, 82, 249). At the age of 4 months, Tyk2 -/- on C57Bl/6 background were significantly heavier than wild type animals, when fed a regular chow diet, as well as on a high fat, high sucrose diet (Fig 3.1A).Tyk2- null mice bred into BALB/c strain showed increased body weigh only, when challenged with the high fat diet (Fig 3.1B). However, both strains of Tyk2 -/- mice displayed abnormal glucose tolerance, when fed the regular chow diet. As depicted in Fig 3.2, glucose levels were higher in the blood of Tyk2- knockout mice in comparison to the control mice. Although C57Bl/6 Tyk2 -/- mice had slightly increased food intake on the chow diet, none of the knockout strains appeared to be hyperphagic. Moreover, Tyk2- null mice consumed the same amount of food as wild type mice on the high fat diet, where obese phenotype was accelerated. These results suggest that Tyk2 -/- animals have reduced energy expenditure.

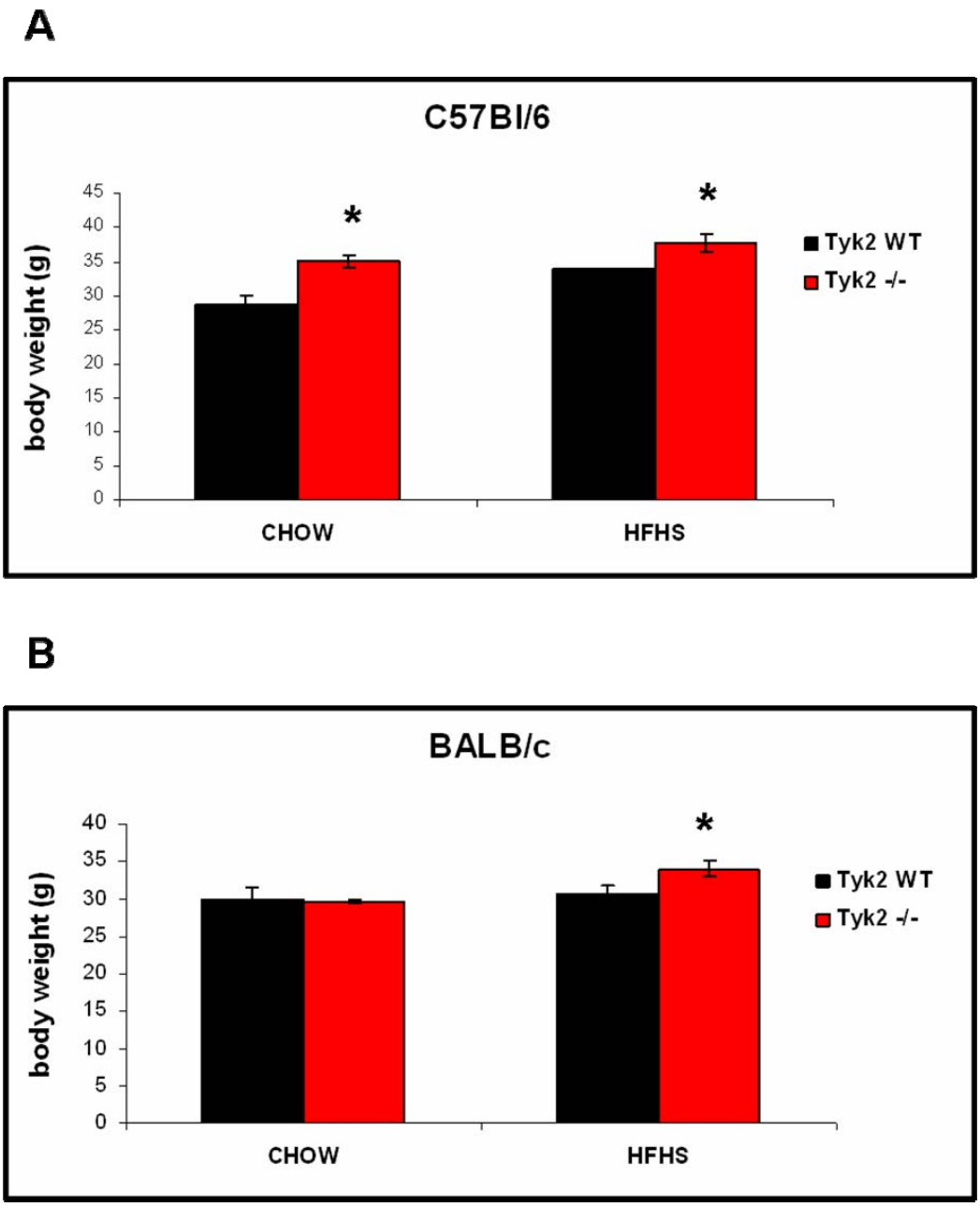

Figure 3.1. Tyk2 deficient mice develop spontaneous obesity. Tyk2 -/- and wild type male mice were fed a regular chow diet or high fat diet for 12 weeks. **(A)** body weight of 4- month old mice on a C57Bl/6 background**. (B)** body weight of 4- month old BALB/c mouse strain. Data are presented as the mean ± SE for n = 5 - 8 mice per group, *$p < 0.05$.

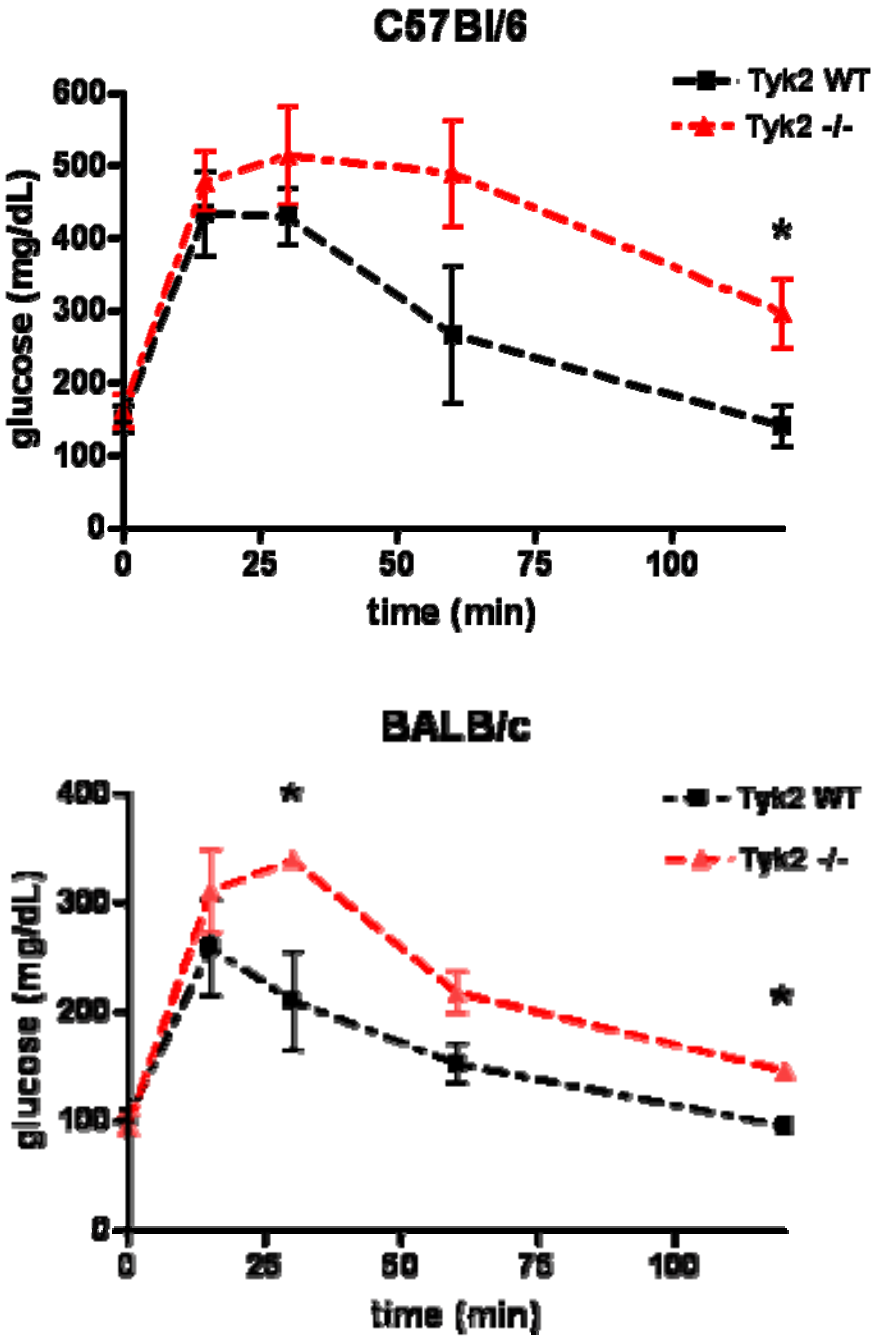

Figure 3.2. Tyk2 -/- mice display abnormal glucose tolerance. Fasting blood glucose levels during glucose tolerance test (GTT) performed on 4- month old C57Bl/6 and BALB/c male mice fed a normal chow diet. Mice were fasted for 16 h. Data are presented as the mean ± SE for n = 5 - 8 mice per group, *$p < 0.05$.

A

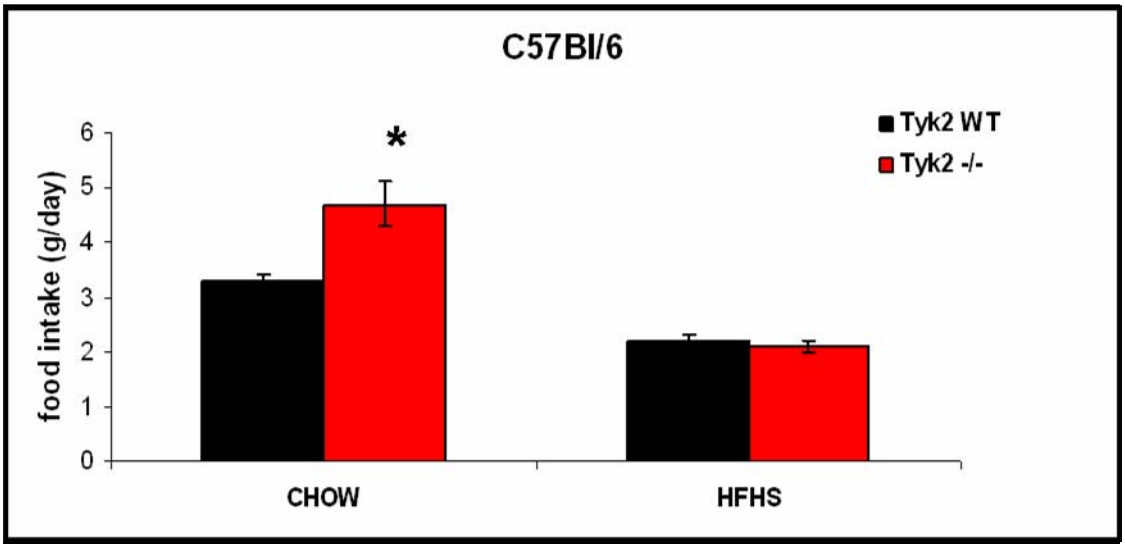

B

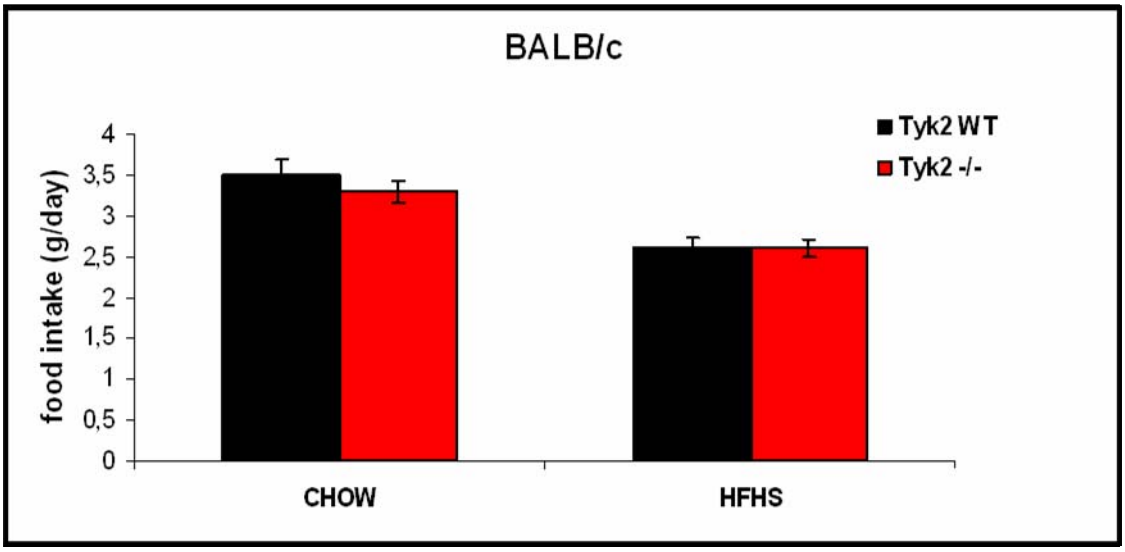

Figure 3.3. Tyk2 deficient mice do not show hyperphagia. Amount of food recorded weekly during 12 weeks of diet study. **(A)** food intake of 4- month old males, C57Bl/6 strain. **(B)** food intake of 4- month old males, BALB/c strain. Values are the mean ± SE for n = 5 - 8 mice per group, *p < 0.05.

3.2 Defective brown adipose tissue (BAT) differentiation in Tyk2 -/- mice

Lack of the larger changes in the food intake with increasing with age body weight, suggest that there is decreased energy expenditure in Tyk2 knockout mice. Therefore, we decided to verify gene expression pattern in BAT, which is one of the major tissues responsible for energy expenditure. Total RNA was isolated from intrascapular BAT depots of wild type and Tyk2 -/- mice and gene expression was analyzed by real-time qPCR (Fig 3.4A and B). Our results showed that brown fat–specific RNA levels (UCP1, PRDM16 and Cidea) are down regulated in both strains of Tyk2 deficient animals. Moreover, the expression of PPARα, the nuclear receptor responsible for transcription of β-oxidation enzymes, was also decreased. We did not observe any significant changes in RNA encoding common adipogenic factors (PPARγ, PGC1α). These data suggest incorrect differentiation of brown adipose tissue and reduced thermogenesis in Tyk2 -/- mice, which may contribute to development of the obese phenotype.

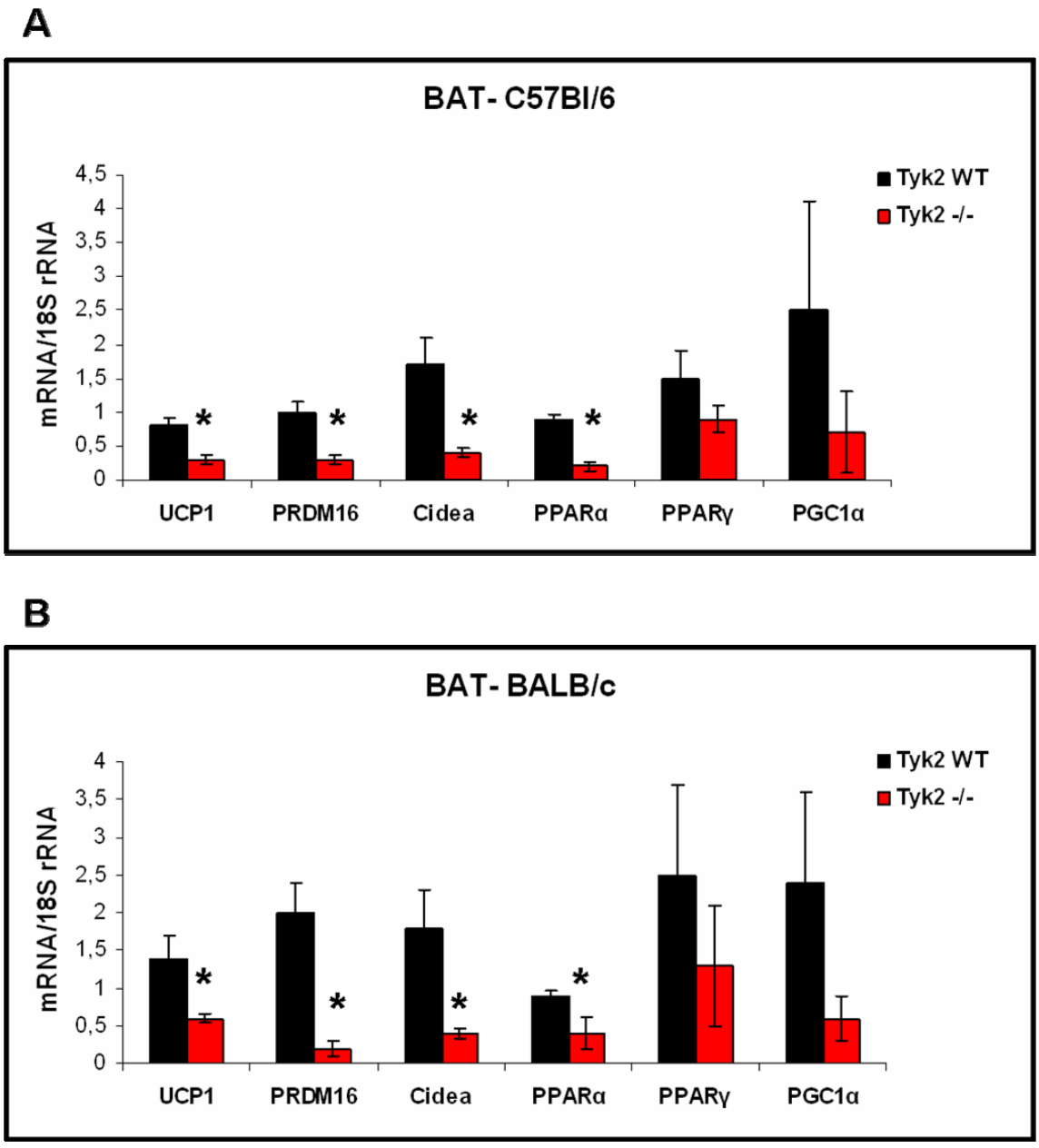

Figure 3.4. Decreased gene expression in BAT from Tyk2 knockout mice. Total RNA was isolated from intrascapular BAT of 3- month old 16 h fasted **(A)** C57Bl/6, **(B)** BALB/c Tyk2 WT and Tyk2 -/- male mice. The expression level of brown fat- specific (UCP1, PRDM16, Cidea) and common adipogenic (PPARα, PPARγ, PGC1α) mRNAs were measured by real-time qPCR. The values represent mean fold decrease ± SE for n = 5 - 8 mice per group, *$p < 0.05$.

3.3 Altered BAT morphology in Tyk2- null mice

Histology performed on the brown adipose tissue revealed big differences in lipid accumulation in Tyk2 -/- mice. Large cells with unilocular fat droplets were observed in Tyk2- null BAT. These cells resemble white adipocytes, instead of the typical small brown fat cells with multiloculat lipid droplets, which are present in wild type mice (Fig 3.5). Altered BAT morphology in Tyk2 deficient mice is likely a consequence of down regulated gene expression observed in Fig 3.4. Due to reduced RNA levels of PPARα, as well as AOX and LCAD (94), Tyk2 -/- mice exhibit insufficient oxidation of fatty acid- a main energy source for adaptive thermogenesis in BAT. The problems with burning the fatty acids were confirmed by the metabolic cages analysis, which showed that respiratory exchange rate (RER) was significantly higher in Tyk2- null mice (0.7) than in wild type mice (0.58).

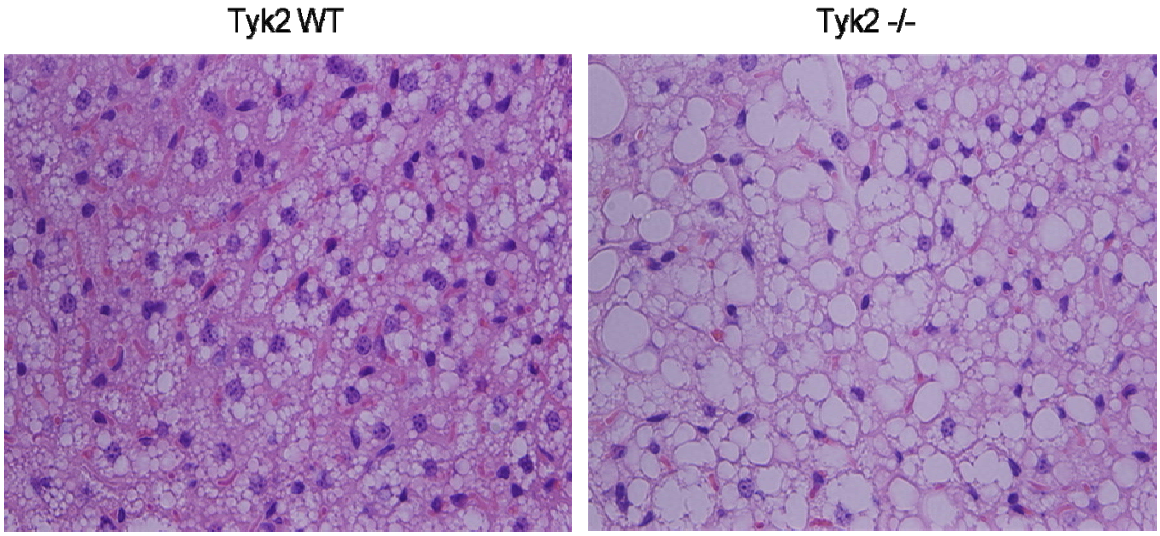

Figure 3.5 Histological analysis of interscapular brown adipose tissue of 3- month old Tyk2 WT and Tyk2 -/- mice. Representative hematoxylin-eosin staining. C57Bl/6 male mice, n = 4 mice per group.

3.4 Tyk2 knockout mice have defective response for acute cold exposure

The primary role of brown adipose tissue is dissipating energy directly as heat, in process described as non-shivering or diet-induced thermogenesis (68). Heat is produced by uncoupling fatty acid oxidation from ATP production by the protein UCP1 regulated by PGC1α. Changes in BAT morphology suggest defective function of this tissue in Tyk2 -/- mice. Since the basal expression level of UCP1 in Tyk2-null BAT is severely decreased, we examined the response of animals to the cold exposure. Wild type and Tyk2 -/- mice were kept at 4° C for 6h. Total RNA was isolated from brown fat and muscle tissue and analyzed for the expression of PGC1α, involved in thermogenic response. PGC1α is upstream regulator of UCP1 expression in BAT (30). Furthermore, it increases oxidative capacity of muscle tissue during shivering, and possible non-shivering thermogenesis, taking place in skeletal muscles in response to temperature insult (195). Real-time qPCR analysis showed a 20 fold, and a 14 fold increase in PGC1α expression in BAT and skeletal muscles of wild type mice maintained at 4° C. The same experimental conditions resulted in a less robust response in Tyk2 deficient animals (11 fold increase of PGC1α RNA in BAT, and 3 fold in skeletal muscles) (Fig 3.6). The results obtained from Tyk2 -/- samples did not reach statistical significance. Our data indicate depressed function of brown adipose tissue, as well as general disturbance of thermogenic response to acute cold exposure in Tyk2 knockout mice. Additionally, metabolic cages studies performed at room temperature revealed that Tyk2 deficient mice followed the trend to produce less heat then wild type animals, which confirm that these mice display defective thermogenesis.

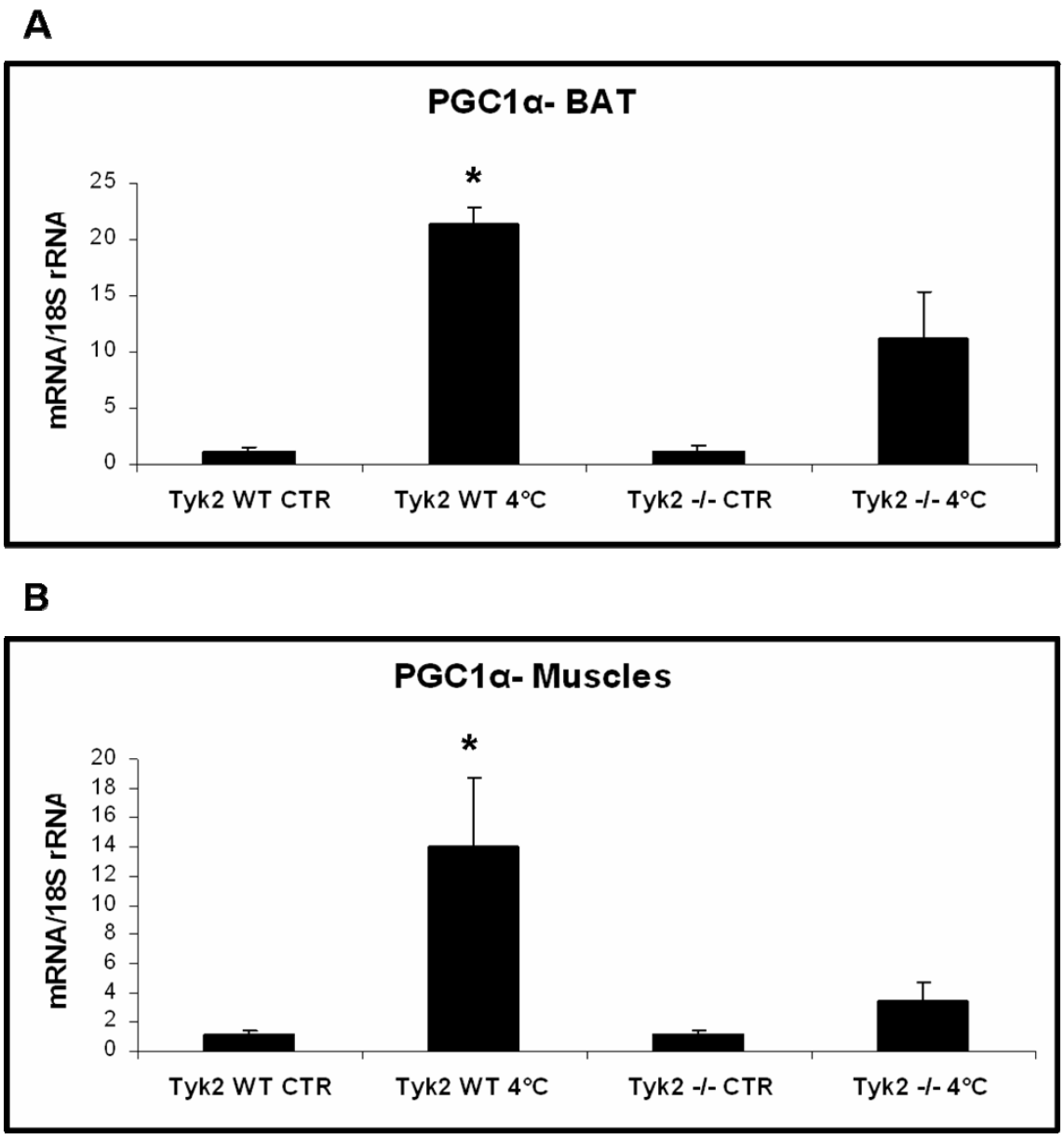

Figure 3.6 Tyk2 -/- mice exhibit reduced PGC1α expression in response to acute cold exposure. Wild type and Tyk2 -/- males on the C57Bl/6 background were maintained at 4° C for 6h. Total RNA from **(A)** BAT and **(B)** skeletal muscles was isolated and analyzed for the expression level of PGC1α using real-time qPCR. The values represent mean fold increase ± SE for n = 5 mice per group, *$p < 0.05$.

3.5 Impaired mitochondrial morphology in thermogenic tissues of Tyk2 deficient mice

Recent research findings have supported previously suggested theory, that mitochondrial dysfunction is closely associated with insulin resistance and might contribute to the progression of diabetes. Results from different laboratories showed that insufficient energy supply can cause insulin insensitivity in myocytes and adipocytes (122, 139). Because of diminished activation of the key player in mitochondrial biogenesis- PGC1α, and impaired thermogenesis, in which mitochondria play a major role, we decided to investigate possible alterations in the mitochondrion. Using electron microscopy, we examined mitochondrial morphology in different tissues of Tyk2-null mice and compare them to wild type mice. EM micrograph revealed abnormal cristae formation in mitochondria from brown adipose and skeletal muscle tissue of Tyk2 -/- mice (Fig 3.7A and B respectively). Surprisingly, we did not observe any changes in other tissues like highly oxidative heart (Fig 3.7C) or liver (data not shown). Mitochondrial function and ultrastructure depend on the proper fusion of the outer and inner membranes. The fusion processes are governed by three large GTPases: mitofusin 1 (Mfn1), mitofusin 2 (Mfn2) and optic atrophy protein 1 (OPA1). Mfn1 and Mfn2 are involved in early steps of outer membrane fusion, whereas OPA1 is associated with inner membrane fusion and cristae remodeling (37, 38). Disorganization of mitochondrial cristae observed in BAT and skeletal muscles from Tyk2 deficient mice can be a result of decreased OPA1 expression in these tissues (Fig 3.8). Reduced mRNA levels of OPA1 were not observed in the control tissues, such as WAT or liver. In contrast to OPA1, the expression levels of Mfn1 and Mfn2 were not significantly changed in any of assayed tissues (Fig 3.8). Since BAT and skeletal muscles originate from the same Myf5 positive progenitor cells (215), these results suggest that Tyk2 kinase may play important role at an early stage of development of these progenitors.

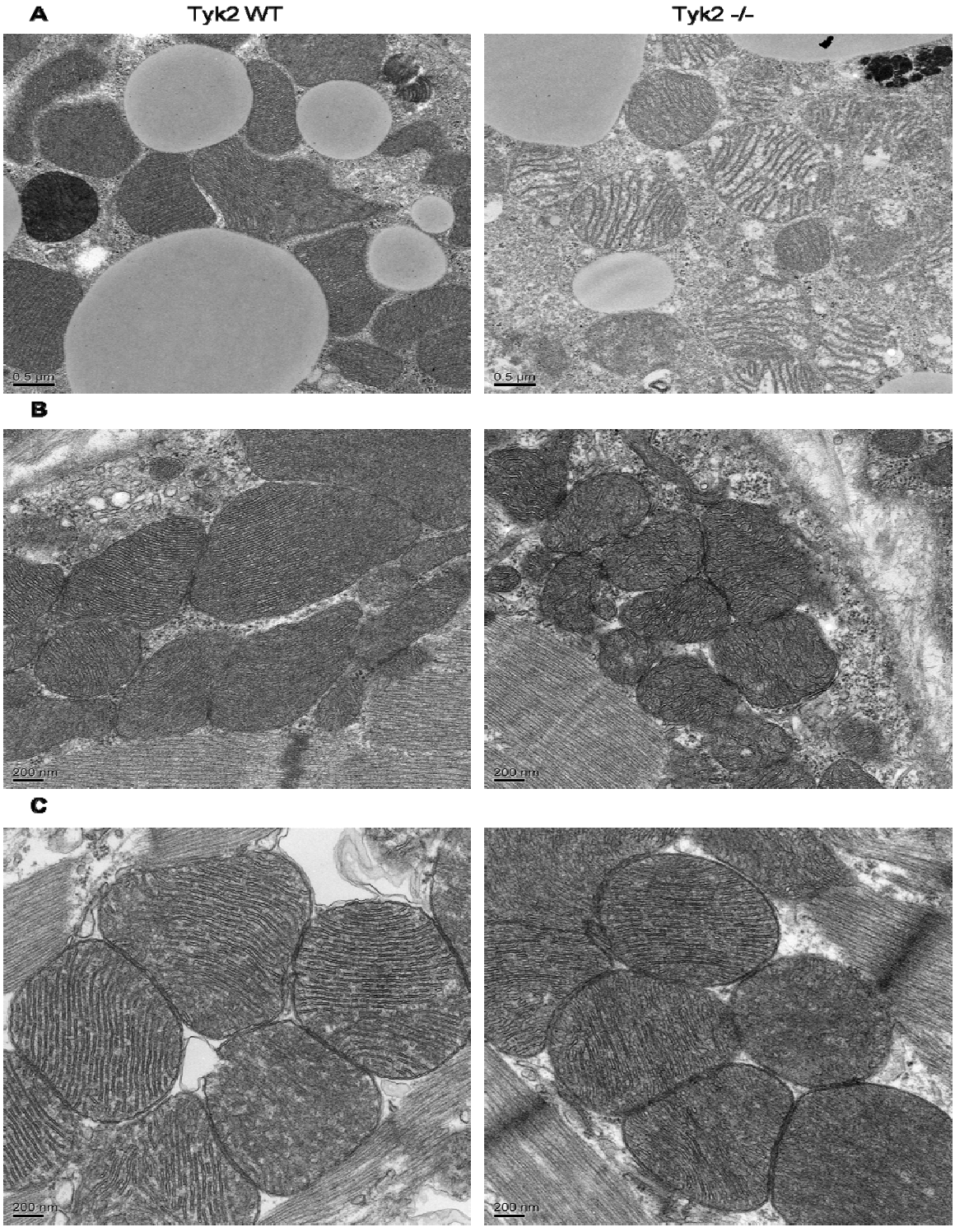

Figure 3.7 Changes in mitochondrial morphology in BAT and skeletal muscles of Tyk2 -/- mice. Representative EM micrograph from **(A)** brown adipose tissue, **(B)** skeletal muscles, **(C)** heart of wild type and Tyk2 -/- males on the C57Bl/6 background, n = 6 mice per group.

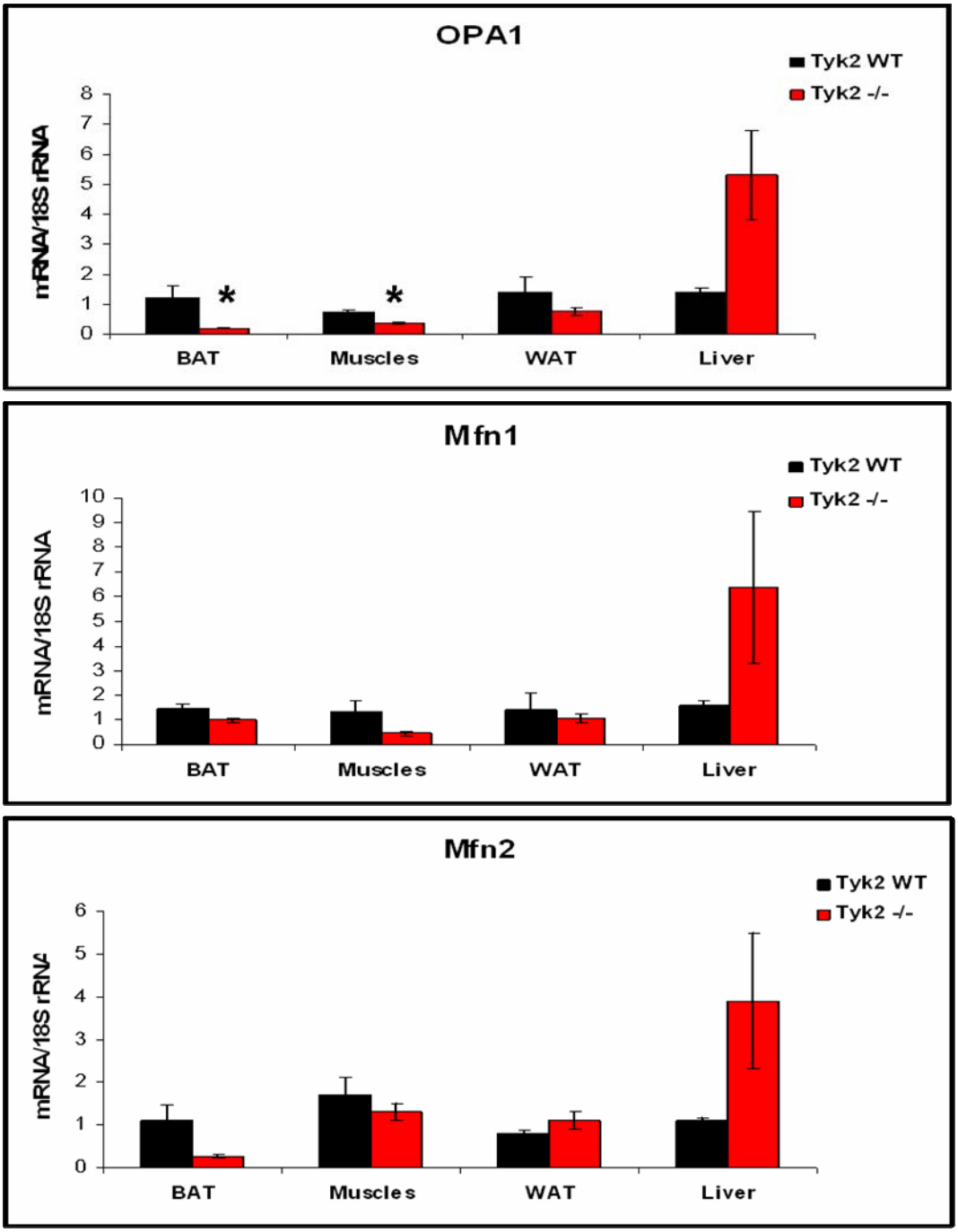

Figure 3.8 Tyk2 knockout mice show reduced expression of OPA1 in BAT and skeletal muscles. Total RNA was isolated from BAT, WAT, skeletal muscles and liver of 3- month old Tyk2 WT and Tyk2 -/- males on the C57Bl/6 background. The expression level of OPA1, Mfn1 and Mfn2 were measured by real-time qPCR. The values represent mean fold decrease ± SE for n = 6 - 8 mice per group, *$p < 0.05$.

3.6 Tyk2- null mice display decreased PGC1α expression in skeletal muscle

It is well described that insulin resistance in skeletal muscles plays an important role in pathogenesis of type 2 diabetes (267). Recently, there also is abundant evidence that insulin insensitivity may emerge as a result of reduced mitochondrial oxidative capacity, which relies on the ability of skeletal muscles to effectively switch from glucose to fatty acid oxidation (59). The transcriptional coactivator PGC1α is a key integrator of skeletal muscle fiber- type switching (194). It increases the number of type I oxidative, high endurance fibers, which contain great number of mitochondria. Microarray expression analysis performed on skeletal muscle samples from patients with insulin resistance, and type 2 diabetes showed decreased RNA levels of PGC1α, as well as genes encoding proteins of mitochondrial electron transport chain (180). Our data indicate that the expression and protein level of PGC1α in the skeletal muscles of Tyk2 -/- mice are down regulated (Fig 3.9A and B). We also assayed RNA levels for two mitochondrial proteins, citrate synthase (CS) and cytochrome c oxidase subunit VIIIb (Cox8b), which were decreased in Tyk2 -/- muscle tissue (Fig 3.9C). Obtained data indicate that there is impaired skeletal muscle fiber-type switching in Tyk2 -/- mice, which can contribute to the progression of diabetic phenotype as the Tyk2 knockout animals age. It has been also reported that Tyk2 -/- mice are relatively exercise intolerant (191), which may be a possible consequence of decreased number of oxidative fibers.

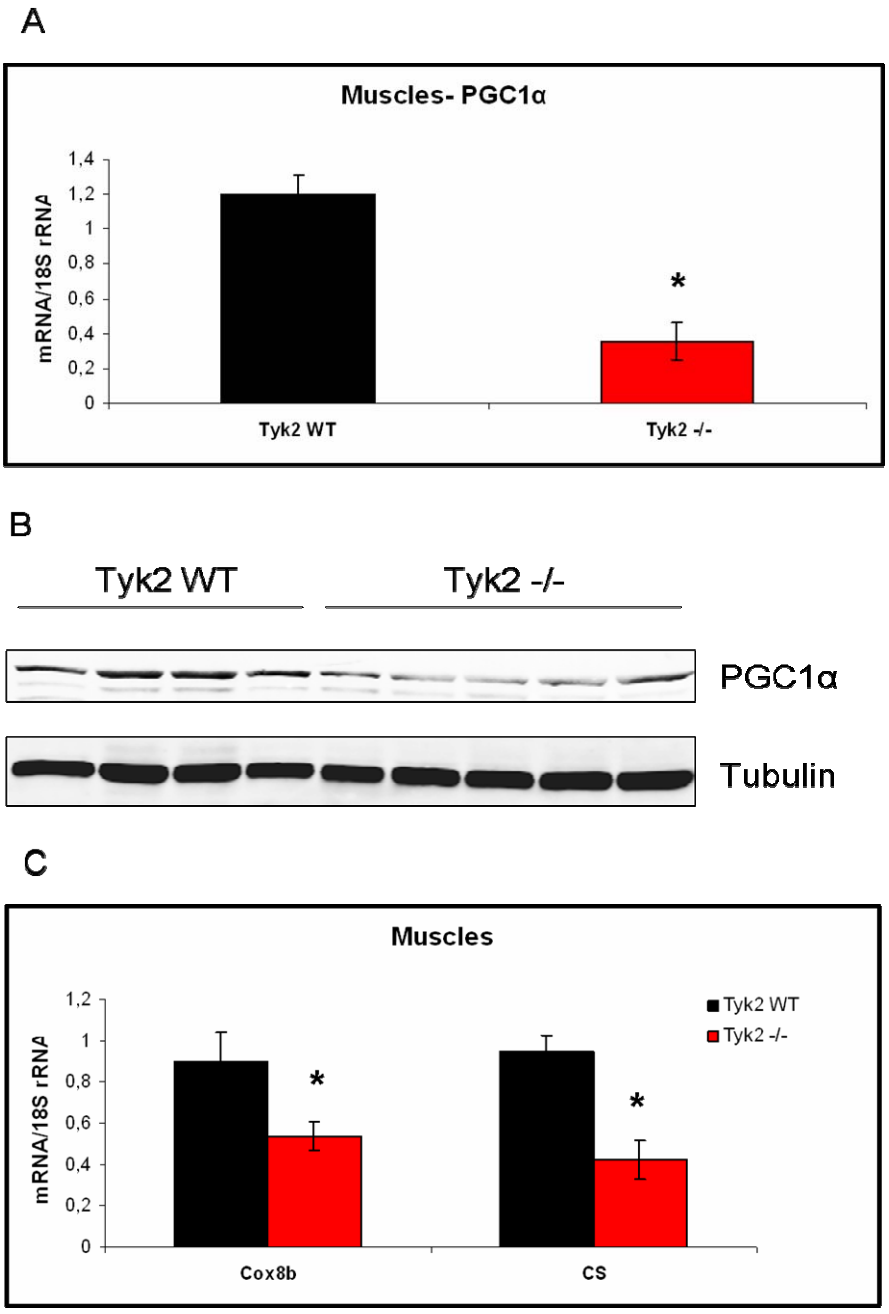

Figure 3.9 The expression of PGC1α, as well as CS and Cox8b are decreased in skeletal muscles of Tyk2 -/- mice. (A) total RNA was extracted from skeletal muscles and analyzed for PGC1α expression by real-time qPCR. **(B)** extracts were isolated from muscle samples and analyzed for PGC1α protein level by western blot. **(C)** RNA samples from skeletal muscles were subjected to real-time qPCR with primers for CS and Cox8b. The values represent mean fold increase ± SE for n = 5-9 mice per group (males on the C57Bl/6 background), *$p < 0.05$.

3.7 In vitro differentiation of immortalized Tyk2 -/- brown adipocytes is defective

The great advantage of an in vitro system in studying signaling pathways led us to create a stable brown adipocyte cell lines. Preadipocytes obtained after digestion of brown adipose tissue from neonatal wild type and Tyk2 knockout mice can be immortalized and differentiated into functional BAT cells (70, 113, 217). To examine the role of Tyk2 in BAT development, we generated also Tyk2 -/- preadipocytes expressing either wild type (Tyk2WT) or a kinase dead (Tyk2KD) version of the kinase, as well as constitutively active Stat3 (Stat3CA) and an empty control vector (MSCV). Since Tyk2 and Stat3 have been cloned into MSCV vector, cells infected with empty MSCV vector serve as the control for experiments and behave exactly like Tyk2 -/- cells (Fig 3.10A). It has been reported, that stimulation of murine Tyk2- null cells with interferon α/β results in absent tyrosine 705 phosphorylation of Stat3 but preserved phosphorylation of tyrosine 701 in Stat1 (191). In order to determine whether all created cell lines were functional, we analyzed their response to interferon beta (IFN β). According to the published data, we did not observe Stat3 phosphorylation in Tyk2 -/- preadipocytes, as well as cells reconstituted with inactive form of the kinase (Tyk2KD) or empty MSCV vector, after IFN β treatment. However, activation of Stat3 in Tyk2 -/- cells was rescued by Tyk2WT and Stat3CA, as expected. Interferon beta- induced Stat1 phosphorylation was comparable in all cell lines using the same experimental conditions (Fig 3.10B). As a next step, all preadipocyte cell lines were subjected to the in vitro differentiation protocol. In comparison to almost 100% efficient differentiation in wild type cells, only 5-10% of Tyk2 -/- cells became Oil Red O- positive (Fig 3.11). Interestingly, full differentiation was restored in Ty2 deficient adipocytes expressing Tyk2KD and Stat3CA. Regardless of proper response to IFN β in Tyk2 -/- + Tyk2WT cells, we noticed only partial differentiation of this cell line. To further analyze our in vitro model, we examined gene expression in all differentiated cell lines. Tyk2 -/- adipocytes exhibit severely reduced brown fat- specific RNAs (UCP1, PRDM16, Cidea, Elovl3), down regulated levels of key transcription factors and coactivators (PPARs, C/EBPs, PGC1α), as well as mitochondrial RNAs (Cox8b, CS) (Table 3.1). These results explain lack of differentiation in Tyk2- null adipocytes. Additionally, they confirm the data obtained from BAT of wild type and Tyk2 knockout mice. Gene expression was recovered by

reconstitution of Tyk2 -/- cells with Tyk2KD and Stat3CA. Protein levels of selected RNAs were also confirmed by Western blot analysis (Fig 3.12).

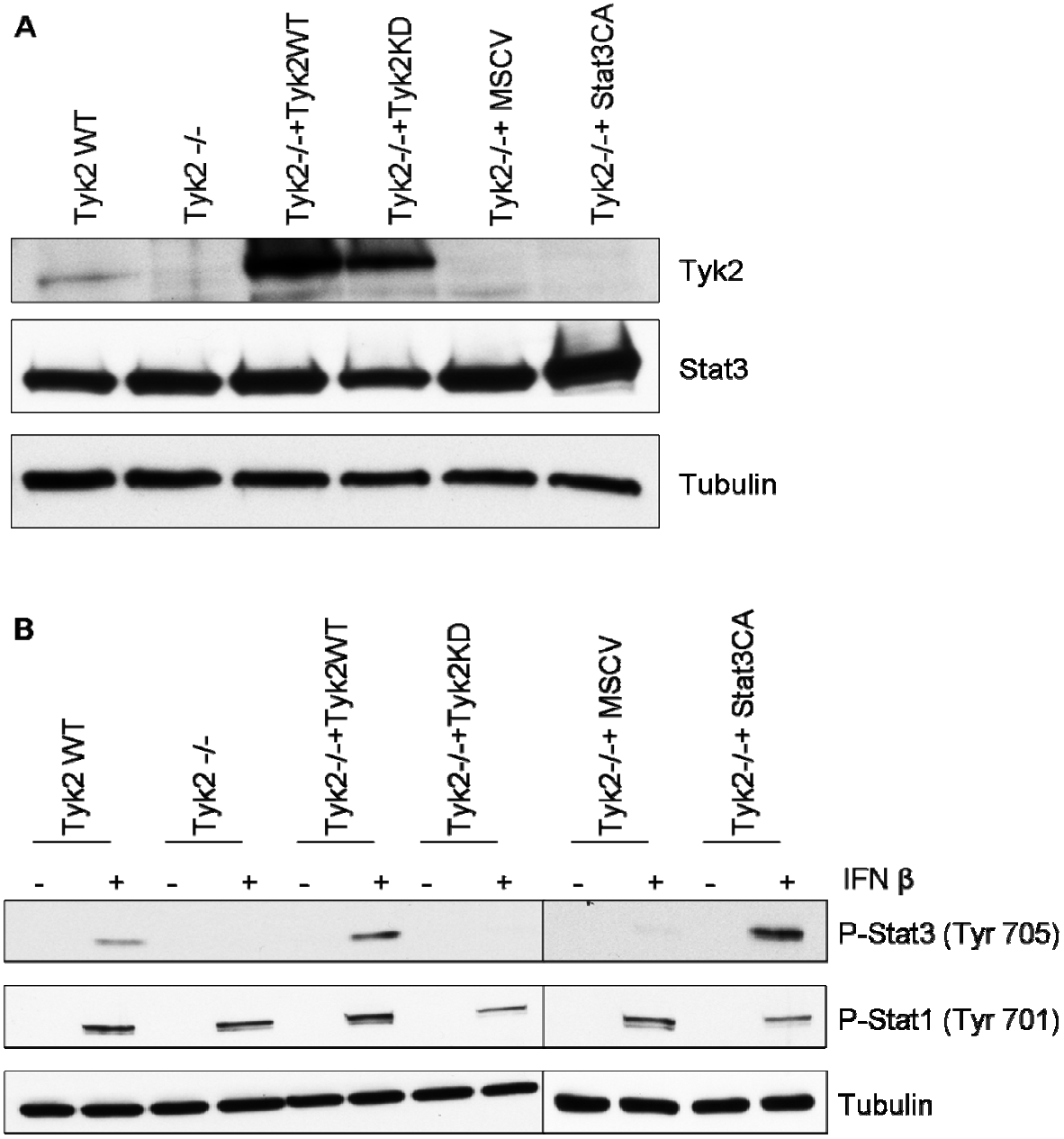

Figure 3.10 Generation of immortalized brown adipocyte cell lines. (A) cell extracts were prepared from immortalized wild type and Tyk2 -/- adipocytes reconstituted with Tyk2WT, Tyk2KD, Stat3CA, MSCV and analyzed for proteins level of Tyk2 and Stat3. Tubulin was used as a loading control. **(B)** Created cell lines were incubated with or

without IFN β (1000U/ml) for 30 min prior to preparing cell extracts and analyzed for tyrosine phosphorylation of Stat3 and Stat1. One representative blot out of three independent experiments is shown.

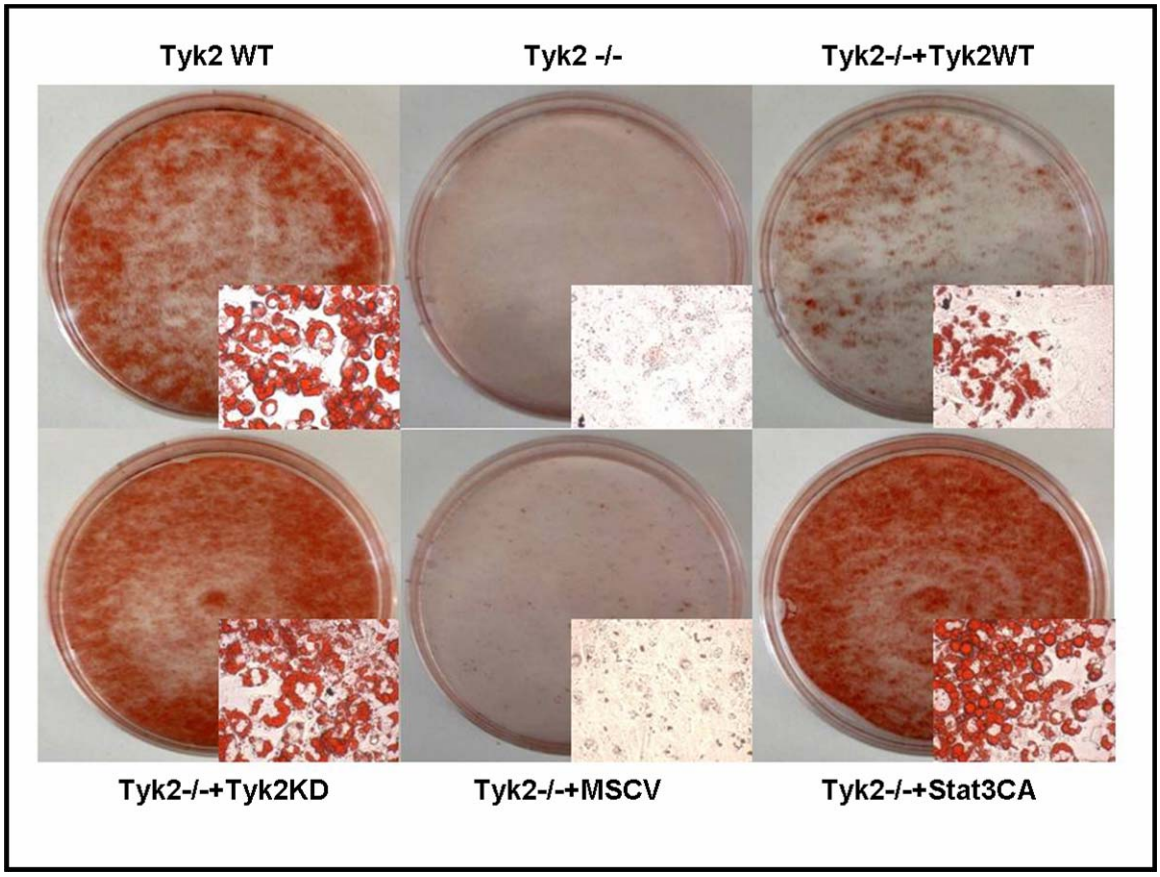

Figure 3.11 Oil Red O staining of immortalized adipocytes. Generated cell lines were subjected to in vitro differentiation, fixed with buffered formalin and stained with working solution of Oil Red O.

	Tyk2 WT	Tyk2-/-	Tyk2-/- +MSCV	Tyk2-/- +Tyk2WT	Tyk2-/- +Tyk2KD	Tyk2-/- +Stat3CA
UCP1	1	0.1 ± 0.03 *	0.1 ± 0.04 *	0.5 ± 0.1	1.8 ± 0.3	1.3 ± 0.4
PRDM16	1	0.1 ± 0.04 *	0.2 ± 0.07 *	0.3 ± 0.09 *	1.2 ± 0.3	1.1 ± 0.4
PPARγ	1	0.2 ± 0.05 *	0.2 ± 0.06 *	0.3 ± 0.07 *	2.2 ± 0.3	1.8 ± 0.4
PGC1α	1	0.1 ± 0.02 *	0.1 ± 0.02 *	0.2 ± 0.09 *	0.9 ± 0.2	1.7 ± 0.7
PPARα	1	0.3 ± 0.1 *	0.3 ± 0.04 *	0.2 ± 0.08 *	1.5 ± 0.5	1.2 ± 0.6
C/EBPα	1	0.2 ± 0.09 *	0.2 ± 0.03 *	0.5 ± 0.1 *	2.2 ± 0.7	2.4 ± 0.7
C/EBPβ	1	0.7 ± 0.1 *	0.6 ± 0.2 *	0.7 ± 0.1 *	1.3 ± 0.2	1.2 ± 0.1
Cidea	1	0.2 ± 0.07 *	0.2 ± 0.07 *	0.4 ± 0.2 *	2.1 ± 0.6	2.3 ± 0.6
Elovl3	1	0.3 ± 0.17 *	0.5 ± 0.2 *	0.6 ± 0.4 *	1.3 ± 0.2	1.5 ± 0.5
Cox8b	1	0.3 ± 0.09 *	0.3 ± 0.1 *	0.6 ± 0.2 *	2.3 ± 0.9	3.6 ± 0.9
CS	1	0.2 ± 0.1 *	0.2 ± 0.07 *	0.5 ± 0.1 *	2.7 ± 0.9	2.9 ± 0.9

Table 3.1 Reduced gene expression in Tyk2 deficient adipocytes is restored by reconstitution with Tyk2KD and Stat3CA. Total RNA was isolated form in vitro differentiated adipocytes and analyzed for selected RNA levels using real- time qPCR. The values represent mean fold decrease ± SE for n = 5 independent experiments, *$p < 0.05$.

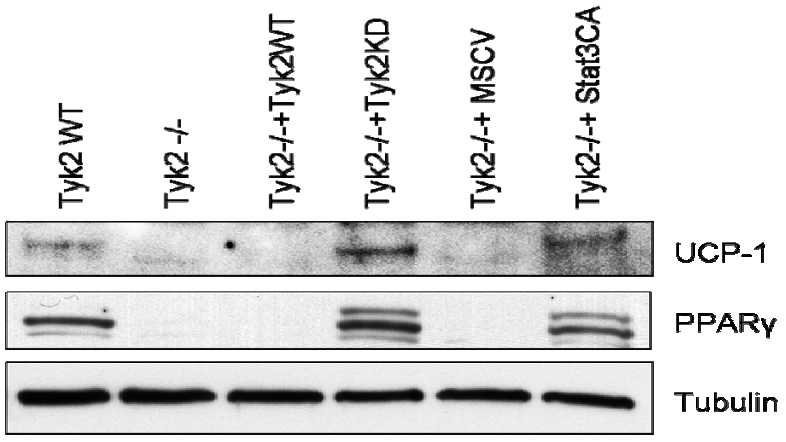

Figure 3.12 UCP1 and PPARγ expression in Tyk2 -/- adipocytes is rescued by expression of Tyk2KD and Stat3CA. Protein extracts from differentiated adipocytes were immunoblotted against UCP1 and PPARγ. Tubulin was used as a loading control. One representative blot out of three independent experiments is shown.

3.8 Response to cAMP treatment is diminished in Tyk2 -/- adipocytes

It is quite well established that norepinephrine released during thermogenesis activates adenylyl cyclase resulting in increased cAMP level in brown fat cells. Stimulation with dibutyryl- cAMP, which can cross the cell membrane, is used as an in vitro model of thermogenic response. This method serves as a functional test for brown adipocytes in cell culture. We therefore examined whether our immortalized brown adipocytes are capable of increasing the UCP1 expression upon cAMP stimulation. Our data revealed abolished thermogenic response in Tyk2 -/- adipocytes, when compared to wild type cells. UCP1 expression, after cAMP treatment, is restored by reconstitution with Tyk2KD and Stat3CA (Fig 3.13). This experiment indicates that our differentiated cell lines behave like fully functional brown fat cells.

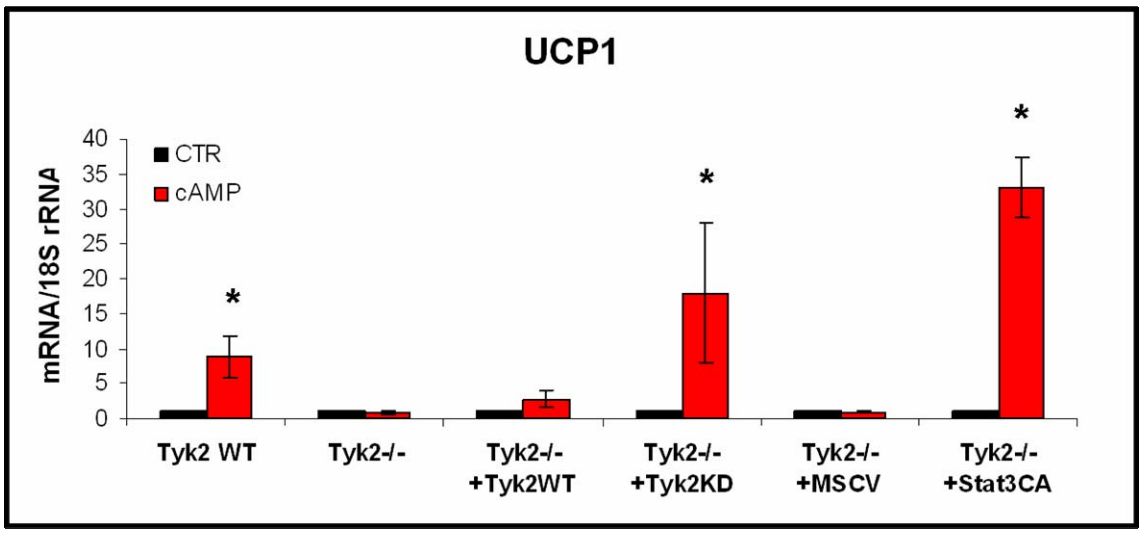

Figure 3.13 Defective response to cAMP in Tyk2-null adipocytes is recovered by Tyk2KD and Stat3 expression. Differentiated adipocytes were stimulated with cAMP (0.5 mM) for 4 h. Total RNA was isolated and analyzed for UCP1 expression by real-time qPCR. The values represent mean fold increase ± SE for n = 3 independent experiments, *$p < 0.05$.

3.9 Tyk2- null adipocytes exhibit increased expression of muscle- specific RNAs

PRDM16 is required for the control of brown fat / skeletal muscle switch (215). Since the PRDM16 expression is down regulated in both: BAT from Tyk2 knockout mice and in vitro differentiated adipocytes, we proceeded with measurement of muscle- related genes in our stable cell lines. The results showed increased expression of common muscle- specific genes like muscle creatine kinase (MCK), or transcription factors MyoD and myogenin (Myg), in Tyk2- null compared to wild type adipocytes (Fig 3.14). Surprisingly, expression of the wild type version of Tyk2 kinase in Tyk2 -/- preadipocytes was much more effective in reducing the expression of muscle- selective markers than TykKD or Stat3CA (Table 3.2).

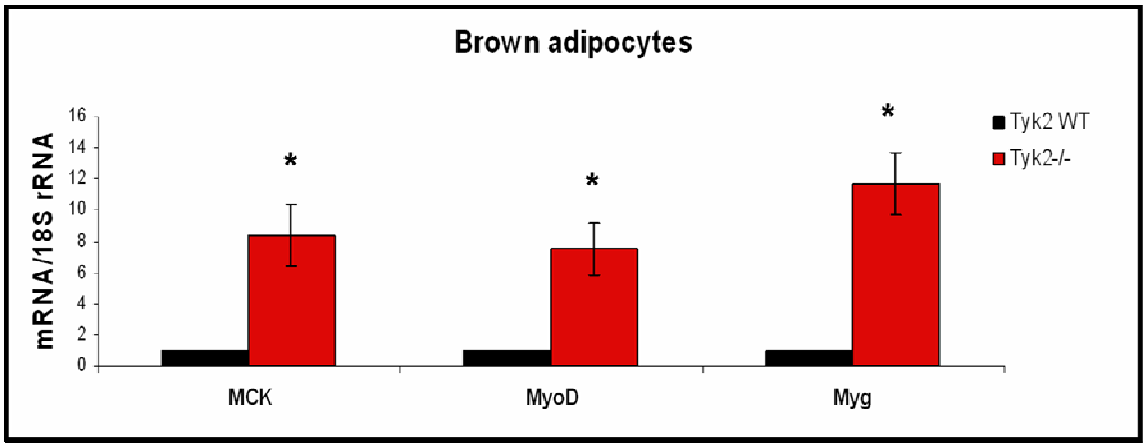

Figure 3.14 Tyk2 -/- adipocytes display increased muscle- specific genes expression. Total RNA was isolated from differentiated wild type and knockout cells. Levels of MCK, MyoD and Myg RNAs were measured by real- time qPCR. The values represent mean fold increase ± SE for n = 3 independent experiments, *p < 0.05.

	Tyk2 WT	Tyk2-/-	Tyk2-/- +MSCV	Tyk2-/- +Tyk2WT	Tyk2-/- +Tyk2KD	Tyk2-/- +Stat3CA
MCK	1	8.4 ± 2.0 *	6.3 ± 1.4 *	2.7 ± 0.5	5 ± 1.7 *	3.4 ± 0.5 *
MyoD	1	7.5 ± 1.7 *	10 ± 2.2 *	2.9 ± 0.5	4.7 ± 1.7 *	4.3 ± 0.7 *
Myg	1	12 ± 2.1 *	29 ± 1.3 *	2.6 ± 0.2	8.2 ± 2.3	3.5 ± 1.7

Table 3.2 Tyk2 WT overexpressed in Tyk2- null adipocytes reduces muscle gene expression. Total RNA was isolated form in vitro differentiated adipocytes and analyzed for selected RNA levels using real- time qPCR. The values represent mean fold decrease ± SE for n = 5 independent experiments, *p < 0.05.

3.10 Reconstitution with PRDM16 does not restore differentiation in Tyk2 -/- adipocytes

Because PRDM16 is a master regulator of BAT development, we tested if its overexpression reverses lack of differentiation in Tyk2 -/- adipocytes. In order to do that cells were infected with a control adenovirus, as well as the vector containing PRDM16. The expression level of PRDM16 in the infected cells was confirmed by western blot and qPCR method respectively (Fig 3.15A and Fig 3.16). The principal role of PRDM16 is to commit Myf5- positive progenitors towards brown adipocytes, by suppressing muscle-specific genes (215, 217). Therefore, we examined if adenoviral PRDM16 overexpression decreases muscle- related RNAs in Tyk2 -/- adipocytes. Elevated MCK, MyoD and Myg expression in Tyk2 -/- cells was diminished almost to the level present in the wild type cells (Fig 3.15B). These experiments showed that PRDM16 is fully functional in the infected cells. However, PRDM16 expression did not restore differentiation in Tyk2- null adipocytes. According to real- time qPCR analysis, none of brown fat- specific or adipogenic genes in Tyk2 -/- cells were up regulated by PRDM16 (Fig 3.16).

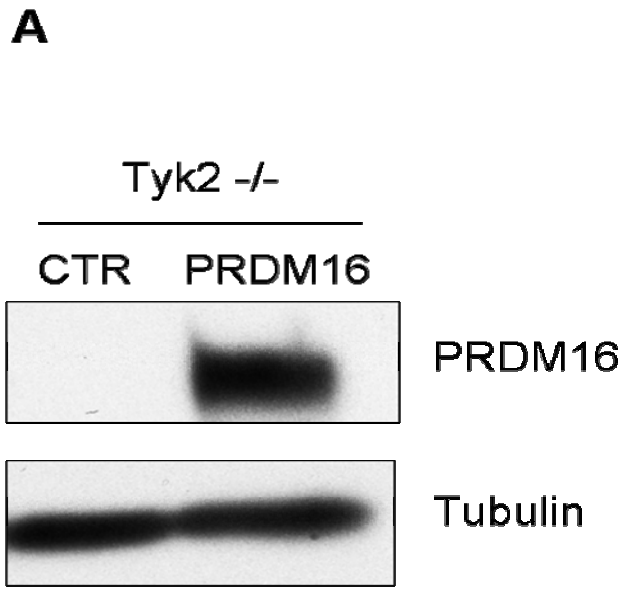

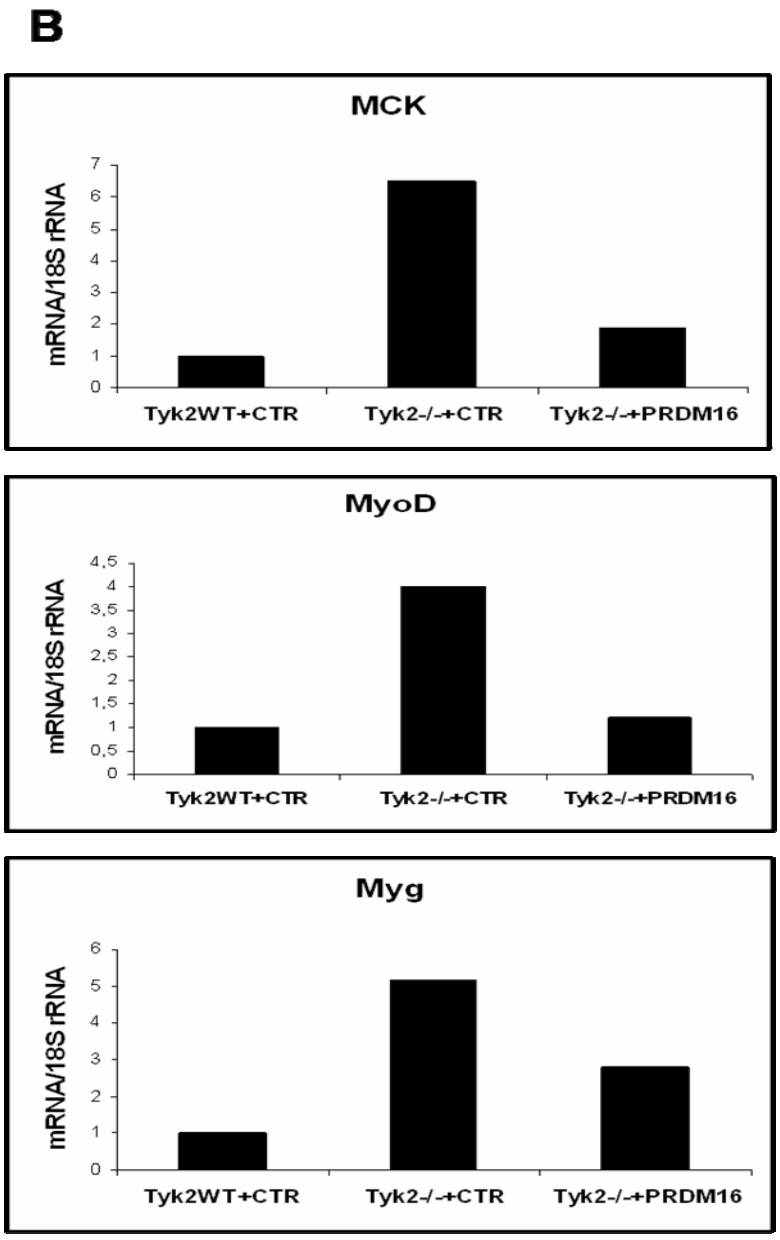

Figure 3.15 Elevated muscle- specific gene expression in Tyk2 -/- adipocytes are decreased by PRDM16 overexpression. Tyk2- null cells were infected with control adenovirus (CTR), as well as adenovirus containing PRDM16. Wild type cells infected with the same vector served as a control of the differentiation in the presence of adenovirus. **(A)** whole cell extracts were analyzed for PRDM16 protein level by western blot. Tubulin was used as a loading control. **(B)** total RNA was assayed for muscle gene expression by real- time qPCR and normalized to 18S rRNA expression. The values represent mean fold increase for n = 2 independent experiments

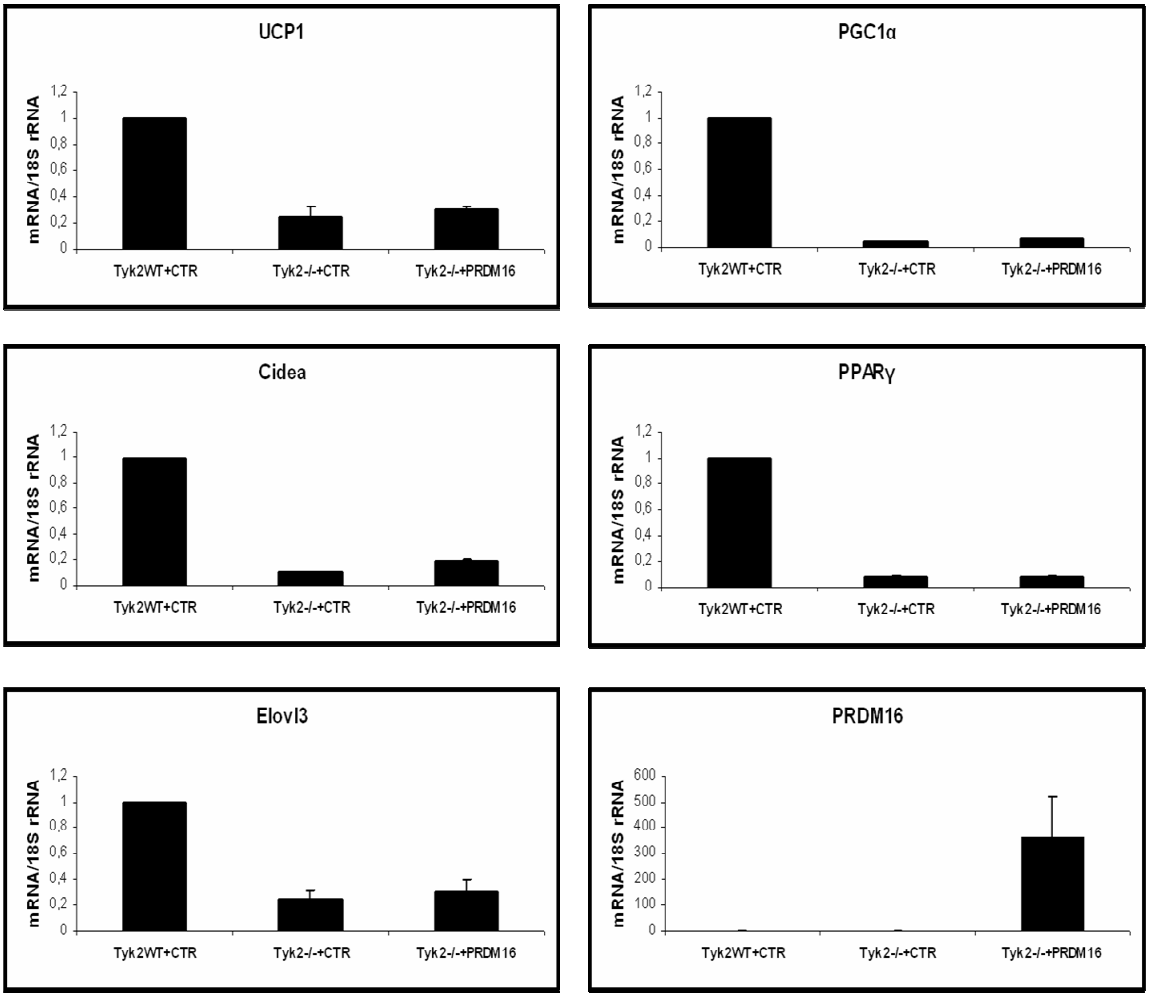

Figure 3.16 PRDM16 overexpression does not restore differentiation in Tyk2 -/- adipocytes. Tyk2- knockout cells were infected with control adenovirus (CTR), as well as adenovirus containing PRDM16. Wild type cells infected with the same vector served as a control of the differentiation in the presence of adenovirus. Total RNA was then isolated from differentiated adipocytes. Levels of brown fat- specific (UCP1, Cidea, Elovl3, PRDM16) and adipogenic (PPARγ, PGC1α) RNAs were measured by real- time qPCR. The values represent mean fold change ± SE for n = 2 independent experiments.

3.11 Stat3 deficient adipocytes exhibit loss of brown fat phenotype in cell culture

It has been reported that mice with Stat3 knocked down in fat tissue become obese (34). Cre-loxP DNA recombination system was used to create mice with disrupted Stat3 expression in adipose tissue (ASKO mice). Published data revealed higher body weights in male mice, which is a result of increased adiposity, fatty liver, reduced serum adiponectin levels and loss of leptin- induced lipolysis. However, Stat3 knockout mice do not show impaired glucose tolerance or any other characteristics of metabolic syndrome. Despite greatly reduced protein levels of Stat3 in white and brown adipose tissue in ASKO mice, previous investigations focused mainly on changes in WAT and liver (34). Our in vitro cell culture model suggests an important role of Stat3 in differentiation of brown adipocytes. Therefore, we examined if lack of Stat3 would change the phenotype of brown adipocytes by creating stable cell lines using shRNA approach. Wild type adipocytes were infected with GFP- expressing lentivirus containing scramble shRNA (SCR), or shRNA targeting Stat3. Total RNA as well as whole cell extracts were prepared from cells subjected to the differentiation. Western blot analysis of protein lysates showed that we were able to silence 100% of Stat3 protein (Fig 3.17A). Real-time qPCR analysis revealed decrease in brown fat- specific gene expression (UCP1, Cidea, Elovl3), but no alterations in RNA levels of adipogenic markers (PPARs, PGC1α, C/EBPβ, aP2) (Fig 3.17B). Gene expression data confirmed lack of changes in morphology between SCR and Stat3 shRNA expressing cells. Both cell lines, subjected to differentiation, become adipocytes but Stat3 knockout cells do not acquire a brown fat phenotype. Based on our results from Tyk2 deficient mice, we can speculate that altered BAT might contribute to the obese phenotype described in ASKO mice. Furthermore, the same phenomenon observed in Stat3 knockout adipocytes is also reported in PRDM16 deficient cells (215), which suggests that these two proteins may be involved in the same signaling cascade regulating BAT development.

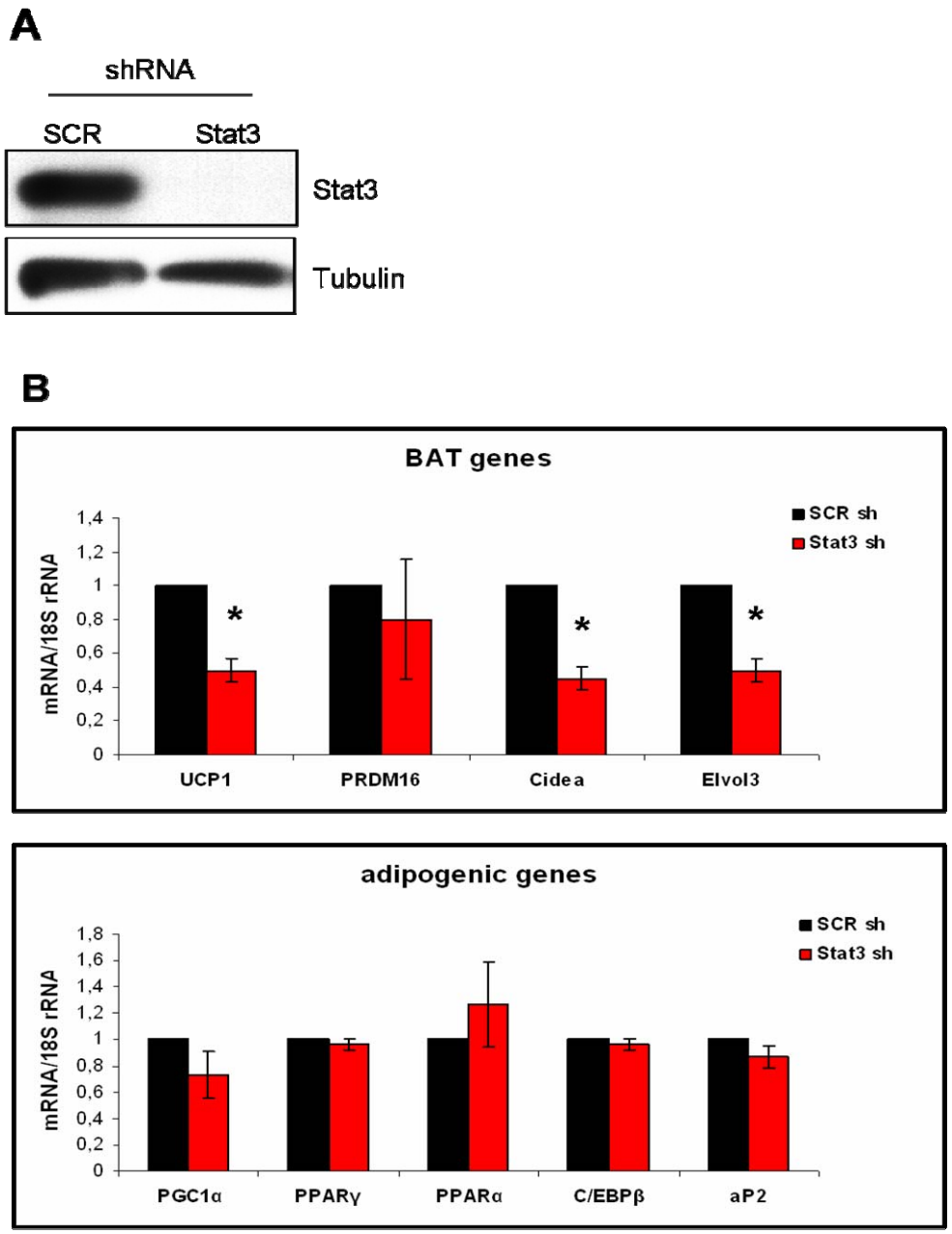

Figure 3.17 Stat3 deficient adipocytes do not acquire brown fat phenotype during differentiation. Wild type cells were infected with lentivirus carrying scramble shRNA (SCR sh) or shRNA against Stat3, and differentiated as described in Materials and Methods. **(A)** whole cell extracts were analyzed for Stat3 protein by western blot. Tubulin was used as a loading control. **(B)** RNA was isolated and analyzed for BAT and adipogenic markers by real- time qPCR. The values represent mean fold change ± SE for n = 3 independent experiments, *$p < 0.05$.

3.12 Tyk2 -/- brown adipocytes display hypermethylation of the C/EBPβ binding sequence in the promoters of BAT- selective genes

Among the different mechanisms that could lead to the defective development of BAT in Tyk2 -/- mice, epigenetic regulation of the gene expression is potentially one of the major contributors. The possible epigenetic changes include DNA methylation, covalent modification to histones and chromatin rearrangements. It has been previously reported that lack of the UCP1 expression in WAT is a result of hypermethylation of UCP1 promoter and enhancer. Moreover, treatment with the DNA methylation inhibitor 5-aza-2'-deoxycytidine causes over 10 fold increase in UCP1 expression (123). On the other hand, abundant UCP1 expression in BAT is associated with reduced methylation of UCP1 enhancer (226). Due to silenced expression of BAT- specific markers in Tyk2 deficient mice and cells, we decided to examine the methylation status of the promoters in BAT genes. Bisulphite sequencing revealed increased methylation of the Cidea and UCP1 promoters in Tyk2 -/- preadipocytes (Fig 3.18A and B respectively). The most striking differences in both promoters were observed in the sequence corresponding to the C/EBPβ binding sites (marked by a red frame in Fig 3.18). As mentioned before, C/EBPβ in complex with PRDM16 plays a crucial role in proper development of brown adipose tissue (113). Therefore, inability of C/EBPβ to regulate its target genes, due to altered methylation, could explain the aberrant phenotype of BAT in Tyk2- null mice/cells. Despite the slight reduction in mRNA level of C/EBPβ noticed in Tyk2 -/- adipocytes (Table 3.1), the increase in total C/EBPβ protein level upon induction of preadipocyte differentiation were not changed between wild type and knockout cells (Fig 3.19A). Surprisingly, C/EBPβ phosphorylation occurring later during the differentiation process was increased in Tyk2 -/- preadipocytes in comparison to the wild type cells, which may be a compensatory mechanism for potential lack of C/EBPβ binding to the DNA (Fig 3.19B). These results suggest that possible insufficient binding of C/EBPβ to the promoters of its target genes, such as Cidea or UCP1 can be the reason of silenced expression of BAT markers in Tyk2 deficient adipocytes.

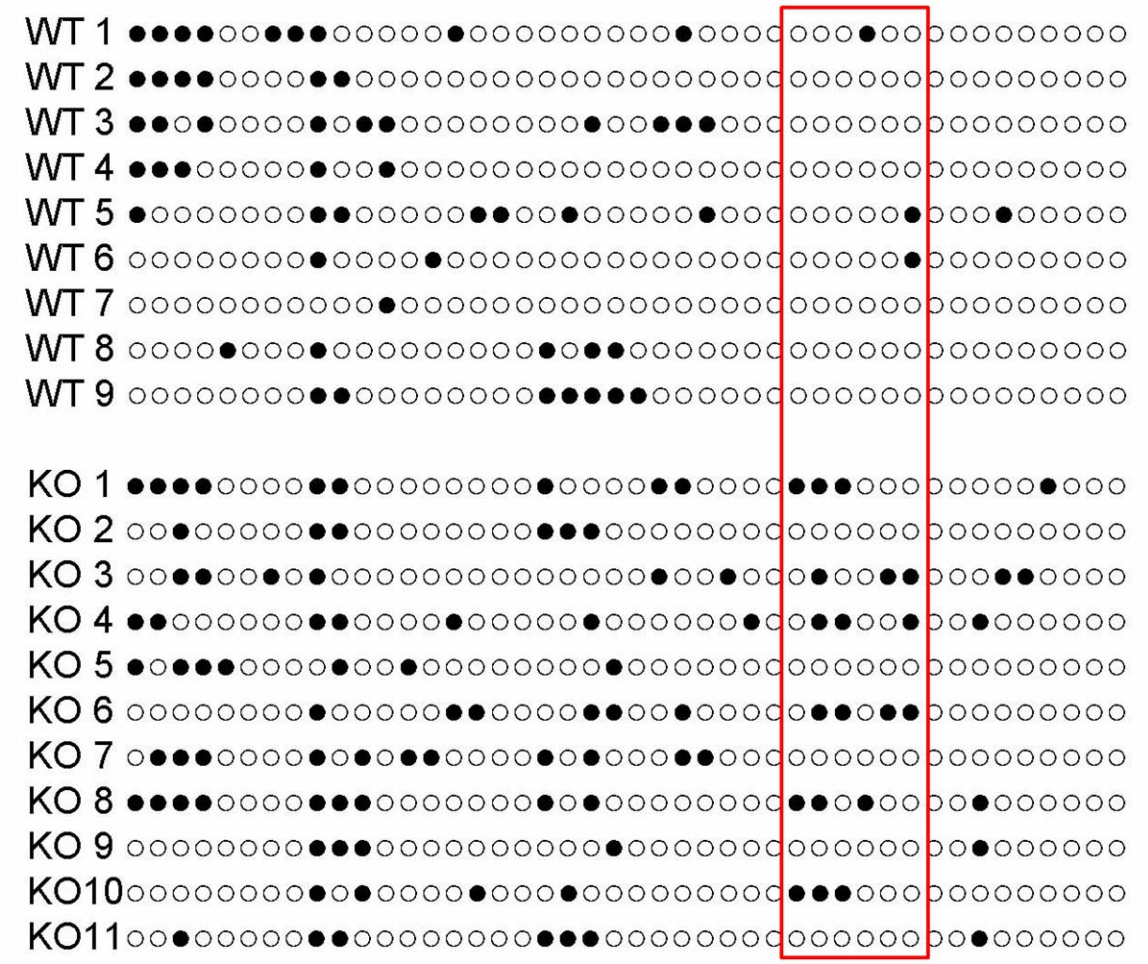
WT 1
WT 2
WT 3
WT 4
WT 5
WT 6
WT 7
WT 8
WT 9
KO 1
KO 2
KO 3
KO 4
KO 5
KO 6
KO 7
KO 8
KO 9
KO10
KO11

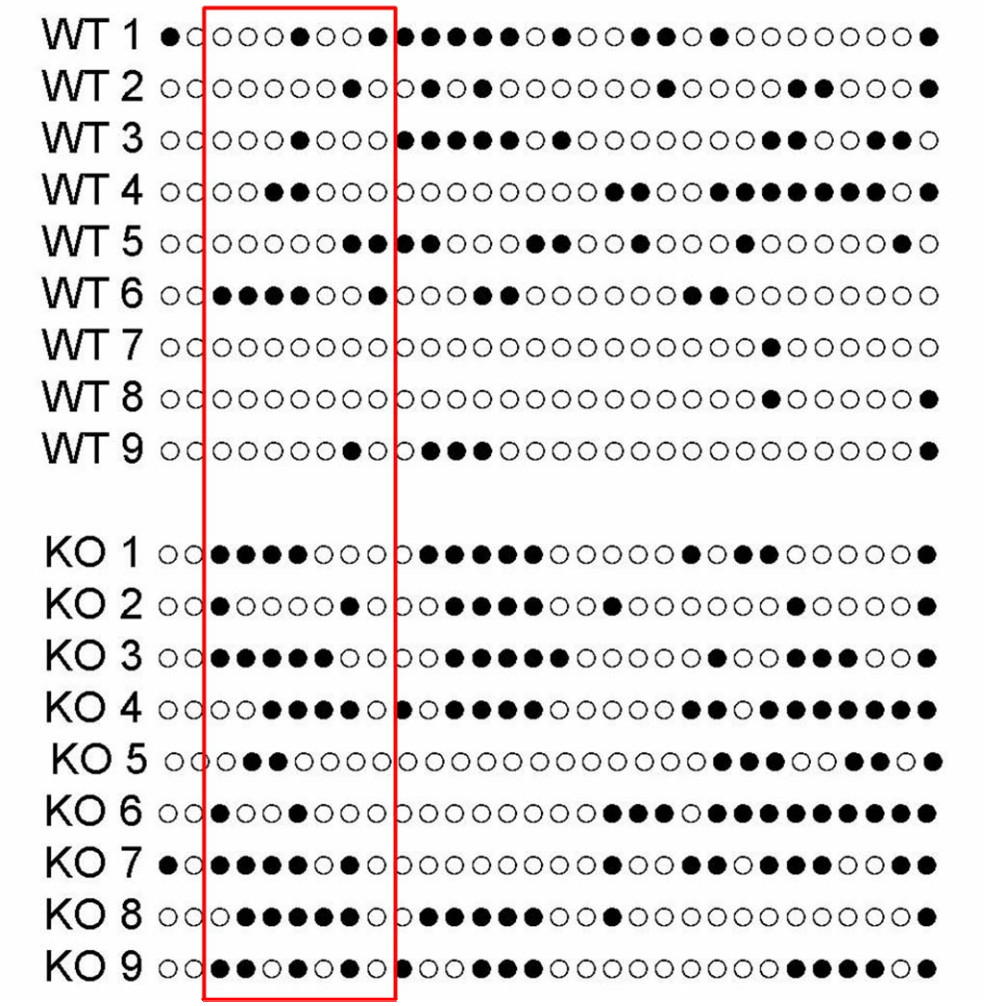

Figure 3.18 Cidea and UCP1 promoters show increased methylation of C/EBPβ binding sites. Bisulphite sequencing of CpGs was carried out after isolation of genomic DNA from Tyk2 WT and Tyk2 -/- preadipocytes. Black and white circles indicate methylated and unmethylated CpGs, respectively. The red frames indicate CpGs overlapping with C/EBPβ binding sites. **(A)** The Cidea promoter contains 44 CpGs (-550 to +250b). **(B)** The UCP1 promoter contains 30 CpGs (-500 to +200b).

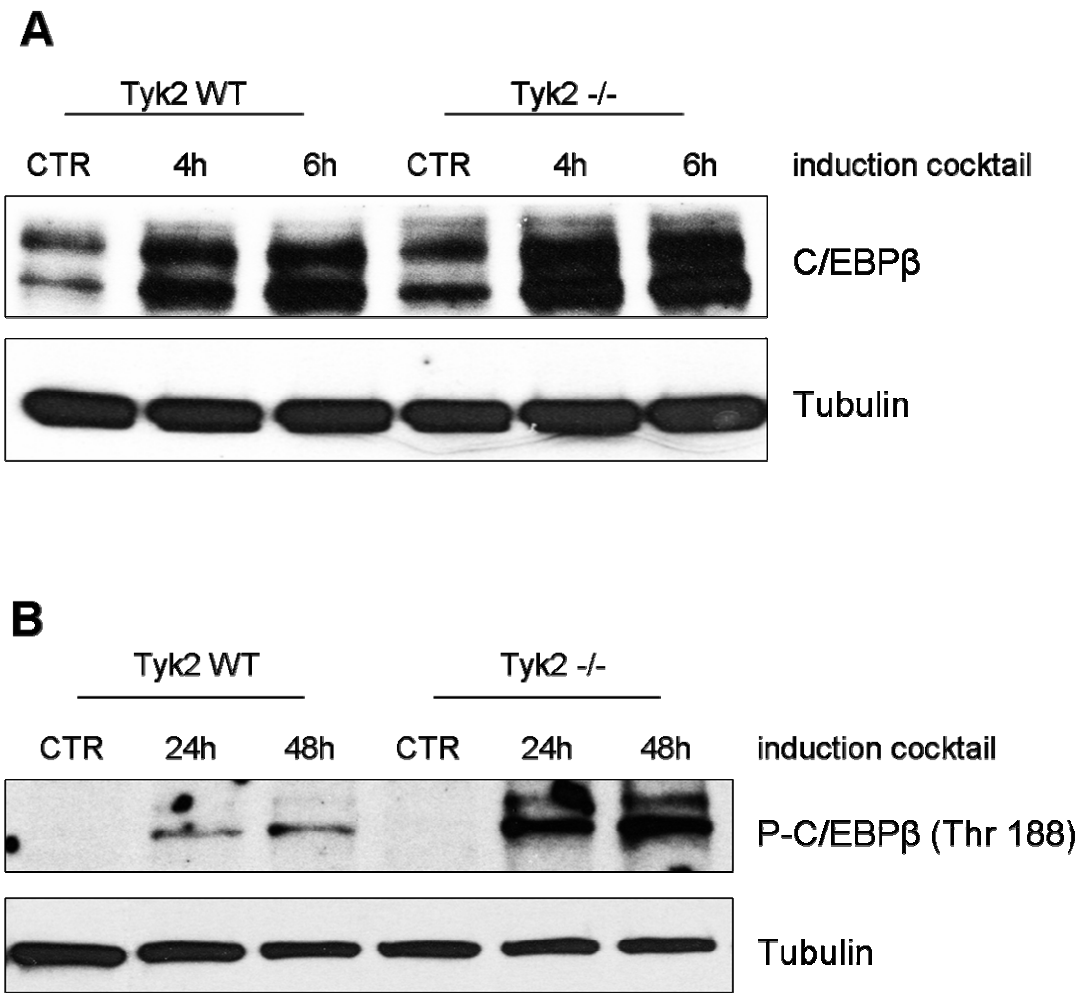

Figure 3.19 Increase in C/EBPβ level and its phosphorylation are preserved in Tyk2- null adipocytes during differentiation. Protein extracts from preadipocytes induced for the differentiation were immunoblotted against **(A)** total C/EBPβ and **(B)** phospho- Thr188 residue within C/EBPβ . Tubulin was used as a loading control. One representative blot out of two independent experiments is shown.

3.13 Expression of constitutively active Stat3 (Stat3CA) in BAT of Tyk2 knockout mice reverses their obese phenotype

Since Stat3CA restores the differentiation in immortalized Tyk2 -/- adipocytes in vitro, we further investigated this phenomenon in an in vivo mice model. Recently, a transgenic mouse has been described that expresses a constitutively active version of Stat3 in AgRP neurons (agouti- related peptide). These animals are lean and display relative resistance to diet- induced obesity due to increased locomotor activity, but without changes in AgRP expression (153). We obtained these mice, as a kind gift of Dr. K. Rajewsky (Harvard Medical School, Boston, USA). Mice with an inactive Stat3CA transgene were crossed with Tyk2 -/- animals. In order to activate the Stat3CA transgene in brown adipose tissue, Tyk2 -/- mice containing Stat3CA DNA (Tyk2-/-/Stat3CA) were mated with aP2- Cre/Tyk2-/- animals, which express Cre recombinase in BAT. The results presented in this dissertation were obtained from mice with Stat3CA transgene expressed selectively in BAT. All experiments were performed on control mice (Tyk2-/- / Stat3CA stated as CTR) and animals with the activated transgene (ap2-Cre/Tyk2-/- /Stat3CA stated as Stat3CA E), coming from the same litter. Expression of Stat3CA transgene in BAT of Tyk2 deficient mice increased the expression of brown fat- specific RNAs (UCP1, PRDM16, Cidea), which are severely diminished in Tyk2- null animals (Fig 3.20A). C/EBPβ, PPARγ and PPARα, which play an important role in BAT development, were also increased (Fig 3.20B). Furthermore, altered Tyk2 -/- BAT morphology depicted on Fig. 3.5 was restored by the Stat3CA expression, and resembled the tissue from wild type animals (Fig 3.21). Importantly, these results confirmed our observations from the in vitro cell culture system. Next step was to study how the restored BAT function in Tyk2 knockout animals influences their obese phenotype. Therefore, we fed mice regular chow diet until the age of 6 month, when Tyk2 -/- mice show many characteristics of metabolic syndrome, and examined their body weigh, insulin and leptin levels. Mice with the Stat3CA expression in brown fat exhibited significantly reduced body weight in comparison to control littermates (Fig. 3.22). Moreover, Stat3CA mice had much lower plasma insulin levels then control animals, which indicates improved insulin sensitivity (Fig. 3.23A). Additionally, animals with the activated transgene showed a tendency toward decreased plasma leptin levels, which

might be a result of reduced adiposity in comparison to control littermates (Fig. 3.23B). However these data did not reach statistical significance. Taken together these results reveal that expression of the constitutively active form of Stat3 in BAT of Tyk2- null mice reverses their obese phenotype. More importantly, our data support the recent hypothesis that brown adipose tissue may play very important role in preventing obesity, and could serve as a potential target for pharmacological approach in the clinic.

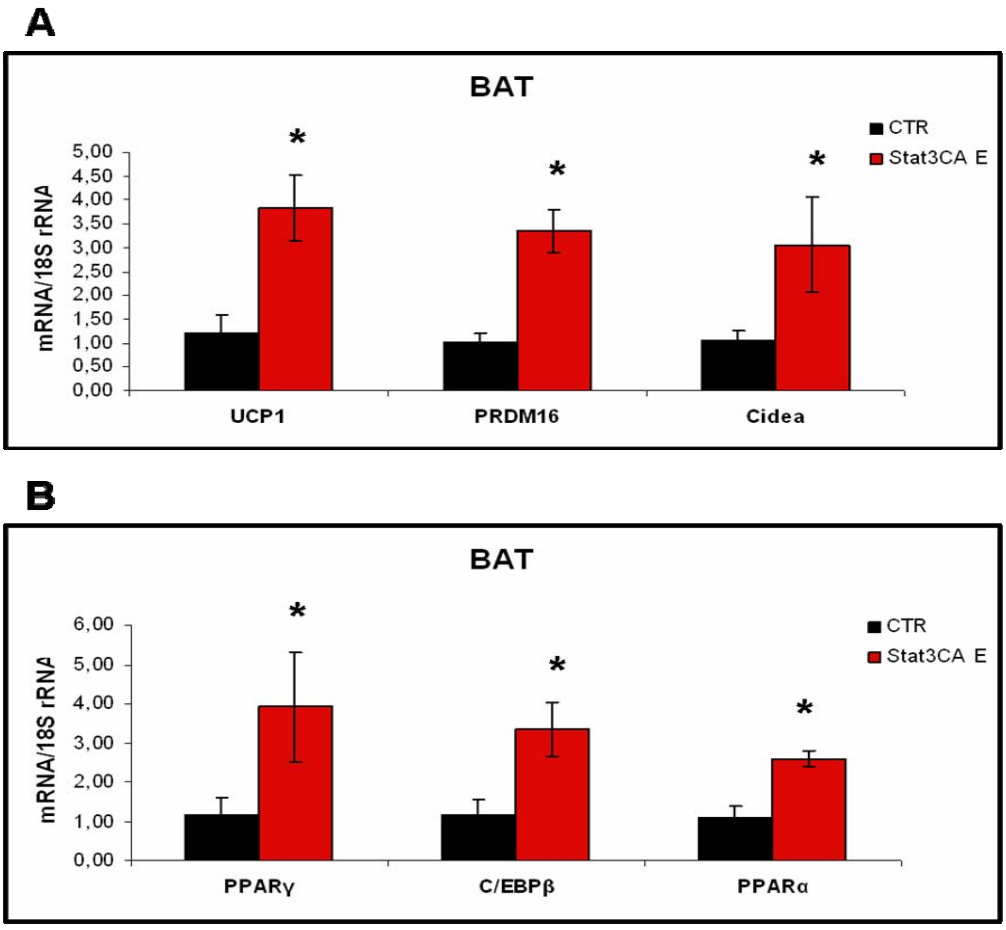

Figure 3.20 Activation of the Stat3CA transgene in BAT of Tyk2- null mice restores brown fat- specific gene expression. Total RNA was isolated from intrascapular BAT of 3- month old fasted for 16 h mice. **(A)** the expression level of brown fat- specific RNAs (UCP1, PRDM16, Cidea), **(B)** and common adipogenic RNAs (PPARs and C/EBPβ) were measured by real-time qPCR. The values represent mean fold increase ± SE for n = 6- 8 mice per group, *$p < 0.05$.

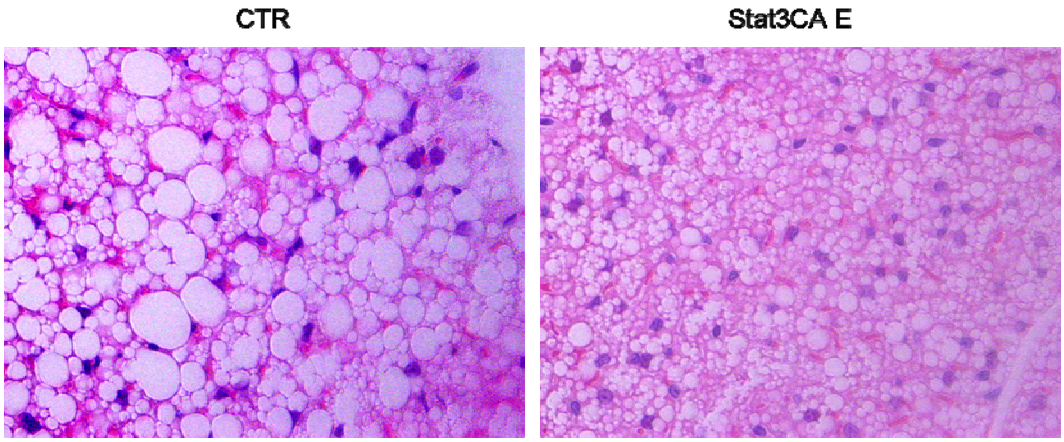

Figure 3.21 Altered BAT morphology in Tyk2 -/- mice is reversed by the expression of the Stat3CA transgene. Histological analysis of intrascapular brown adipose tissue of 3- month old mice expressing Stat3CA transgene in Tyk2 -/- BAT and control littermates. Representative hematoxylin- eosin staining, n = 5 mice per group.

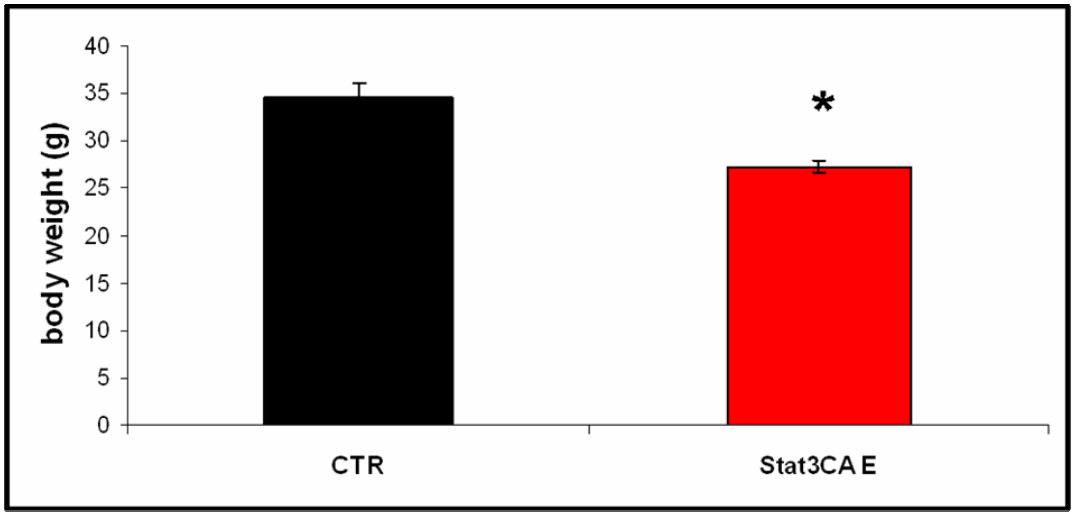

Figure 3.22 Tyk2 -/- mice expressing the Stat3CA transgene in BAT exhibit lower body weight. Body weight of 6- month old Stat3CA E and control mice fed a regular chow diet. Data are presented as the mean ± SE for n = 10 - 12 mice per group, *$p < 0.05$.

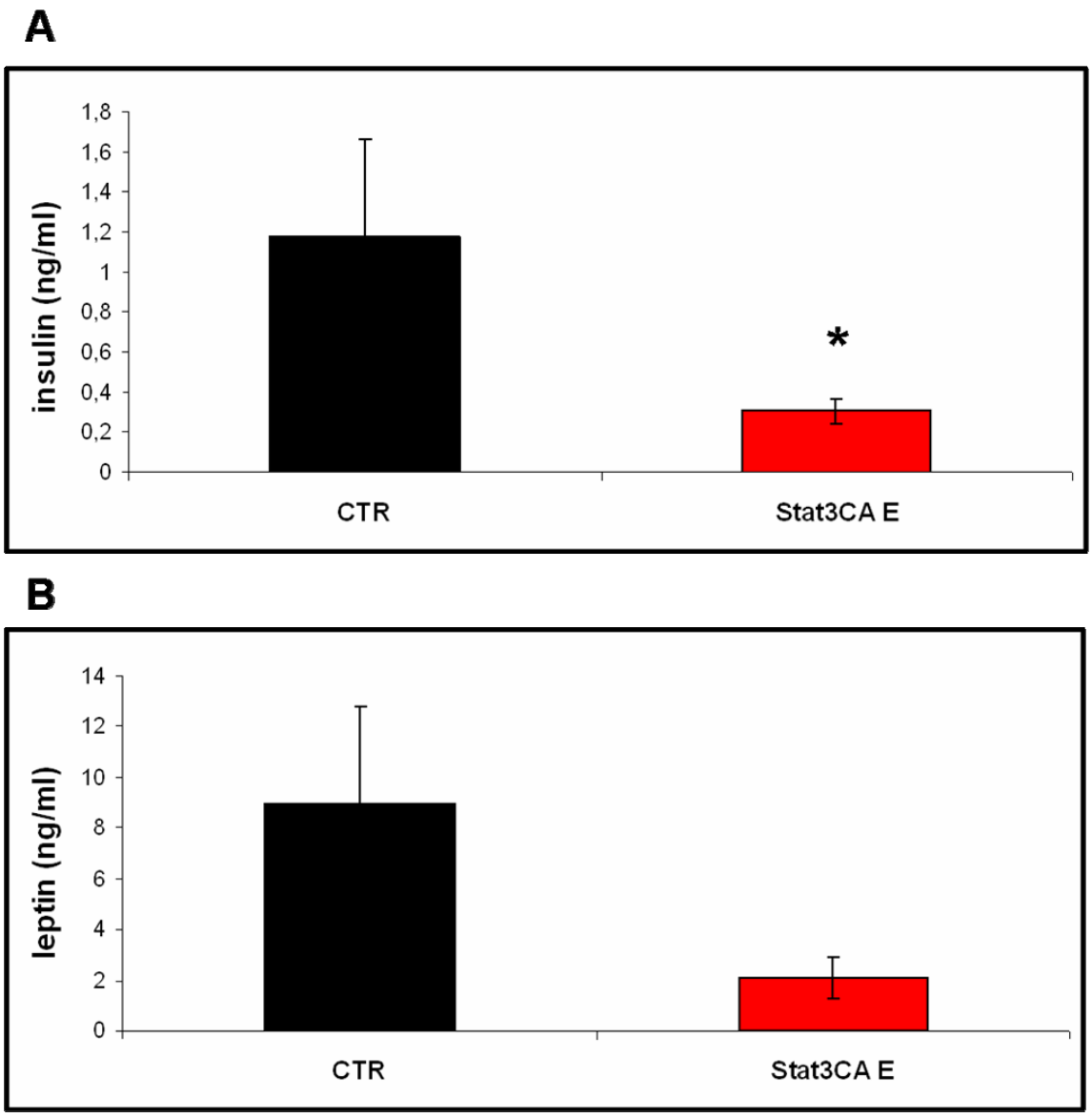

Figure 3.23 Restored BAT function in Tyk2 deficient mice improves insulin sensitivity and down regulates plasma leptin level. 6- month old mice were fasted overnight and bled from tail vein. **(A)** Plasma insulin level, and **(B)** plasma leptin level were measured by ELISA assay. Data are presented as the mean ± SE for n = 10 - 12 mice per group, *$p < 0.05$.

CHAPTER IV

DISCUSSION

The Jak/Stat pathway is well recognized regulator of many basic cell processes, such as growth, survival, development and differentiation. Numerous cytokines and growth factors utilize the Jak/Stat pathway to activate gene expression. Tyk2, which belongs to the Jak family of tyrosine kinases, has been shown to be critical for the biological actions of type I interferons, some interleukins such as IL- 12 or IL- 10 and to lesser degree the cytokines that signal through the gp130 receptor like IL-6 family. So far there are no published reports showing Tyk2 participation in signaling cascades that regulate metabolic homeostasis. We have made the novel observation that Tyk2 is involved in energy expenditure and maintenance of overall energy balance.

Metabolic syndrome is a very complex disorder, involving many organs and tissues. Therefore, it is extremely important to investigate all components of signaling cascades that are responsible for maintaining proper metabolic balance. Mice with the deletion of Tyk2 become spontaneously obese with age. Importantly, as shown in this work the obese phenotype is not influenced by the genetic background of animals. Three different strains: SV129 (94), C57Bl/6 and BALB/c of mice were used during the course of experiments and all of the Tyk2 -/- animals showed similar abnormalities. The obese phenotype of Tyk2- null mice become more severe with age and leads to the development of type 2 diabetes. Mice lacking Tyk2 have impaired glucose tolerance, insulin resistance, increased leptin levels, and changes in the expression of enzymes regulating glucose and lipid metabolism, as previously described by A. Górnicka (94).

Despite the higher body weights of Tyk2 knockout mice in comparison to the wild type animals, none of the Tyk2 deficient strains appeared to by hyperphagic. This observation strongly suggested that Tyk2 -/- mice had decreased energy expenditure. Brown adipose tissue has been well described as one of the main tissues responsible for energy consumption. More importantly, it has been proven, using rodent models, that

BAT influences entire energy balance in the organism, which when disturbed can lead to the obesity (73, 99, 146). Over the past 3 years there has been evident that BAT exists in adult humans and it is inversely correlated with the body mass index (54, 210, 265). Functional BAT is a big contributor to maintaining a lean phenotype through its effects on diet- induced thermogenesis, which permits excessive caloric intake to be dissipated as heat. Tyk2 -/- mice showed reduced RNA levels of BAT- specific genes such as UCP1, Cidea or PRDM16, which possibly cause impaired development and function of this tissue. Tyk2 ablation resulted also in decreased expression of PPARα, which regulates the transcription of β- oxidation enzymes. Altered gene expression was reflected in BAT morphology. Histology performed on the brown adipose tissue from Tyk2 -/- and wild type animals showed differences in lipid content. Cells with unilocular fat droplets, observed in Tyk2 -/- BAT, are characteristic for white adipose tissue. Small adipocytes with multilocular lipid droplets presented in wild type mice are typical for brown fat morphology (79). These changes in BAT morphology are likely the consequence of down regulated expression of PPARα, which lead to the excessive accumulation of lipids in the brown adipose tissue of Tyk2- null animals. PRDM16 serves as a key regulator during the BAT development process. It orchestrates the expression of brown fat-specific genes and at the same time inhibits a white fat- specific transcription program (114). Therefore, greatly reduced PRDM16 may also explain impaired morphology of the brown fat in Tyk2 -/- mice. Observed features of Tyk2 -/- mice were confirmed by metabolic cages studies, which are a standard method for overall metabolic analysis. Higher respiratory exchange ratio, recorded in case of Tyk2 knockout mice are consistent with their lower capacity to burn fat for energy production. Since fatty acids are the main substrate for BAT function, inability of Tyk2 -/- mice to process lipids efficiently can seriously affect diet- induced thermogenesis, which can greatly contribute to their obese phenotype.

The primary role of brown adipose tissue is to produce heat. Defective development of BAT and greatly decreased expression of UCP1 lead to depressed non-shivering thermogenesis. Brown adipose tissue from Tyk2 knockout mice exhibited a poor response to temperature insult. PGC1α is well described regulator of thermogenic response and one of the most potent activators of UCP1 expression, which drives the entire thermogenic program. Acute cold exposure resulted in 2-fold lower PGC1α

induction in Tyk2 -/- then in wild type mice. Additionally, metabolic cage analysis showed lower heat production by Tyk2- null animals in comparison to control mice at room temperature. These results provide in vivo evidence of severe defects in BAT in Tyk2 -/- mice. Alterations in brown fat function have been repeatedly shown to influence metabolic balance and cause obesity, which results in other metabolic abnormalities as the syndrome develops. As mentioned earlier, due to the extreme complexity of metabolic syndrome, the primary tissue/defect remains unknown. We hypothesized that BAT could be the primary site and major contributor to the obese phenotype presented by Tyk2 deficient mice. Although, the role of other tissues such as skeletal muscles, WAT or liver cannot be ruled out at this stage of our studies.

Interestingly, cold exposure experiments revealed a 4- fold lower induction of PGC1α, as well as reduced basal level of PGC1α in skeletal muscles of Tyk2 -/- mice than wild type mice. These observations indicate that there are the defects in BAT-regulated thermogenesis in Tyk2- null animals. PGC1α orchestrates multiple functions in skeletal muscles, all of which have been reported as necessary to maintain insulin sensitivity. PGC1α increases oxidative capacity during shivering thermogenesis, stimulates mitochondrial biogenesis and regulates muscle fiber- type switching (194). Thus, decreased PGC1α level contributes to insulin resistance, observed previously in skeletal muscles in Tyk2 deficient mice (94). Additionally, diminished expression of LCAD in the muscle tissue from Tyk2 -/- mice (94) may participate in occurring with age insulin insensitivity. It has been demonstrated that inhibition of fat oxidation in rodents increased intracellular lipid amount and decreased insulin sensitivity in vivo (63). Moreover, our group reported also that Tyk2 -/- mice are exercise intolerant (191), possibly as a consequence of decreased numbers of oxidative fibers resulting in lower oxidative capacity.

Skeletal muscles and brown fat are highly enriched in mitochondria and rely on their proper function. Studies of the etiology of insulin resistance have shown that dysfunction of the “power houses” of the cell is relevant in this disorder. The fact that Tyk2 -/- mice were insulin insensitive, have defective thermogenesis, showed decreased level of PGC1α, as well as some mitochondrial RNAs (CS and Cox8b), suggested

possible mitochondrial dysfunction. It has been also reported that pro B-cells from Tyk2 -/- mice have lower oxygen consumption and impaired electron transport chain activity compared to wild type cells. Electron microscopy revealed altered mitochondrial morphology in skeletal muscles and BAT of Tyk2- null mice compared to wild type animals. These changes concerned mainly abnormal cristae structure. The major proteins controlling mitochondrial membranes formation are mitofusins and optic atrophy protein 1. OPA1 has been described to regulate cristae remodeling (37, 38). Its expression was down regulated in Tyk2 -/- muscle and BAT samples, which explains abnormal cristae formation in these tissues in Tyk2 knockout mice. Unexpectedly, changes in the mitochondrial ultrastrucure and lower OPA1 expression were observed only in the skeletal muscles and brown fat, but not in the other tissues in Tyk2 -/- mice, such as heart, liver or WAT. This observation suggests a tissue- specific action of Tyk2 kinase. BAT and skeletal muscles have been shown to derive from the common Myf5 expressing progenitors (113). These results indicate a possible role of Tyk2 during development of these progenitor cells.

Due to severe alterations in BAT development and a possibility that changes in the function of this tissue can actually cause the obese phenotype in Tyk2 -/- mice, we decided to further examine this phenomenon. We took an advantage of the cell culture model, where we had opportunity to investigate the molecular mechanisms by witch Tyk2 mediates differentiation of brown adipocytes. Preadipocytes isolated from neonatal mice were immortalized and stable cell lines were generated expressing either wild type (Tyk2WT) or catalytically inactive (Tyk2KD- kinase dead) version of the kinase, as well as constitutively active Stat3 (Stat3CA) and empty vector control (MSCV). In order to confirm that all created cell lines were functional, their interferon response was analyzed. As expected, Stat3 phosphorylation was lost in the Tyk2 -/- cells and cells expressing Tyk2KD or MSCV, whereas it was present in the wild type cells and knockout cells reconstituted with Tyk2WT. Stat1 phosphorylation was preserved in all cell lines. These results showed that the cell lines behave according to the well described paradigm for Jak/Stat signaling. Then the cells were subjected to in vitro differentiation. As demonstrated by the Oil Red O staining, wild type cells were fully differentiated, whereas Tyk2 -/- cells were differentiation- incompetent. Surprisingly, the differentiation was

totally rescued by the expression of Tyk2KD and Stat3CA. Despite the proper function during the interferon response, Tyk2 -/- preadipocytes reconstituted with Tyk2WT presented only partial differentiation. Consistent with the Oil Red O staining, control (MSCV) and Tyk2 -/- adipocytes displayed severely decreased BAT- specific RNAs such asUCP1, PRDM16, Cidea and Elovl3, which reproduced the results seen in brown adipose tissue from Tyk2 -/- mice. Tyk2 deficient adipocytes also showed down regulated expression of mitochondrial genes (CS and Cox8b), which is consistent with diminished differentiation. Reduced levels of key transcription factors and co- activators (PPARs, C/EBPs and PGC1α), which are required for adipogenesis explains very poor lipid accumulation in the Tyk2- null adipocytes. The altered RNA levels for UCP1 and PPARγ were also confirmed at the protein level by Western blot analysis. Gene expression and protein levels were completely restored by the reconstitution of Tyk2- null cells with Tyk2KD and Stat3CA, and were partially restored by the expression of Tyk2WT.

In order to ensure that the cells behave like functional brown adipocytes, when differentiated, the response for the cyclic AMP was tested. It is well known that catecholamines, such as norepinephrine released during a thermogenic response, activate adenylyl cyclase resulting in increased cAMP and subsequent elevated UCP1 levels in brown fat cells. Preadipocytes were differentiated in vitro and UCP1 expression was assayed upon incubation with cell- permeable dibutyryl- cAMP. As expected, the response to cAMP was blunted in Tyk2 -/- adipocytes, when compared to the wild type cells. Reconstitution with either Tyk2KD or Stat3CA rescued cAMP- induced expression of UCP1 in Tyk2 -/- cells. Expression of Tyk2WT in the knockout cells resulted in much weaker UCP1 induction. This experiment indicated that the cell lines are capable of increasing UCP1 levels during a thermogenic response, similar to brown adipocyte tissue.

The fact that the kinase dead version of the Tyk2 kinase fully restores the differentiation in the Tyk2 -/- cells was very surprising. The explanation as to why there is not complete reconstitution of BAT- selective markers in Tyk2 -/- cells expressing Tyk2WT is still not clear. Interestingly, there are the reports in the literature suggesting that catalytically inactive forms of kinases, called pseudokinases, can still have biological functions. Protein kinases are critical for the regulation of numerous events regulating

cellular homeostasis. However, according to the clinical data, nearly 10% of the human kinome can be classified as pseudokinases due to mutations occurring in the residues that are essential for catalysis (115, 294). It has been reported that version of CASK (CA^{2+}/calmodulin-activated serine-threonine kinase), which was missing catalytic residues, still displayed catalytic activity under physiological conditions in vivo. It appeared that pseudokinase domain of CASK can adopt constitutively active conformation and phosphorylate itself, as well as one of its physiological substrates-neurexin-1. In this case, CASK kinase serves as a scaffold protein with an unusual kinase activity allowing phosphorylation of the substrate recruited by the scaffold activity (161). Another uncommon pseudokinase example was BRAF, a proto- oncogene serine-threonine protein kinase involved in MAPK / ERK signaling pathway (mitogen and extracellular- signal regulated protein kinases). Mutations in the components of MAPK / ERK cascade were discovered in many types of cancer. Over 30 mutants of BRAF, classified as catalytically inactive, have been found in human cancers. Some of the described mutations in BRAF occur always together with RAS (small guanine-nucleotide binding protein in the MAPK / ERK cascade) mutations. The kinase dead BRAF was shown to mediate tumor progression in the presence of oncogenic RAS. This observation provides important insight into the cancer genetics. It is also extremely valuable for clinical practice, where patients with these particular combination of mutations in BARF and RAS can be identified prior to administering BRAF- selective drugs, which in these cases could lead to even faster tumorigenesis (100). Furthermore, it has been shown that inhibition of catalytic activity of tyrosine kinase Zap70 could be a potential therapeutic tool. Zap70 kinase is normally required for T cells proliferation and activation. Patients with Zap70 deficiency suffer from a form of severe combined immunodeficiency characterized by a lack of peripheral $CD8^+$ T cells and presence of dysfunctional $CD4^+$ T cells. In contrast, the catalytic activity of Zap70 was not needed for signals promoting suppressive activity of regulatory T cells (11). In summary, it is clear that so called pseudokinases can transduce signals by connecting and assembling components of different signaling networks. These observations have changed our understanding of kinome function and reveal potential clinical applications of pseudokinases.

Despite the similarities in the signaling pathways that govern lipid metabolism in both brown and white adipose tissue, recent studies showed that they have distinct developmental origins. Lineage tracking experiments revealed that brown adipose tissue and skeletal muscles share common Myf5 positive progenitors. PRDM16 has been identified as a major regulator required for the control of brown fat / skeletal muscle switch (215). As mentioned earlier, PRDM16 expression was significantly decreased in BAT from Tyk2 -/- mice and Tyk2 -/- preadipocytes differentiated in vitro. Therefore, muscle- specific RNAs were measured in our stable cell lines. The results demonstrated augmented expression of muscle markers (MCK, Myg and MyoD) in Tyk2 -/- cells compared to wild type adipocytes. Interestingly, the expression of Tyk2KD or Stat3CA was much less effective in reducing the expression of muscle RNAs than Tyk2WT. These observations suggest that Tyk2 has two different functions during BAT development. One is to repress the expression of skeletal muscle genes, which takes place during the commitment phase of differentiation and seems to require the kinase activity of Tyk2, thus is poorly executed by Tyk2KD or Stat3CA. The other one is the induction of brown fat- specific gene expression, which is effectively accomplished by the expression of Tyk2KD or Stat3CA.

Because PRDM16 is the master regulator of BAT development, we overexpressed it in the Tyk2 -/- preadipocytes using adenovirus and monitored the differentiation of the infected cells. The principal role of PRDM16 during BAT development is suppression of muscle- specific gene and induction of BAT- selective genes. PRDM16 expression decreased muscle- related RNAs in Tyk2- null preadipocytes, indicating that PRDM16 functions properly in our system. Nevertheless, PRDM16 expression did not restore the differentiation in Tyk2 deficient preadipocytes or the expression of brown fat markers. These results indicate that the actions of Tyk2 and PEDM16 are on separate pathways or PRDM16 is functioning upstream of Tyk2 so overexpression of PRDM16 cannot overcome the defects caused by the absence of Tyk2. The fact that PRDM16 can inhibit the expression of muscle RNAs, but not induce the expression of BAT RNAs reinforces our hypothesis that these two events involved in BAT development can be experimentally separated.

Since Stat3CA rescued the differentiation in Tyk2 -/- preadipocytes we examined whether Stat3 was required for this process, using shRNA approach. Preadipocytes with Stat3 knocked down showed normal lipid accumulation, confirmed by the lack of changes in the expression of common adipogenic marker, such as PPARs or aP2. However, BAT- specific RNAs (UCP1, Cidea, Elovl3) were significantly decreased in the adipocytes expressing shRNA targeting Stat3, indicating that they did not acquire a brown fat phenotype during differentiation. Interestingly, the exact same phenotype was also presented in PRDM16 deficient cells (215), suggesting that Stat3 and PRDM16 may be involved in the same signaling cascade regulating BAT development. Additionally, PRDM16 has been recently shown to promote stem cell maintenance in various tissues (46). The role of Stat3 as one of essential stem cell transcription factors has been known for years (137). This also links these two proteins and suggests their mutual operation at the stage of progenitor cells, where PRDM16 is most need to commit Myf5 expressing cells towards brown adipocytes.

Over past couple of years, the field of chromatin structure and epigenetic changes in the regulation of gene expression has been under intensive investigation. Chromatin can regulate transcriptional processes thorough modifications of both its components: DNA and histones. Genome- wide mapping of DNA methylation patterns at the promoters in mouse embryonic stem cells showed that most methylated genes are associated with differentiation (77). In mammalian cells DNA methylation has been demonstrated to be involved in genome stability, repression of endogenous retroviral and transposable elements, genomic imprinting and developmental gene regulation (77). Thus, defects in DNA methylation can lead to various diseases, ranging from imprinting-associated disorders, cancer, neurological problems and obesity (42, 188). DNA methylation and histones modifications are connected. Recent findings have shown that disruption of the histone H3 lysine 9- specific demethylase Jhdm2a causes obesity and hyperlipidemia in mice due to defects in brown adipose tissue and muscles. The absence of Jhdm2a results in reduced of β- adrenergic- stimulated glycerol release and oxygen consumption in BAT, as well as decreased fat oxidation and glycerol release in skeletal muscles. Additionally, Jhdm2a directly regulates PPARγ and UCP1 expression (240). Several reports indicated that UCP1 expression in BAT is influenced by the DNA

methylation and chromatin remodeling (226). Since UCP1 and other BAT gene expression was ablated in Tyk2 -/- mice and cells, the epigenetic alterations within the promoters in these genes seemed to be a possible mechanism explaining the observed phenotype. Therefore, we examined whether expression of Tyk2 influences DNA methylation patterns of the UCP1 and Cidea promoters. Bisulfite sequencing analysis revealed that DNA within the entire promoters of both genes was hypermethylated in Tyk2- null preadipocytes. Moreover, the degree of methylation in the sequence adjacent to the C/EBPβ binding site was even higher in Tyk2 -/- cells. Since protein level and activation of C/EBPβ during differentiation was not affected in Tyk2 -/- cells in comparison to wild type cells, it is highly likely that C/EBPβ binding to the promoters of target genes is prevented due to their hypermethylation. Nevertheless, this assumption has to be confirmed by the chromatin immunoprecipitation assay. C/EBPβ plays an important role during BAT development, working in the complex with PRDM16 (113). Additionally, C/EBPβ and Stat3 have been reported to function synergistically (172, 189), thus we hypothesize that Stat3 in combination with PRDM16 and C/EBPβ are required at some stage of differentiation, possibly at the commitment phase. Interestingly, it has been indicated that a pool of Jak2 and Tyk2 are located within the nucleus and Jak2 directly phosphorylates tyrosine 41 on histone H3, which displaces HP1α (heterochromatin protein1α) from chromatin and allows transcription (58, 197). It is possible that Tyk2 may work in similar manner, either directly phosphorylating histones or serving as a scaffold protein recruiting/activating other enzymes that modify histones, which affects gene expression. Figure 4.1 is a model that summarizes our present understanding of how the expression of Tyk2 mediates BAT differentiation.

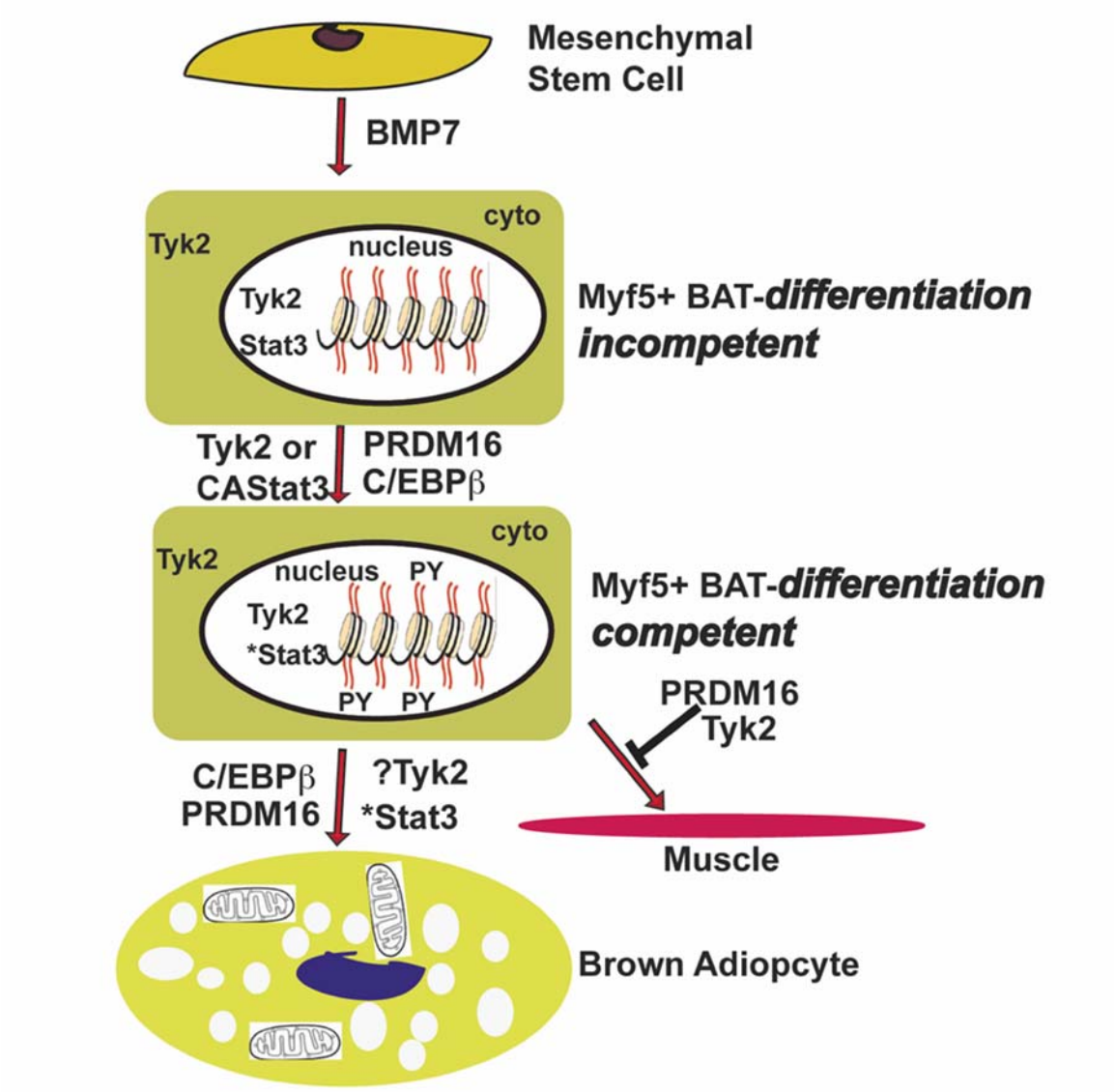

Figure 4.1 Model of Tyk2 and Stat3 function in brown adipose tissue differentiation. WAT and BAT are derived from mesenchymal stem cells. However, they have different progenitors. WAT originates from adipoblasts while BAT and muscles share common Myf5 positive progenitors, which require PRDM16 and BMP7 for further differentiation. Our results indicate that expression of Tyk2 is also required for progenitors to become committed brown preadipocytes, where PRDM16 and BMP7 can perform their functions. Stat3 is needed for differentiation as well. The data are consistent with the possibility that Tyk2 -/- preadipocytes are differentiation- incompetent and are at the earlier stage in differentiation then wild type cells. We hypothesize that Tyk2 mediates the progression in the differentiation to a stage such that preadipocytes can be developed into BAT by

PRDM16 and C/EBPβ in combination with other proteins. We speculate that Tyk2 allows Stat3 to be activated (*Stat3), which permits progression of differentiation- competent preadipocytes. Tyk2- mediated activation of Stat3 probably does not involve tyrosine phosphorylation, but requires some other modification of the protein such as serine phosphorylation, acetylation or methylation, all of witch have been reported for Stat3 (287, 293). It is possible that nuclear localized Tyk2 can phosphorylate histones (PY), which facilitates transcriptional activity of PRDM16 / C/EBPβ complex. Additionally, Tyk2 is needed to repress muscle- specific gene expression either in coordination with or independent of PRDM16.

Because expression of constitutively active Stat3 restored the differentiation of immortalized Tyk2 -/- preadipocytes, we obtained a transgenic mouse that carries a Stat3CA, which can be activated by Cre recombinase. Stat3CA mice were crossed into Tyk2 -/- animals and then mated with aP2-Cre/Tyk2 -/- , which expresses Cre recombinase specifically in BAT. Expression of the Stat3CA transgene in BAT of Tyk2 -/- mice increased the level of BAT- specific RNAs (UCP1, Cidea, PRDM16), which were significantly reduced in Tyk2 deficient mice. Additionally, the expression of adipogenic markers such as PPARγ, C/EBPβ and PPARα were also up regulated. Histology showed that BAT of Stat3CA expressing mice resembled tissue in wild type animals. More importantly, mice with Stat3CA expression in BAT exhibited significantly lower body weights than control mice at the age of 6 months, when normally Tyk2- null animals are grossly obese and show characteristics of metabolic syndrome. Furthermore, Stat3CA expressors had reduced plasma insulin levels, indicative of improved insulin sensitivity. These results demonstrate that the obese phenotype observed in Tyk2 -/- mice is most likely a result of a defect in BAT development occurring in these animals. Interestingly, improved BAT function has been previously reported to affect body weight in rodents. Cidea deficient mice are lean and resistant to diet- induced obesity due to increased metabolic rate and lipolysis in BAT. The lean phenotype of Cidea knockout mice is partially the result of direct suppressive action of Cidea on UCP1 activity (302). Surprisingly, it has been shown that lack of TNFα converting enzyme (TACE) causes elevated sympathetic activity, which leads to increased levels of UCP1 in BAT. Therefore, TACE- null mice display a hypermetabolic and lean phenotype (86).

Moreover, some studies indicated that recruitment of brown fat- like cells within white adipose tissue can influence energy balance and prevent weight gain. The manipulations leading to "creation" of BAT within WAT have been even proposed as a potential therapeutic approach in obesity treatment. Recent studies showed that administration of β_3-adrenergic receptor agonist CL 316, 243 promotes thermogenesis and appearance of brown adipocytes in white adipose tissue in rats. This in turn can delay high fat diet-induced obesity and reverse already existing diet- initiated overweight (89). Genetic approaches such as transgenic expression of PRDM16 also leads to robust induction of brown fat cells in WAT in mice. These animals exhibit increased energy expenditure and decreased weight gain, as well as improved glucose tolerance in the response to high fat feeding (216).

Therapeutic approaches to enhance the beneficial effects of brown adipose tissue in protecting against obesity and metabolic syndrome are now being seriously considered. It has been recently shown that depots of functional BAT can be found not only in newborns but also in adult humans. Moreover, BAT activity correlates with body weight in patients. Animal models provided multiple examples proving that brown adipose tissue influences the entire metabolic homeostasis. In order to apply our knowledge about brown adipose tissue to the clinic, signaling networks regulating its development and function have to be understood. To date there is no evidence that Tyk2 kinase has any role in the pathogenesis of obesity or brown adipose tissue differentiation. Therefore, the data presented in this dissertation add another piece into the puzzle of our understanding of energy balance.

STRESZCZENIE

Otyłość jest chorobą ogólnoustrojową, która charakteryzuje się nadmiernym nagromadzeniem tkanki tłuszczowej, przekraczającym energetyczne potrzeby organizmu. Często prowadzi ona do rozwoju wielu stanów patologicznych takich jak: cukrzyca typu drugiego, nadciśnienie tętnicze, miażdżyca, choroby serca, zwyrodnienia kręgosłupa oraz niektóre typy nowotworów. Kombinacje powyższych zaburzeń powodują rozwój niezwykle niebezpiecznego syndromu metabolicznego.

Kinaza tyrozynowa Tyk2 zaliczana jest do niereceptorowych kinaz z rodziny Janus (JAK), biorących udział w wewnątrzkomórkowej ścieżce przekazu sygnału Jak/Stat. Kinaza ta została zidentyfikowana po raz pierwszy jako element niezbędny do odpowiedzi komórki na interferony typu I. Dalsze badania wykazały, iż Tyk2 jest aktywowana także przez wiele innych cytokin takich jak: IL-6, IL-10, IL-12 oraz IL-23. Ścieżka transdukcji sygnału Jak/Stat wykorzystywana jest także przez czynniki regulujące procesy metaboliczne takie jak leptyna oraz insulina. Zaburzenia w działaniu obu hormonów prowadzą do rozwoju otyłości, cukrzycy typy drugiego oraz w konsekwencji do zespołu metabolicznego.

Dotychczasowe badania z wykorzystaniem myszy Tyk2-/- wykazały nieprawidłowości w działaniu układu immunologicznego tych myszy w związku z rolą jaką kinaza Tyk2 pełni w działaniu interferonów oraz innych cytokin. Analiza metaboliczna wykonana w naszym laboratorium nieoczekiwanie pokazała, iż myszy Tyk2-/- posiadają także wiele cech zespołu metabolicznego takich jak: otyłość, insulinooporność oraz zaburzenia w metabolizmie cukrów i tłuszczy. Celem tej pracy było potwierdzenie powyższego fenotypu w różnych szczepach myszy Tyk2-/- różniących się podatnością na związane z otyłością choroby metaboliczne, oraz znalezienie mechanizmu odpowiadającego za rozwój otyłości. Wykazano, że masa ciała myszy Tyk2-/- zarówno szczepu C57Bl/6 oraz BALB/c była statystycznie większa niż myszy typu dzikiego. Ponadto, oba szczepy myszy z delecją Tyk2 posiadały zaburzony test tolerancji na glukozę, co świadczy o insulinooporności. Najnowsze badania pokazały, że nieprawidłowe funkcjonowanie brunatnej tkanki tłuszczowej prowadzi do rozwoju

otyłości. W niniejszej pracy wykazano, że ekspresja genów kodujących czynniki odpowiedzialne za prawidłowy rozwój i funkcjonowanie brunatnej tkanki tłuszczowej, była znacznie obniżona u myszy Tyk2-/- w porównaniu z myszami typu dzikiego. Zaobserwowane zmiany zostały potwierdzone przy użyciu modelu *in vitro*. Preadipocyty wyizolowane z brunatnej tkanki tłuszczowej myszy Tyk2-/- wykazywały tylko częściowe różnicowanie w warunkach *in vitro* w porównaniu do prawie całkowitego różnicowania komórek typu dzikiego. Różnicowanie preadipocytów Tyk2-/- zostało przywrócone poprzez ekspresję kinazy Tyk2 oraz konstytutywnie aktywnej formy białka Stat3 (Stat3CA). Brak ekspresji czynników potrzebnych do prawidłowego rozwoju poszczególnych typów komórek związany jest często ze zmianami epigenetycznymi. Wzrost metylacji części regulatorowych genów wpływa hamująco na ich ekspresję. W przypadku preadipocytów z delecją Tyk2, analiza sekwencji DNA kodującego białka specyficzne dla brunatnej tkanki tłuszczowej wykazała zwiększoną metylację ich promotorów. Ponadto, największe różnice w poziomie metylacji zaobserwowano w obrębie sekwencji rozpoznawanej przez czynnik transkrypcyjny C/EBPβ, który odpowiada za regulację różnicowania preadipocytów w brunatnej tkance tłuszczowej. Zmiany zaobserwowane we wzorze metylacji DNA w komórkach Tyk2-/- sugerują spadek wiązania C/EBPβ do jego specyficznej sekwencji DNA, co w konsekwencji może powodować obniżenie ekspresji genów kodujących białka niezbędne do różnicowania brunatnych preadipocytów. Ponieważ konstytutywnie aktywna forma białka Stat3 przywraca różnicowanie preadipocytów z delecją Tyk2 w warunkach *in vitro*, otrzymano również mysz transgeniczną Tyk2-/- z ekspresją Stat3CA w komórkach brunatnej tkanki tłuszczowej. Profil ekspresji genów wykazał statystycznie istotny wzrost poziomu czynników regulujących rozwój i funkcjonowanie brunatnej tkanki tłuszczowej u myszy z ekspresją transgenu Stat3CA. Ponadto, waga ciała sześciomiesięcznych zwierząt z ekspresja Stat3CA była znacznie niższa niż myszy kontrolnych. Otrzymane wyniki sugerują, że zaburzenia w brunatnej tkance tłuszczowej zaobserwowane u myszy Tyk2-/- prowadzą do rozwoju otyłości u tych zwierząt.

Podsumowując, uzyskane w tej rozprawie wyniki wskazują na zupełnie nową rolę ścieżki przekazywania sygnału Jak/Stat w rozwoju brunatnej tkanki tłuszczowej, która może wpływać na regulację metabolizmu całego organizmu. Otrzymane dane sugerują,

że poprawa funkcjonowania brunatnej tkanki tłuszczowej jest w stanie zapobiec otyłości, występującej u myszy z delecją Tyk2. Dalszych badań wymaga kwestia molekularnego mechanizmu, który wyjaśniłby dokładnie w jaki sposób Tyk2 i Stat3 oddziałują z innymi białkami regulującymi różnicowanie brunatnej tkanki tłuszczowej. Być może pozwoli to w przyszłości na wykorzystanie białek Tyk2 oraz Stat3 w terapii farmakologicznej skierowanej przeciwko rozwojowi otyłości.

BIBLIOGRAPHY

1. **Abbas AK, Murphy KM, and Sher A**. Functional diversity of helper T lymphocytes. *Nature* 383: 787-793, 1996.
2. **Achenbach P, Bonifacio E, Koczwara K, and Ziegler AG**. Natural history of type 1 diabetes. *Diabetes* 54 Suppl 2: S25-31, 2005.
3. **Aizu K, Li W, Yajima T, Arai T, Shimoda K, Nimura Y, and Yoshikai Y**. An important role of Tyk2 in APC function of dendritic cells for priming CD8+ T cells producing IFN-gamma. *Eur J Immunol* 36: 3060-3070, 2006.
4. **Akaishi H, Takeda K, Kaisho T, Shineha R, Satomi S, Takeda J, and Akira S**. Defective IL-2-mediated IL-2 receptor alpha chain expression in Stat3-deficient T lymphocytes. *Int Immunol* 10: 1747-1751, 1998.
5. **al-Adsani H, Hoffer LJ, and Silva JE**. Resting energy expenditure is sensitive to small dose changes in patients on chronic thyroid hormone replacement. *J Clin Endocrinol Metab* 82: 1118-1125, 1997.
6. **Almind K, Manieri M, Sivitz WI, Cinti S, and Kahn CR**. Ectopic brown adipose tissue in muscle provides a mechanism for differences in risk of metabolic syndrome in mice. *Proc Natl Acad Sci U S A* 104: 2366-2371, 2007.
7. **Arbouzova NI, and Zeidler MP**. JAK/STAT signalling in Drosophila: insights into conserved regulatory and cellular functions. *Development* 133: 2605-2616, 2006.
8. **Aringer M, Cheng A, Nelson JW, Chen M, Sudarshan C, Zhou YJ, and O'Shea JJ**. Janus kinases and their role in growth and disease. *Life Sci* 64: 2173-2186, 1999.
9. **Arsenijevic D, Onuma H, Pecqueur C, Raimbault S, Manning BS, Miroux B, Couplan E, Alves-Guerra MC, Goubern M, Surwit R, Bouillaud F, Richard D, Collins S, and Ricquier D**. Disruption of the uncoupling protein-2 gene in mice reveals a role in immunity and reactive oxygen species production. *Nat Genet* 26: 435-439, 2000.
10. **Atit R, Sgaier SK, Mohamed OA, Taketo MM, Dufort D, Joyner AL, Niswander L, and Conlon RA**. Beta-catenin activation is necessary and sufficient to specify the dorsal dermal fate in the mouse. *Dev Biol* 296: 164-176, 2006.
11. **Au-Yeung BB, Levin SE, Zhang C, Hsu LY, Cheng DA, Killeen N, Shokat KM, and Weiss A**. A genetically selective inhibitor demonstrates a function for the kinase Zap70 in regulatory T cells independent of its catalytic activity. *Nat Immunol* 11: 1085-1092.
12. **Avram AS, Avram MM, and James WD**. Subcutaneous fat in normal and diseased states: 2. Anatomy and physiology of white and brown adipose tissue. *J Am Acad Dermatol* 53: 671-683, 2005.
13. **Bacon CM, McVicar DW, Ortaldo JR, Rees RC, O'Shea JJ, and Johnston JA**. Interleukin 12 (IL-12) induces tyrosine phosphorylation of JAK2 and TYK2: differential use of Janus family tyrosine kinases by IL-2 and IL-12. *J Exp Med* 181: 399-404, 1995.
14. **Barahmand-Pour F, Meinke A, Groner B, and Decker T**. Jak2-Stat5 interactions analyzed in yeast. *J Biol Chem* 273: 12567-12575, 1998.
15. **Barak Y, Nelson MC, Ong ES, Jones YZ, Ruiz-Lozano P, Chien KR, Koder A, and Evans RM**. PPAR gamma is required for placental, cardiac, and adipose tissue development. *Mol Cell* 4: 585-595, 1999.

16. **Bates SH, Stearns WH, Dundon TA, Schubert M, Tso AW, Wang Y, Banks AS, Lavery HJ, Haq AK, Maratos-Flier E, Neel BG, Schwartz MW, and Myers MG, Jr.** STAT3 signalling is required for leptin regulation of energy balance but not reproduction. *Nature* 421: 856-859, 2003.
17. **Becker S, Groner B, and Muller CW**. Three-dimensional structure of the Stat3beta homodimer bound to DNA. *Nature* 394: 145-151, 1998.
18. **Begitt A, Meyer T, van Rossum M, and Vinkemeier U**. Nucleocytoplasmic translocation of Stat1 is regulated by a leucine-rich export signal in the coiled-coil domain. *Proc Natl Acad Sci U S A* 97: 10418-10423, 2000.
19. **Ben-Haroush A, Yogev Y, and Hod M**. Epidemiology of gestational diabetes mellitus and its association with Type 2 diabetes. *Diabet Med* 21: 103-113, 2004.
20. **Beuvink I, Hess D, Flotow H, Hofsteenge J, Groner B, and Hynes NE**. Stat5a serine phosphorylation. Serine 779 is constitutively phosphorylated in the mammary gland, and serine 725 phosphorylation influences prolactin-stimulated in vitro DNA binding activity. *J Biol Chem* 275: 10247-10255, 2000.
21. **Bhattacharya S, Eckner R, Grossman S, Oldread E, Arany Z, D'Andrea A, and Livingston DM**. Cooperation of Stat2 and p300/CBP in signalling induced by interferon-alpha. *Nature* 383: 344-347, 1996.
22. **Boden G, and Shulman GI**. Free fatty acids in obesity and type 2 diabetes: defining their role in the development of insulin resistance and beta-cell dysfunction. *Eur J Clin Invest* 32 Suppl 3: 14-23, 2002.
23. **Bost F, Aouadi M, Caron L, and Binetruy B**. The role of MAPKs in adipocyte differentiation and obesity. *Biochimie* 87: 51-56, 2005.
24. **Bromberg J**. Stat proteins and oncogenesis. *J Clin Invest* 109: 1139-1142, 2002.
25. **Brownlee M**. Biochemistry and molecular cell biology of diabetic complications. *Nature* 414: 813-820, 2001.
26. **Butler AE, Janson J, Bonner-Weir S, Ritzel R, Rizza RA, and Butler PC**. Beta-cell deficit and increased beta-cell apoptosis in humans with type 2 diabetes. *Diabetes* 52: 102-110, 2003.
27. **Caldenhoven E, van Dijk TB, Solari R, Armstrong J, Raaijmakers JA, Lammers JW, Koenderman L, and de Groot RP**. STAT3beta, a splice variant of transcription factor STAT3, is a dominant negative regulator of transcription. *J Biol Chem* 271: 13221-13227, 1996.
28. **Cannon B, and Nedergaard J**. The biochemistry of an inefficient tissue: brown adipose tissue. *Essays Biochem* 20: 110-164, 1985.
29. **Cannon B, and Nedergaard J**. Brown adipose tissue: function and physiological significance. *Physiol Rev* 84: 277-359, 2004.
30. **Cao W, Daniel KW, Robidoux J, Puigserver P, Medvedev AV, Bai X, Floering LM, Spiegelman BM, and Collins S**. p38 mitogen-activated protein kinase is the central regulator of cyclic AMP-dependent transcription of the brown fat uncoupling protein 1 gene. *Mol Cell Biol* 24: 3057-3067, 2004.
31. **Carmona MC, Hondares E, Rodriguez de la Concepcion ML, Rodriguez-Sureda V, Peinado-Onsurbe J, Poli V, Iglesias R, Villarroya F, and Giralt M**. Defective thermoregulation, impaired lipid metabolism, but preserved adrenergic induction of gene expression in brown fat of mice lacking C/EBPbeta. *Biochem J* 389: 47-56, 2005.

32. **Carmona MC, Iglesias R, Obregon MJ, Darlington GJ, Villarroya F, and Giralt M**. Mitochondrial biogenesis and thyroid status maturation in brown fat require CCAAT/enhancer-binding protein alpha. *J Biol Chem* 277: 21489-21498, 2002.
33. **Carr SR**. Screening for gestational diabetes mellitus. A perspective in 1998. *Diabetes Care* 21 Suppl 2: B14-18, 1998.
34. **Cernkovich ER, Deng J, Bond MC, Combs TP, and Harp JB**. Adipose-specific disruption of signal transducer and activator of transcription 3 increases body weight and adiposity. *Endocrinology* 149: 1581-1590, 2008.
35. **Chan CB, De Leo D, Joseph JW, McQuaid TS, Ha XF, Xu F, Tsushima RG, Pennefather PS, Salapatek AM, and Wheeler MB**. Increased uncoupling protein-2 levels in beta-cells are associated with impaired glucose-stimulated insulin secretion: mechanism of action. *Diabetes* 50: 1302-1310, 2001.
36. **Chatterjee-Kishore M, Wright KL, Ting JP, and Stark GR**. How Stat1 mediates constitutive gene expression: a complex of unphosphorylated Stat1 and IRF1 supports transcription of the LMP2 gene. *Embo J* 19: 4111-4122, 2000.
37. **Chen H, and Chan DC**. Physiological functions of mitochondrial fusion. *Ann N Y Acad Sci* 1201: 21-25.
38. **Chen H, Vermulst M, Wang YE, Chomyn A, Prolla TA, McCaffery JM, and Chan DC**. Mitochondrial fusion is required for mtDNA stability in skeletal muscle and tolerance of mtDNA mutations. *Cell* 141: 280-289.
39. **Chen M, Cheng A, Candotti F, Zhou YJ, Hymel A, Fasth A, Notarangelo LD, and O'Shea JJ**. Complex effects of naturally occurring mutations in the JAK3 pseudokinase domain: evidence for interactions between the kinase and pseudokinase domains. *Mol Cell Biol* 20: 947-956, 2000.
40. **Chen M, Cheng A, Chen YQ, Hymel A, Hanson EP, Kimmel L, Minami Y, Taniguchi T, Changelian PS, and O'Shea JJ**. The amino terminus of JAK3 is necessary and sufficient for binding to the common gamma chain and confers the ability to transmit interleukin 2-mediated signals. *Proc Natl Acad Sci U S A* 94: 6910-6915, 1997.
41. **Chen X, Vinkemeier U, Zhao Y, Jeruzalmi D, Darnell JE, Jr., and Kuriyan J**. Crystal structure of a tyrosine phosphorylated STAT-1 dimer bound to DNA. *Cell* 93: 827-839, 1998.
42. **Cheng X, and Blumenthal RM**. Coordinated chromatin control: structural and functional linkage of DNA and histone methylation. *Biochemistry* 49: 2999-3008.
43. **Cho ML, Kang JW, Moon YM, Nam HJ, Jhun JY, Heo SB, Jin HT, Min SY, Ju JH, Park KS, Cho YG, Yoon CH, Park SH, Sung YC, and Kim HY**. STAT3 and NF-kappaB signal pathway is required for IL-23-mediated IL-17 production in spontaneous arthritis animal model IL-1 receptor antagonist-deficient mice. *J Immunol* 176: 5652-5661, 2006.
44. **Christ B, Yazici E, and Nath A**. Phosphatidylinositol 3-kinase and protein kinase C contribute to the inhibition by interleukin 6 of phosphoenolpyruvate carboxykinase gene expression in cultured rat hepatocytes. *Hepatology* 31: 461-468, 2000.
45. **Christian M, Kiskinis E, Debevec D, Leonardsson G, White R, and Parker MG**. RIP140-targeted repression of gene expression in adipocytes. *Mol Cell Biol* 25: 9383-9391, 2005.

46. **Chuikov S, Levi BP, Smith ML, and Morrison SJ**. Prdm16 promotes stem cell maintenance in multiple tissues, partly by regulating oxidative stress. *Nat Cell Biol* 12: 999-1006.
47. **Chung BM, Kang HC, Han SY, Heo HS, Lee JJ, Jeon J, Lim JY, Shin I, Hong SH, Cho YS, and Kim CG**. Jak2 and Tyk2 are necessary for lineage-specific differentiation, but not for the maintenance of self-renewal of mouse embryonic stem cells. *Biochem Biophys Res Commun* 351: 682-688, 2006.
48. **Civitarese AE, Ukropcova B, Carling S, Hulver M, DeFronzo RA, Mandarino L, Ravussin E, and Smith SR**. Role of adiponectin in human skeletal muscle bioenergetics. *Cell Metab* 4: 75-87, 2006.
49. **Collins S, Cao W, and Robidoux J**. Learning new tricks from old dogs: beta-adrenergic receptors teach new lessons on firing up adipose tissue metabolism. *Mol Endocrinol* 18: 2123-2131, 2004.
50. **Collum RG, Brutsaert S, Lee G, and Schindler C**. A Stat3-interacting protein (StIP1) regulates cytokine signal transduction. *Proc Natl Acad Sci U S A* 97: 10120-10125, 2000.
51. **Copeland NG, Gilbert DJ, Schindler C, Zhong Z, Wen Z, Darnell JE, Jr., Mui AL, Miyajima A, Quelle FW, Ihle JN, and et al.** Distribution of the mammalian Stat gene family in mouse chromosomes. *Genomics* 29: 225-228, 1995.
52. **Crisan M, Casteilla L, Lehr L, Carmona M, Paoloni-Giacobino A, Yap S, Sun B, Leger B, Logar A, Penicaud L, Schrauwen P, Cameron-Smith D, Russell AP, Peault B, and Giacobino JP**. A reservoir of brown adipocyte progenitors in human skeletal muscle. *Stem Cells* 26: 2425-2433, 2008.
53. **Cui X, Zhang L, Luo J, Rajasekaran A, Hazra S, Cacalano N, and Dubinett SM**. Unphosphorylated STAT6 contributes to constitutive cyclooxygenase-2 expression in human non-small cell lung cancer. *Oncogene* 26: 4253-4260, 2007.
54. **Cypess AM, Lehman S, Williams G, Tal I, Rodman D, Goldfine AB, Kuo FC, Palmer EL, Tseng YH, Doria A, Kolodny GM, and Kahn CR**. Identification and importance of brown adipose tissue in adult humans. *N Engl J Med* 360: 1509-1517, 2009.
55. **Darlington GJ, Wang N, and Hanson RW**. C/EBP alpha: a critical regulator of genes governing integrative metabolic processes. *Curr Opin Genet Dev* 5: 565-570, 1995.
56. **Darnell JE, Jr.** Reflections on STAT3, STAT5, and STAT6 as fat STATs. *Proc Natl Acad Sci U S A* 93: 6221-6224, 1996.
57. **Darnell JE, Jr.** STATs and gene regulation. *Science* 277: 1630-1635, 1997.
58. **Dawson MA, Bannister AJ, Gottgens B, Foster SD, Bartke T, Green AR, and Kouzarides T**. JAK2 phosphorylates histone H3Y41 and excludes HP1alpha from chromatin. *Nature* 461: 819-822, 2009.
59. **De Pauw A, Tejerina S, Raes M, Keijer J, and Arnould T**. Mitochondrial (dys)function in adipocyte (de)differentiation and systemic metabolic alterations. *Am J Pathol* 175: 927-939, 2009.
60. **Decker T, Lew DJ, and Darnell JE, Jr.** Two distinct alpha-interferon-dependent signal transduction pathways may contribute to activation of transcription of the guanylate-binding protein gene. *Mol Cell Biol* 11: 5147-5153, 1991.
61. **DeFronzo RA**. Pathogenesis of type 2 diabetes mellitus. *Med Clin North Am* 88: 787-835, ix, 2004.

62. **Deng J, Hua K, Lesser SS, and Harp JB**. Activation of signal transducer and activator of transcription-3 during proliferative phases of 3T3-L1 adipogenesis. *Endocrinology* 141: 2370-2376, 2000.
63. **Dobbins RL, Szczepaniak LS, Bentley B, Esser V, Myhill J, and McGarry JD**. Prolonged inhibition of muscle carnitine palmitoyltransferase-1 promotes intramyocellular lipid accumulation and insulin resistance in rats. *Diabetes* 50: 123-130, 2001.
64. **Doria A, Patti ME, and Kahn CR**. The emerging genetic architecture of type 2 diabetes. *Cell Metab* 8: 186-200, 2008.
65. **Durbin JE, Hackenmiller R, Simon MC, and Levy DE**. Targeted disruption of the mouse Stat1 gene results in compromised innate immunity to viral disease. *Cell* 84: 443-450, 1996.
66. **Enerback S**. Human brown adipose tissue. *Cell Metab* 11: 248-252.
67. **Enerback S, Jacobsson A, Simpson EM, Guerra C, Yamashita H, Harper ME, and Kozak LP**. Mice lacking mitochondrial uncoupling protein are cold-sensitive but not obese. *Nature* 387: 90-94, 1997.
68. **Erlanson-Albertsson C**. The role of uncoupling proteins in the regulation of metabolism. *Acta Physiol Scand* 178: 405-412, 2003.
69. **Erol A**. Insulin resistance is an evolutionarily conserved physiological mechanism at the cellular level for protection against increased oxidative stress. *Bioessays* 29: 811-818, 2007.
70. **Fasshauer M, Klein J, Kriauciunas KM, Ueki K, Benito M, and Kahn CR**. Essential role of insulin receptor substrate 1 in differentiation of brown adipocytes. *Mol Cell Biol* 21: 319-329, 2001.
71. **Fasshauer M, Klein J, Ueki K, Kriauciunas KM, Benito M, White MF, and Kahn CR**. Essential role of insulin receptor substrate-2 in insulin stimulation of Glut4 translocation and glucose uptake in brown adipocytes. *J Biol Chem* 275: 25494-25501, 2000.
72. **Fearnside JF, Dumas ME, Rothwell AR, Wilder SP, Cloarec O, Toye A, Blancher C, Holmes E, Tatoud R, Barton RH, Scott J, Nicholson JK, and Gauguier D**. Phylometabonomic patterns of adaptation to high fat diet feeding in inbred mice. *PLoS One* 3: e1668, 2008.
73. **Feldmann HM, Golozoubova V, Cannon B, and Nedergaard J**. UCP1 ablation induces obesity and abolishes diet-induced thermogenesis in mice exempt from thermal stress by living at thermoneutrality. *Cell Metab* 9: 203-209, 2009.
74. **Finbloom DS, and Larner AC**. Regulation of the Jak/STAT signalling pathway. *Cell Signal* 7: 739-745, 1995.
75. **Firmbach-Kraft I, Byers M, Shows T, Dalla-Favera R, and Krolewski JJ**. tyk2, prototype of a novel class of non-receptor tyrosine kinase genes. *Oncogene* 5: 1329-1336, 1990.
76. **Forner F, Kumar C, Luber CA, Fromme T, Klingenspor M, and Mann M**. Proteome differences between brown and white fat mitochondria reveal specialized metabolic functions. *Cell Metab* 10: 324-335, 2009.
77. **Fouse SD, Shen Y, Pellegrini M, Cole S, Meissner A, Van Neste L, Jaenisch R, and Fan G**. Promoter CpG methylation contributes to ES cell gene regulation in

parallel with Oct4/Nanog, PcG complex, and histone H3 K4/K27 trimethylation. *Cell Stem Cell* 2: 160-169, 2008.
78. **Freytag SO, Paielli DL, and Gilbert JD**. Ectopic expression of the CCAAT/enhancer-binding protein alpha promotes the adipogenic program in a variety of mouse fibroblastic cells. *Genes Dev* 8: 1654-1663, 1994.
79. **Fruhbeck G, Becerril S, Sainz N, Garrastachu P, and Garcia-Velloso MJ**. BAT: a new target for human obesity? *Trends Pharmacol Sci* 30: 387-396, 2009.
80. **Fujitani Y, Hibi M, Fukada T, Takahashi-Tezuka M, Yoshida H, Yamaguchi T, Sugiyama K, Yamanaka Y, Nakajima K, and Hirano T**. An alternative pathway for STAT activation that is mediated by the direct interaction between JAK and STAT. *Oncogene* 14: 751-761, 1997.
81. **Fukuchi K, Tatsumi M, Ishida Y, Oku N, Hatazawa J, and Wahl RL**. Radionuclide imaging metabolic activity of brown adipose tissue in a patient with pheochromocytoma. *Exp Clin Endocrinol Diabetes* 112: 601-603, 2004.
82. **Gallou-Kabani C, Vige A, Gross MS, Rabes JP, Boileau C, Larue-Achagiotis C, Tome D, Jais JP, and Junien C**. C57BL/6J and A/J mice fed a high-fat diet delineate components of metabolic syndrome. *Obesity (Silver Spring)* 15: 1996-2005, 2007.
83. **Gao Q, Wolfgang MJ, Neschen S, Morino K, Horvath TL, Shulman GI, and Fu XY**. Disruption of neural signal transducer and activator of transcription 3 causes obesity, diabetes, infertility, and thermal dysregulation. *Proc Natl Acad Sci U S A* 101: 4661-4666, 2004.
84. **Gaster M, Rustan AC, Aas V, and Beck-Nielsen H**. Reduced lipid oxidation in skeletal muscle from type 2 diabetic subjects may be of genetic origin: evidence from cultured myotubes. *Diabetes* 53: 542-548, 2004.
85. **Gauzzi MC, Barbieri G, Richter MF, Uze G, Ling L, Fellous M, and Pellegrini S**. The amino-terminal region of Tyk2 sustains the level of interferon alpha receptor 1, a component of the interferon alpha/beta receptor. *Proc Natl Acad Sci U S A* 94: 11839-11844, 1997.
86. **Gelling RW, Yan W, Al-Noori S, Pardini A, Morton GJ, Ogimoto K, Schwartz MW, and Dempsey PJ**. Deficiency of TNFalpha converting enzyme (TACE/ADAM17) causes a lean, hypermetabolic phenotype in mice. *Endocrinology* 149: 6053-6064, 2008.
87. **Gesta S, Tseng YH, and Kahn CR**. Developmental origin of fat: tracking obesity to its source. *Cell* 131: 242-256, 2007.
88. **Ghilardi N, Ziegler S, Wiestner A, Stoffel R, Heim MH, and Skoda RC**. Defective STAT signaling by the leptin receptor in diabetic mice. *Proc Natl Acad Sci U S A* 93: 6231-6235, 1996.
89. **Ghorbani M, and Himms-Hagen J**. Appearance of brown adipocytes in white adipose tissue during CL 316,243-induced reversal of obesity and diabetes in Zucker fa/fa rats. *Int J Obes Relat Metab Disord* 21: 465-475, 1997.
90. **Ghoreschi K, Laurence A, and O'Shea JJ**. Janus kinases in immune cell signaling. *Immunol Rev* 228: 273-287, 2009.
91. **Gingras S, Simard J, Groner B, and Pfitzner E**. p300/CBP is required for transcriptional induction by interleukin-4 and interacts with Stat6. *Nucleic Acids Res* 27: 2722-2729, 1999.

92. **Gong DW, He Y, and Reitman ML**. Genomic organization and regulation by dietary fat of the uncoupling protein 3 and 2 genes. *Biochem Biophys Res Commun* 256: 27-32, 1999.
93. **Gong J, Sun Z, and Li P**. CIDE proteins and metabolic disorders. *Curr Opin Lipidol* 20: 121-126, 2009.
94. **Górnicka A**. Deficiency in the tyrosine kinase Tyk2 in mice facilitates the development of metabolic syndrome. In: *Immunology*. Cleveland: Cleveland Clinic Foundation, 2009.
95. **Gregory L, Came PJ, and Brown S**. Stem cell regulation by JAK/STAT signaling in Drosophila. *Semin Cell Dev Biol* 19: 407-413, 2008.
96. **Gupta A, and Gupta V**. Metabolic syndrome: what are the risks for humans? *Biosci Trends* 4: 204-212.
97. **Gupta S, Yan H, Wong LH, Ralph S, Krolewski J, and Schindler C**. The SH2 domains of Stat1 and Stat2 mediate multiple interactions in the transduction of IFN-alpha signals. *Embo J* 15: 1075-1084, 1996.
98. **Haan C, Kreis S, Margue C, and Behrmann I**. Jaks and cytokine receptors--an intimate relationship. *Biochem Pharmacol* 72: 1538-1546, 2006.
99. **Hansen JB, and Kristiansen K**. Regulatory circuits controlling white versus brown adipocyte differentiation. *Biochem J* 398: 153-168, 2006.
100. **Heidorn SJ, Milagre C, Whittaker S, Nourry A, Niculescu-Duvas I, Dhomen N, Hussain J, Reis-Filho JS, Springer CJ, Pritchard C, and Marais R**. Kinase-dead BRAF and oncogenic RAS cooperate to drive tumor progression through CRAF. *Cell* 140: 209-221.
101. **Heilbronn L, Smith SR, and Ravussin E**. Failure of fat cell proliferation, mitochondrial function and fat oxidation results in ectopic fat storage, insulin resistance and type II diabetes mellitus. *Int J Obes Relat Metab Disord* 28 Suppl 4: S12-21, 2004.
102. **Himpe E, and Kooijman R**. Insulin-like growth factor-I receptor signal transduction and the Janus Kinase/Signal Transducer and Activator of Transcription (JAK-STAT) pathway. *Biofactors* 35: 76-81, 2009.
103. **Horvath CM, Stark GR, Kerr IM, and Darnell JE, Jr.** Interactions between STAT and non-STAT proteins in the interferon-stimulated gene factor 3 transcription complex. *Mol Cell Biol* 16: 6957-6964, 1996.
104. **Huang LJ, Constantinescu SN, and Lodish HF**. The N-terminal domain of Janus kinase 2 is required for Golgi processing and cell surface expression of erythropoietin receptor. *Mol Cell* 8: 1327-1338, 2001.
105. **Ihle JN**. Cytokine receptor signalling. *Nature* 377: 591-594, 1995.
106. **Imada K, and Leonard WJ**. The Jak-STAT pathway. *Mol Immunol* 37: 1-11, 2000.
107. **Imai T, Takakuwa R, Marchand S, Dentz E, Bornert JM, Messaddeq N, Wendling O, Mark M, Desvergne B, Wahli W, Chambon P, and Metzger D**. Peroxisome proliferator-activated receptor gamma is required in mature white and brown adipocytes for their survival in the mouse. *Proc Natl Acad Sci U S A* 101: 4543-4547, 2004.
108. **Inoue H, Ogawa W, Ozaki M, Haga S, Matsumoto M, Furukawa K, Hashimoto N, Kido Y, Mori T, Sakaue H, Teshigawara K, Jin S, Iguchi H, Hiramatsu R, LeRoith D, Takeda K, Akira S, and Kasuga M**. Role of STAT-3 in

regulation of hepatic gluconeogenic genes and carbohydrate metabolism in vivo. *Nat Med* 10: 168-174, 2004.
109. **Iyer J, and Reich NC**. Constitutive nuclear import of latent and activated STAT5a by its coiled coil domain. *Faseb J* 22: 391-400, 2008.
110. **Jahromi MM, and Eisenbarth GS**. Cellular and molecular pathogenesis of type 1A diabetes. *Cell Mol Life Sci* 64: 865-872, 2007.
111. **Jakobsson A, Jorgensen JA, and Jacobsson A**. Differential regulation of fatty acid elongation enzymes in brown adipocytes implies a unique role for Elovl3 during increased fatty acid oxidation. *Am J Physiol Endocrinol Metab* 289: E517-526, 2005.
112. **Jia JJ, Tian YB, Cao ZH, Tao LL, Zhang X, Gao SZ, Ge CR, Lin QY, and Jois M**. The polymorphisms of UCP1 genes associated with fat metabolism, obesity and diabetes. *Mol Biol Rep* 37: 1513-1522.
113. **Kajimura S, Seale P, Kubota K, Lunsford E, Frangioni JV, Gygi SP, and Spiegelman BM**. Initiation of myoblast to brown fat switch by a PRDM16-C/EBP-beta transcriptional complex. *Nature* 460: 1154-1158, 2009.
114. **Kajimura S, Seale P, Tomaru T, Erdjument-Bromage H, Cooper MP, Ruas JL, Chin S, Tempst P, Lazar MA, and Spiegelman BM**. Regulation of the brown and white fat gene programs through a PRDM16/CtBP transcriptional complex. *Genes Dev* 22: 1397-1409, 2008.
115. **Kannan N, and Taylor SS**. Rethinking pseudokinases. *Cell* 133: 204-205, 2008.
116. **Kaplan MH, Schindler U, Smiley ST, and Grusby MJ**. Stat6 is required for mediating responses to IL-4 and for development of Th2 cells. *Immunity* 4: 313-319, 1996.
117. **Kaplan MH, Sun YL, Hoey T, and Grusby MJ**. Impaired IL-12 responses and enhanced development of Th2 cells in Stat4-deficient mice. *Nature* 382: 174-177, 1996.
118. **Karaghiosoff M, Neubauer H, Lassnig C, Kovarik P, Schindler H, Pircher H, McCoy B, Bogdan C, Decker T, Brem G, Pfeffer K, and Muller M**. Partial impairment of cytokine responses in Tyk2-deficient mice. *Immunity* 13: 549-560, 2000.
119. **Karamanlidis G, Karamitri A, Docherty K, Hazlerigg DG, and Lomax MA**. C/EBPbeta reprograms white 3T3-L1 preadipocytes to a Brown adipocyte pattern of gene expression. *J Biol Chem* 282: 24660-24669, 2007.
120. **Kashyap SR, Belfort R, Berria R, Suraamornkul S, Pratipranawatr T, Finlayson J, Barrentine A, Bajaj M, Mandarino L, DeFronzo R, and Cusi K**. Discordant effects of a chronic physiological increase in plasma FFA on insulin signaling in healthy subjects with or without a family history of type 2 diabetes. *Am J Physiol Endocrinol Metab* 287: E537-546, 2004.
121. **Kawamura M, McVicar DW, Johnston JA, Blake TB, Chen YQ, Lal BK, Lloyd AR, Kelvin DJ, Staples JE, Ortaldo JR, and et al.** Molecular cloning of L-JAK, a Janus family protein-tyrosine kinase expressed in natural killer cells and activated leukocytes. *Proc Natl Acad Sci U S A* 91: 6374-6378, 1994.
122. **Kelley DE, He J, Menshikova EV, and Ritov VB**. Dysfunction of mitochondria in human skeletal muscle in type 2 diabetes. *Diabetes* 51: 2944-2950, 2002.
123. **Kiskinis E, Hallberg M, Christian M, Olofsson M, Dilworth SM, White R, and Parker MG**. RIP140 directs histone and DNA methylation to silence Ucp1 expression in white adipocytes. *Embo J* 26: 4831-4840, 2007.

124. **Kisseleva T, Bhattacharya S, Braunstein J, and Schindler CW**. Signaling through the JAK/STAT pathway, recent advances and future challenges. *Gene* 285: 1-24, 2002.
125. **Klingenberg M, and Echtay KS**. Uncoupling proteins: the issues from a biochemist point of view. *Biochim Biophys Acta* 1504: 128-143, 2001.
126. **Kopecky J, Clarke G, Enerback S, Spiegelman B, and Kozak LP**. Expression of the mitochondrial uncoupling protein gene from the aP2 gene promoter prevents genetic obesity. *J Clin Invest* 96: 2914-2923, 1995.
127. **Kozak LP, and Anunciado-Koza R**. UCP1: its involvement and utility in obesity. *Int J Obes (Lond)* 32 Suppl 7: S32-38, 2008.
128. **Krolewski JJ, Lee R, Eddy R, Shows TB, and Dalla-Favera R**. Identification and chromosomal mapping of new human tyrosine kinase genes. *Oncogene* 5: 277-282, 1990.
129. **Krssak M, and Roden M**. The role of lipid accumulation in liver and muscle for insulin resistance and type 2 diabetes mellitus in humans. *Rev Endocr Metab Disord* 5: 127-134, 2004.
130. **Kus V, Prazak T, Brauner P, Hensler M, Kuda O, Flachs P, Janovska P, Medrikova D, Rossmeisl M, Jilkova Z, Stefl B, Pastalkova E, Drahota Z, Houstek J, and Kopecky J**. Induction of muscle thermogenesis by high-fat diet in mice: association with obesity-resistance. *Am J Physiol Endocrinol Metab* 295: E356-367, 2008.
131. **Leonard WJ**. STATs and cytokine specificity. *Nat Med* 2: 968-969, 1996.
132. **Leonard WJ, and O'Shea JJ**. Jaks and STATs: biological implications. *Annu Rev Immunol* 16: 293-322, 1998.
133. **Lettner A, and Roden M**. Ectopic fat and insulin resistance. *Curr Diab Rep* 8: 185-191, 2008.
134. **Levy DE, and Darnell JE, Jr.** Stats: transcriptional control and biological impact. *Nat Rev Mol Cell Biol* 3: 651-662, 2002.
135. **Li WX**. Canonical and non-canonical JAK-STAT signaling. *Trends Cell Biol* 18: 545-551, 2008.
136. **Li X, Leung S, Kerr IM, and Stark GR**. Functional subdomains of STAT2 required for preassociation with the alpha interferon receptor and for signaling. *Mol Cell Biol* 17: 2048-2056, 1997.
137. **Li YQ**. Master stem cell transcription factors and signaling regulation. *Cell Reprogram* 12: 3-13.
138. **Liang P, Hughes V, and Fukagawa NK**. Increased prevalence of mitochondrial DNA deletions in skeletal muscle of older individuals with impaired glucose tolerance: possible marker of glycemic stress. *Diabetes* 46: 920-923, 1997.
139. **Lim JH, Lee JI, Suh YH, Kim W, Song JH, and Jung MH**. Mitochondrial dysfunction induces aberrant insulin signalling and glucose utilisation in murine C2C12 myotube cells. *Diabetologia* 49: 1924-1936, 2006.
140. **Lin B, Coughlin S, and Pilch PF**. Bidirectional regulation of uncoupling protein-3 and GLUT-4 mRNA in skeletal muscle by cold. *Am J Physiol* 275: E386-391, 1998.
141. **Lin J, Wu PH, Tarr PT, Lindenberg KS, St-Pierre J, Zhang CY, Mootha VK, Jager S, Vianna CR, Reznick RM, Cui L, Manieri M, Donovan MX, Wu Z, Cooper MP, Fan MC, Rohas LM, Zavacki AM, Cinti S, Shulman GI, Lowell BB,**

Krainc D, and Spiegelman BM. Defects in adaptive energy metabolism with CNS-linked hyperactivity in PGC-1alpha null mice. *Cell* 119: 121-135, 2004.
142. **Liu L, McBride KM, and Reich NC**. STAT3 nuclear import is independent of tyrosine phosphorylation and mediated by importin-alpha3. *Proc Natl Acad Sci U S A* 102: 8150-8155, 2005.
143. **Liu X, Robinson GW, Wagner KU, Garrett L, Wynshaw-Boris A, and Hennighausen L**. Stat5a is mandatory for adult mammary gland development and lactogenesis. *Genes Dev* 11: 179-186, 1997.
144. **Lowell BB, and Bachman ES**. Beta-Adrenergic receptors, diet-induced thermogenesis, and obesity. *J Biol Chem* 278: 29385-29388, 2003.
145. **Lowell BB, and Spiegelman BM**. Towards a molecular understanding of adaptive thermogenesis. *Nature* 404: 652-660, 2000.
146. **Lowell BB, V SS, Hamann A, Lawitts JA, Himms-Hagen J, Boyer BB, Kozak LP, and Flier JS**. Development of obesity in transgenic mice after genetic ablation of brown adipose tissue. *Nature* 366: 740-742, 1993.
147. **Lufei C, Ma J, Huang G, Zhang T, Novotny-Diermayr V, Ong CT, and Cao X**. GRIM-19, a death-regulatory gene product, suppresses Stat3 activity via functional interaction. *Embo J* 22: 1325-1335, 2003.
148. **Macchi P, Villa A, Giliani S, Sacco MG, Frattini A, Porta F, Ugazio AG, Johnston JA, Candotti F, O'Shea JJ, and et al.** Mutations of Jak-3 gene in patients with autosomal severe combined immune deficiency (SCID). *Nature* 377: 65-68, 1995.
149. **Maechler P, and Wollheim CB**. Mitochondrial function in normal and diabetic beta-cells. *Nature* 414: 807-812, 2001.
150. **Mallone R, and Perin PC**. Anti-CD38 autoantibodies in type? diabetes. *Diabetes Metab Res Rev* 22: 284-294, 2006.
151. **Manning G, Whyte DB, Martinez R, Hunter T, and Sudarsanam S**. The protein kinase complement of the human genome. *Science* 298: 1912-1934, 2002.
152. **Meraz MA, White JM, Sheehan KC, Bach EA, Rodig SJ, Dighe AS, Kaplan DH, Riley JK, Greenlund AC, Campbell D, Carver-Moore K, DuBois RN, Clark R, Aguet M, and Schreiber RD**. Targeted disruption of the Stat1 gene in mice reveals unexpected physiologic specificity in the JAK-STAT signaling pathway. *Cell* 84: 431-442, 1996.
153. **Mesaros A, Koralov SB, Rother E, Wunderlich FT, Ernst MB, Barsh GS, Rajewsky K, and Bruning JC**. Activation of Stat3 signaling in AgRP neurons promotes locomotor activity. *Cell Metab* 7: 236-248, 2008.
154. **Minegishi Y, Saito M, Morio T, Watanabe K, Agematsu K, Tsuchiya S, Takada H, Hara T, Kawamura N, Ariga T, Kaneko H, Kondo N, Tsuge I, Yachie A, Sakiyama Y, Iwata T, Bessho F, Ohishi T, Joh K, Imai K, Kogawa K, Shinohara M, Fujieda M, Wakiguchi H, Pasic S, Abinun M, Ochs HD, Renner ED, Jansson A, Belohradsky BH, Metin A, Shimizu N, Mizutani S, Miyawaki T, Nonoyama S, and Karasuyama H**. Human tyrosine kinase 2 deficiency reveals its requisite roles in multiple cytokine signals involved in innate and acquired immunity. *Immunity* 25: 745-755, 2006.
155. **Miranda PJ, DeFronzo RA, Califf RM, and Guyton JR**. Metabolic syndrome: definition, pathophysiology, and mechanisms. *Am Heart J* 149: 33-45, 2005.

156. **Mootha VK, Lindgren CM, Eriksson KF, Subramanian A, Sihag S, Lehar J, Puigserver P, Carlsson E, Ridderstrale M, Laurila E, Houstis N, Daly MJ, Patterson N, Mesirov JP, Golub TR, Tamayo P, Spiegelman B, Lander ES, Hirschhorn JN, Altshuler D, and Groop LC**. PGC-1alpha-responsive genes involved in oxidative phosphorylation are coordinately downregulated in human diabetes. *Nat Genet* 34: 267-273, 2003.
157. **Moriggl R, Gouilleux-Gruart V, Jahne R, Berchtold S, Gartmann C, Liu X, Hennighausen L, Sotiropoulos A, Groner B, and Gouilleux F**. Deletion of the carboxyl-terminal transactivation domain of MGF-Stat5 results in sustained DNA binding and a dominant negative phenotype. *Mol Cell Biol* 16: 5691-5700, 1996.
158. **Moriggl R, Topham DJ, Teglund S, Sexl V, McKay C, Wang D, Hoffmeyer A, van Deursen J, Sangster MY, Bunting KD, Grosveld GC, and Ihle JN**. Stat5 is required for IL-2-induced cell cycle progression of peripheral T cells. *Immunity* 10: 249-259, 1999.
159. **Morrison SF, Nakamura K, and Madden CJ**. Central control of thermogenesis in mammals. *Exp Physiol* 93: 773-797, 2008.
160. **Mowen KA, Tang J, Zhu W, Schurter BT, Shuai K, Herschman HR, and David M**. Arginine methylation of STAT1 modulates IFNalpha/beta-induced transcription. *Cell* 104: 731-741, 2001.
161. **Mukherjee K, Sharma M, Urlaub H, Bourenkov GP, Jahn R, Sudhof TC, and Wahl MC**. CASK Functions as a Mg2+-independent neurexin kinase. *Cell* 133: 328-339, 2008.
162. **Muller M, Briscoe J, Laxton C, Guschin D, Ziemiecki A, Silvennoinen O, Harpur AG, Barbieri G, Witthuhn BA, Schindler C, and et al.** The protein tyrosine kinase JAK1 complements defects in interferon-alpha/beta and -gamma signal transduction. *Nature* 366: 129-135, 1993.
163. **Murphy TL, Geissal ED, Farrar JD, and Murphy KM**. Role of the Stat4 N domain in receptor proximal tyrosine phosphorylation. *Mol Cell Biol* 20: 7121-7131, 2000.
164. **Murray PJ**. The JAK-STAT signaling pathway: input and output integration. *J Immunol* 178: 2623-2629, 2007.
165. **Musso T, Johnston JA, Linnekin D, Varesio L, Rowe TK, O'Shea JJ, and McVicar DW**. Regulation of JAK3 expression in human monocytes: phosphorylation in response to interleukins 2, 4, and 7. *J Exp Med* 181: 1425-1431, 1995.
166. **Nedergaard J, Bengtsson T, and Cannon B**. Unexpected evidence for active brown adipose tissue in adult humans. *Am J Physiol Endocrinol Metab* 293: E444-452, 2007.
167. **Neubauer H, Cumano A, Muller M, Wu H, Huffstadt U, and Pfeffer K**. Jak2 deficiency defines an essential developmental checkpoint in definitive hematopoiesis. *Cell* 93: 397-409, 1998.
168. **Newbold RR**. Impact of environmental endocrine disrupting chemicals on the development of obesity. *Hormones (Athens)* 9: 206-217.
169. **Nishikata I, Sasaki H, Iga M, Tateno Y, Imayoshi S, Asou N, Nakamura T, and Morishita K**. A novel EVI1 gene family, MEL1, lacking a PR domain (MEL1S) is expressed mainly in t(1;3)(p36;q21)-positive AML and blocks G-CSF-induced myeloid differentiation. *Blood* 102: 3323-3332, 2003.

170. **Nosaka T, van Deursen JM, Tripp RA, Thierfelder WE, Witthuhn BA, McMickle AP, Doherty PC, Grosveld GC, and Ihle JN**. Defective lymphoid development in mice lacking Jak3. *Science* 270: 800-802, 1995.
171. **O'Shea JJ, Gadina M, and Schreiber RD**. Cytokine signaling in 2002: new surprises in the Jak/Stat pathway. *Cell* 109 Suppl: S121-131, 2002.
172. **Ochrietor JD, Harrison KA, Zahedi K, and Mortensen RF**. Role of STAT3 and C/EBP in cytokine-dependent expression of the mouse serum amyloid P-component (SAP) and C-reactive protein (CRP) genes. *Cytokine* 12: 888-899, 2000.
173. **Otto TC, and Lane MD**. Adipose development: from stem cell to adipocyte. *Crit Rev Biochem Mol Biol* 40: 229-242, 2005.
174. **Ouchi T, Lee SW, Ouchi M, Aaronson SA, and Horvath CM**. Collaboration of signal transducer and activator of transcription 1 (STAT1) and BRCA1 in differential regulation of IFN-gamma target genes. *Proc Natl Acad Sci U S A* 97: 5208-5213, 2000.
175. **Parganas E, Wang D, Stravopodis D, Topham DJ, Marine JC, Teglund S, Vanin EF, Bodner S, Colamonici OR, van Deursen JM, Grosveld G, and Ihle JN**. Jak2 is essential for signaling through a variety of cytokine receptors. *Cell* 93: 385-395, 1998.
176. **Parham C, Chirica M, Timans J, Vaisberg E, Travis M, Cheung J, Pflanz S, Zhang R, Singh KP, Vega F, To W, Wagner J, O'Farrell AM, McClanahan T, Zurawski S, Hannum C, Gorman D, Rennick DM, Kastelein RA, de Waal Malefyt R, and Moore KW**. A receptor for the heterodimeric cytokine IL-23 is composed of IL-12Rbeta1 and a novel cytokine receptor subunit, IL-23R. *J Immunol* 168: 5699-5708, 2002.
177. **Park C, Li S, Cha E, and Schindler C**. Immune response in Stat2 knockout mice. *Immunity* 13: 795-804, 2000.
178. **Park OK, Schaefer LK, Wang W, and Schaefer TS**. Dimer stability as a determinant of differential DNA binding activity of Stat3 isoforms. *J Biol Chem* 275: 32244-32249, 2000.
179. **Park SY, Saijo K, Takahashi T, Osawa M, Arase H, Hirayama N, Miyake K, Nakauchi H, Shirasawa T, and Saito T**. Developmental defects of lymphoid cells in Jak3 kinase-deficient mice. *Immunity* 3: 771-782, 1995.
180. **Patti ME, Butte AJ, Crunkhorn S, Cusi K, Berria R, Kashyap S, Miyazaki Y, Kohane I, Costello M, Saccone R, Landaker EJ, Goldfine AB, Mun E, DeFronzo R, Finlayson J, Kahn CR, and Mandarino LJ**. Coordinated reduction of genes of oxidative metabolism in humans with insulin resistance and diabetes: Potential role of PGC1 and NRF1. *Proc Natl Acad Sci U S A* 100: 8466-8471, 2003.
181. **Paulson M, Pisharody S, Pan L, Guadagno S, Mui AL, and Levy DE**. Stat protein transactivation domains recruit p300/CBP through widely divergent sequences. *J Biol Chem* 274: 25343-25349, 1999.
182. **Pearse RN, Feinman R, and Ravetch JV**. Characterization of the promoter of the human gene encoding the high-affinity IgG receptor: transcriptional induction by gamma-interferon is mediated through common DNA response elements. *Proc Natl Acad Sci U S A* 88: 11305-11309, 1991.
183. **Pellegrini S, and Dusanter-Fourt I**. The structure, regulation and function of the Janus kinases (JAKs) and the signal transducers and activators of transcription (STATs). *Eur J Biochem* 248: 615-633, 1997.

184. **Pesu M, Takaluoma K, Aittomaki S, Lagerstedt A, Saksela K, Kovanen PE, and Silvennoinen O**. Interleukin-4-induced transcriptional activation by stat6 involves multiple serine/threonine kinase pathways and serine phosphorylation of stat6. *Blood* 95: 494-502, 2000.
185. **Petersen KF, Dufour S, Befroy D, Garcia R, and Shulman GI**. Impaired mitochondrial activity in the insulin-resistant offspring of patients with type 2 diabetes. *N Engl J Med* 350: 664-671, 2004.
186. **Petersen KF, Dufour S, and Shulman GI**. Decreased insulin-stimulated ATP synthesis and phosphate transport in muscle of insulin-resistant offspring of type 2 diabetic parents. *PLoS Med* 2: e233, 2005.
187. **Pietropaolo M, Barinas-Mitchell E, and Kuller LH**. The heterogeneity of diabetes: unraveling a dispute: is systemic inflammation related to islet autoimmunity? *Diabetes* 56: 1189-1197, 2007.
188. **Plagemann A, Harder T, Brunn M, Harder A, Roepke K, Wittrock-Staar M, Ziska T, Schellong K, Rodekamp E, Melchior K, and Dudenhausen JW**. Hypothalamic proopiomelanocortin promoter methylation becomes altered by early overfeeding: an epigenetic model of obesity and the metabolic syndrome. *J Physiol* 587: 4963-4976, 2009.
189. **Poli V**. The role of C/EBP isoforms in the control of inflammatory and native immunity functions. *J Biol Chem* 273: 29279-29282, 1998.
190. **Postic C, and Girard J**. Contribution of de novo fatty acid synthesis to hepatic steatosis and insulin resistance: lessons from genetically engineered mice. *J Clin Invest* 118: 829-838, 2008.
191. **Potla R, Koeck T, Wegrzyn J, Cherukuri S, Shimoda K, Baker DP, Wolfman J, Planchon SM, Esposito C, Hoit B, Dulak J, Wolfman A, Stuehr D, and Larner AC**. Tyk2 tyrosine kinase expression is required for the maintenance of mitochondrial respiration in primary pro-B lymphocytes. *Mol Cell Biol* 26: 8562-8571, 2006.
192. **Powelka AM, Seth A, Virbasius JV, Kiskinis E, Nicoloro SM, Guilherme A, Tang X, Straubhaar J, Cherniack AD, Parker MG, and Czech MP**. Suppression of oxidative metabolism and mitochondrial biogenesis by the transcriptional corepressor RIP140 in mouse adipocytes. *J Clin Invest* 116: 125-136, 2006.
193. **Puigserver P, Rhee J, Lin J, Wu Z, Yoon JC, Zhang CY, Krauss S, Mootha VK, Lowell BB, and Spiegelman BM**. Cytokine stimulation of energy expenditure through p38 MAP kinase activation of PPARgamma coactivator-1. *Mol Cell* 8: 971-982, 2001.
194. **Puigserver P, and Spiegelman BM**. Peroxisome proliferator-activated receptor-gamma coactivator 1 alpha (PGC-1 alpha): transcriptional coactivator and metabolic regulator. *Endocr Rev* 24: 78-90, 2003.
195. **Puigserver P, Wu Z, Park CW, Graves R, Wright M, and Spiegelman BM**. A cold-inducible coactivator of nuclear receptors linked to adaptive thermogenesis. *Cell* 92: 829-839, 1998.
196. **Ragimbeau J, Dondi E, Alcover A, Eid P, Uze G, and Pellegrini S**. The tyrosine kinase Tyk2 controls IFNAR1 cell surface expression. *Embo J* 22: 537-547, 2003.

197. **Ragimbeau J, Dondi E, Vasserot A, Romero P, Uze G, and Pellegrini S**. The receptor interaction region of Tyk2 contains a motif required for its nuclear localization. *J Biol Chem* 276: 30812-30818, 2001.
198. **Rawlings JS, Rosler KM, and Harrison DA**. The JAK/STAT signaling pathway. *J Cell Sci* 117: 1281-1283, 2004.
199. **Reich NC, and Liu L**. Tracking STAT nuclear traffic. *Nat Rev Immunol* 6: 602-612, 2006.
200. **Ren D, Collingwood TN, Rebar EJ, Wolffe AP, and Camp HS**. PPARgamma knockdown by engineered transcription factors: exogenous PPARgamma2 but not PPARgamma1 reactivates adipogenesis. *Genes Dev* 16: 27-32, 2002.
201. **Ripperger JA, Fritz S, Richter K, Hocke GM, Lottspeich F, and Fey GH**. Transcription factors Stat3 and Stat5b are present in rat liver nuclei late in an acute phase response and bind interleukin-6 response elements. *J Biol Chem* 270: 29998-30006, 1995.
202. **Roden M**. Muscle triglycerides and mitochondrial function: possible mechanisms for the development of type 2 diabetes. *Int J Obes (Lond)* 29 Suppl 2: S111-115, 2005.
203. **Rodgers JT, Lerin C, Haas W, Gygi SP, Spiegelman BM, and Puigserver P**. Nutrient control of glucose homeostasis through a complex of PGC-1alpha and SIRT1. *Nature* 434: 113-118, 2005.
204. **Rodig SJ, Meraz MA, White JM, Lampe PA, Riley JK, Arthur CD, King KL, Sheehan KC, Yin L, Pennica D, Johnson EM, Jr., and Schreiber RD**. Disruption of the Jak1 gene demonstrates obligatory and nonredundant roles of the Jaks in cytokine-induced biologic responses. *Cell* 93: 373-383, 1998.
205. **Rosen ED, Walkey CJ, Puigserver P, and Spiegelman BM**. Transcriptional regulation of adipogenesis. *Genes Dev* 14: 1293-1307, 2000.
206. **Rousset S, Alves-Guerra MC, Mozo J, Miroux B, Cassard-Doulcier AM, Bouillaud F, and Ricquier D**. The biology of mitochondrial uncoupling proteins. *Diabetes* 53 Suppl 1: S130-135, 2004.
207. **Russell SM, Tayebi N, Nakajima H, Riedy MC, Roberts JL, Aman MJ, Migone TS, Noguchi M, Markert ML, Buckley RH, O'Shea JJ, and Leonard WJ**. Mutation of Jak3 in a patient with SCID: essential role of Jak3 in lymphoid development. *Science* 270: 797-800, 1995.
208. **Saharinen P, and Silvennoinen O**. The pseudokinase domain is required for suppression of basal activity of Jak2 and Jak3 tyrosine kinases and for cytokine-inducible activation of signal transduction. *J Biol Chem* 277: 47954-47963, 2002.
209. **Saharinen P, Takaluoma K, and Silvennoinen O**. Regulation of the Jak2 tyrosine kinase by its pseudokinase domain. *Mol Cell Biol* 20: 3387-3395, 2000.
210. **Saito M, Okamatsu-Ogura Y, Matsushita M, Watanabe K, Yoneshiro T, Nio-Kobayashi J, Iwanaga T, Miyagawa M, Kameya T, Nakada K, Kawai Y, and Tsujisaki M**. High incidence of metabolically active brown adipose tissue in healthy adult humans: effects of cold exposure and adiposity. *Diabetes* 58: 1526-1531, 2009.
211. **Schaefer TS, Sanders LK, Park OK, and Nathans D**. Functional differences between Stat3alpha and Stat3beta. *Mol Cell Biol* 17: 5307-5316, 1997.
212. **Schindler C, Fu XY, Improta T, Aebersold R, and Darnell JE, Jr.** Proteins of transcription factor ISGF-3: one gene encodes the 91-and 84-kDa ISGF-3 proteins that are activated by interferon alpha. *Proc Natl Acad Sci U S A* 89: 7836-7839, 1992.

213. **Schrauwen P, and Hesselink M**. UCP2 and UCP3 in muscle controlling body metabolism. *J Exp Biol* 205: 2275-2285, 2002.
214. **Schrauwen P, Hoppeler H, Billeter R, Bakker AH, and Pendergast DR**. Fiber type dependent upregulation of human skeletal muscle UCP2 and UCP3 mRNA expression by high-fat diet. *Int J Obes Relat Metab Disord* 25: 449-456, 2001.
215. **Seale P, Bjork B, Yang W, Kajimura S, Chin S, Kuang S, Scime A, Devarakonda S, Conroe HM, Erdjument-Bromage H, Tempst P, Rudnicki MA, Beier DR, and Spiegelman BM**. PRDM16 controls a brown fat/skeletal muscle switch. *Nature* 454: 961-967, 2008.
216. **Seale P, Conroe HM, Estall J, Kajimura S, Frontini A, Ishibashi J, Cohen P, Cinti S, and Spiegelman BM**. Prdm16 determines the thermogenic program of subcutaneous white adipose tissue in mice. *J Clin Invest*.
217. **Seale P, Kajimura S, Yang W, Chin S, Rohas LM, Uldry M, Tavernier G, Langin D, and Spiegelman BM**. Transcriptional control of brown fat determination by PRDM16. *Cell Metab* 6: 38-54, 2007.
218. **Seto Y, Nakajima H, Suto A, Shimoda K, Saito Y, Nakayama KI, and Iwamoto I**. Enhanced Th2 cell-mediated allergic inflammation in Tyk2-deficient mice. *J Immunol* 170: 1077-1083, 2003.
219. **Sharfe N, Dadi HK, O'Shea JJ, and Roifman CM**. Jak3 activation in human lymphocyte precursor cells. *Clin Exp Immunol* 108: 552-556, 1997.
220. **Shaw MH, Boyartchuk V, Wong S, Karaghiosoff M, Ragimbeau J, Pellegrini S, Muller M, Dietrich WF, and Yap GS**. A natural mutation in the Tyk2 pseudokinase domain underlies altered susceptibility of B10.Q/J mice to infection and autoimmunity. *Proc Natl Acad Sci U S A* 100: 11594-11599, 2003.
221. **Shi S, Calhoun HC, Xia F, Li J, Le L, and Li WX**. JAK signaling globally counteracts heterochromatic gene silencing. *Nat Genet* 38: 1071-1076, 2006.
222. **Shi S, Larson K, Guo D, Lim SJ, Dutta P, Yan SJ, and Li WX**. Drosophila STAT is required for directly maintaining HP1 localization and heterochromatin stability. *Nat Cell Biol* 10: 489-496, 2008.
223. **Shimoda K, Kato K, Aoki K, Matsuda T, Miyamoto A, Shibamori M, Yamashita M, Numata A, Takase K, Kobayashi S, Shibata S, Asano Y, Gondo H, Sekiguchi K, Nakayama K, Nakayama T, Okamura T, Okamura S, Niho Y, and Nakayama K**. Tyk2 plays a restricted role in IFN alpha signaling, although it is required for IL-12-mediated T cell function. *Immunity* 13: 561-571, 2000.
224. **Shimoda K, Tsutsui H, Aoki K, Kato K, Matsuda T, Numata A, Takase K, Yamamoto T, Nukina H, Hoshino T, Asano Y, Gondo H, Okamura T, Okamura S, Nakayama K, Nakanishi K, Niho Y, and Harada M**. Partial impairment of interleukin-12 (IL-12) and IL-18 signaling in Tyk2-deficient mice. *Blood* 99: 2094-2099, 2002.
225. **Shimoda K, van Deursen J, Sangster MY, Sarawar SR, Carson RT, Tripp RA, Chu C, Quelle FW, Nosaka T, Vignali DA, Doherty PC, Grosveld G, Paul WE, and Ihle JN**. Lack of IL-4-induced Th2 response and IgE class switching in mice with disrupted Stat6 gene. *Nature* 380: 630-633, 1996.
226. **Shore A, Karamitri A, Kemp P, Speakman JR, and Lomax MA**. Role of Ucp1 enhancer methylation and chromatin remodelling in the control of Ucp1 expression in murine adipose tissue. *Diabetologia* 53: 1164-1173.

227. **Shuai K**. The STAT family of proteins in cytokine signaling. *Prog Biophys Mol Biol* 71: 405-422, 1999.
228. **Shuai K, Horvath CM, Huang LH, Qureshi SA, Cowburn D, and Darnell JE, Jr.** Interferon activation of the transcription factor Stat91 involves dimerization through SH2-phosphotyrosyl peptide interactions. *Cell* 76: 821-828, 1994.
229. **Shuai K, Liao J, and Song MM**. Enhancement of antiproliferative activity of gamma interferon by the specific inhibition of tyrosine dephosphorylation of Stat1. *Mol Cell Biol* 16: 4932-4941, 1996.
230. **Silva JE**. Thyroid hormone control of thermogenesis and energy balance. *Thyroid* 5: 481-492, 1995.
231. **Skarulis MC, Celi FS, Mueller E, Zemskova M, Malek R, Hugendubler L, Cochran C, Solomon J, Chen C, and Gorden P**. Thyroid hormone induced brown adipose tissue and amelioration of diabetes in a patient with extreme insulin resistance. *J Clin Endocrinol Metab* 95: 256-262.
232. **Spiegelman BM, and Flier JS**. Obesity and the regulation of energy balance. *Cell* 104: 531-543, 2001.
233. **Stephens JM, Morrison RF, and Pilch PF**. The expression and regulation of STATs during 3T3-L1 adipocyte differentiation. *J Biol Chem* 271: 10441-10444, 1996.
234. **Strehlow I, and Schindler C**. Amino-terminal signal transducer and activator of transcription (STAT) domains regulate nuclear translocation and STAT deactivation. *J Biol Chem* 273: 28049-28056, 1998.
235. **Takeda K, Clausen BE, Kaisho T, Tsujimura T, Terada N, Forster I, and Akira S**. Enhanced Th1 activity and development of chronic enterocolitis in mice devoid of Stat3 in macrophages and neutrophils. *Immunity* 10: 39-49, 1999.
236. **Takeda K, Kaisho T, Yoshida N, Takeda J, Kishimoto T, and Akira S**. Stat3 activation is responsible for IL-6-dependent T cell proliferation through preventing apoptosis: generation and characterization of T cell-specific Stat3-deficient mice. *J Immunol* 161: 4652-4660, 1998.
237. **Takeda K, Noguchi K, Shi W, Tanaka T, Matsumoto M, Yoshida N, Kishimoto T, and Akira S**. Targeted disruption of the mouse Stat3 gene leads to early embryonic lethality. *Proc Natl Acad Sci U S A* 94: 3801-3804, 1997.
238. **Tanaka T, Yoshida N, Kishimoto T, and Akira S**. Defective adipocyte differentiation in mice lacking the C/EBPbeta and/or C/EBPdelta gene. *Embo J* 16: 7432-7443, 1997.
239. **Tang QQ, Zhang JW, and Daniel Lane M**. Sequential gene promoter interactions of C/EBPbeta, C/EBPalpha, and PPARgamma during adipogenesis. *Biochem Biophys Res Commun* 319: 235-239, 2004.
240. **Tateishi K, Okada Y, Kallin EM, and Zhang Y**. Role of Jhdm2a in regulating metabolic gene expression and obesity resistance. *Nature* 458: 757-761, 2009.
241. **Teglund S, McKay C, Schuetz E, van Deursen JM, Stravopodis D, Wang D, Brown M, Bodner S, Grosveld G, and Ihle JN**. Stat5a and Stat5b proteins have essential and nonessential, or redundant, roles in cytokine responses. *Cell* 93: 841-850, 1998.
242. **Teyssier C, Ma H, Emter R, Kralli A, and Stallcup MR**. Activation of nuclear receptor coactivator PGC-1alpha by arginine methylation. *Genes Dev* 19: 1466-1473, 2005.

243. **Thierfelder WE, van Deursen JM, Yamamoto K, Tripp RA, Sarawar SR, Carson RT, Sangster MY, Vignali DA, Doherty PC, Grosveld GC, and Ihle JN**. Requirement for Stat4 in interleukin-12-mediated responses of natural killer and T cells. *Nature* 382: 171-174, 1996.
244. **Thomis DC, Gurniak CB, Tivol E, Sharpe AH, and Berg LJ**. Defects in B lymphocyte maturation and T lymphocyte activation in mice lacking Jak3. *Science* 270: 794-797, 1995.
245. **Timmons JA, Wennmalm K, Larsson O, Walden TB, Lassmann T, Petrovic N, Hamilton DL, Gimeno RE, Wahlestedt C, Baar K, Nedergaard J, and Cannon B**. Myogenic gene expression signature establishes that brown and white adipocytes originate from distinct cell lineages. *Proc Natl Acad Sci U S A* 104: 4401-4406, 2007.
246. **Tokumasa N, Suto A, Kagami S, Furuta S, Hirose K, Watanabe N, Saito Y, Shimoda K, Iwamoto I, and Nakajima H**. Expression of Tyk2 in dendritic cells is required for IL-12, IL-23, and IFN-gamma production and the induction of Th1 cell differentiation. *Blood* 110: 553-560, 2007.
247. **Tontonoz P, Hu E, and Spiegelman BM**. Stimulation of adipogenesis in fibroblasts by PPAR gamma 2, a lipid-activated transcription factor. *Cell* 79: 1147-1156, 1994.
248. **Tortolani PJ, Lal BK, Riva A, Johnston JA, Chen YQ, Reaman GH, Beckwith M, Longo D, Ortaldo JR, Bhatia K, McGrath I, Kehrl J, Tuscano J, McVicar DW, and O'Shea JJ**. Regulation of JAK3 expression and activation in human B cells and B cell malignancies. *J Immunol* 155: 5220-5226, 1995.
249. **Toye AA, Lippiat JD, Proks P, Shimomura K, Bentley L, Hugill A, Mijat V, Goldsworthy M, Moir L, Haynes A, Quarterman J, Freeman HC, Ashcroft FM, and Cox RD**. A genetic and physiological study of impaired glucose homeostasis control in C57BL/6J mice. *Diabetologia* 48: 675-686, 2005.
250. **Tran TT, and Kahn CR**. Transplantation of adipose tissue and stem cells: role in metabolism and disease. *Nat Rev Endocrinol* 6: 195-213.
251. **Truett GE, Heeger P, Mynatt RL, Truett AA, Walker JA, and Warman ML**. Preparation of PCR-quality mouse genomic DNA with hot sodium hydroxide and tris (HotSHOT). *Biotechniques* 29: 52, 54, 2000.
252. **Tseng YH, Kokkotou E, Schulz TJ, Huang TL, Winnay JN, Taniguchi CM, Tran TT, Suzuki R, Espinoza DO, Yamamoto Y, Ahrens MJ, Dudley AT, Norris AW, Kulkarni RN, and Kahn CR**. New role of bone morphogenetic protein 7 in brown adipogenesis and energy expenditure. *Nature* 454: 1000-1004, 2008.
253. **Udy GB, Towers RP, Snell RG, Wilkins RJ, Park SH, Ram PA, Waxman DJ, and Davey HW**. Requirement of STAT5b for sexual dimorphism of body growth rates and liver gene expression. *Proc Natl Acad Sci U S A* 94: 7239-7244, 1997.
254. **Uldry M, Yang W, St-Pierre J, Lin J, Seale P, and Spiegelman BM**. Complementary action of the PGC-1 coactivators in mitochondrial biogenesis and brown fat differentiation. *Cell Metab* 3: 333-341, 2006.
255. **Vaisse C, Halaas JL, Horvath CM, Darnell JE, Jr., Stoffel M, and Friedman JM**. Leptin activation of Stat3 in the hypothalamus of wild-type and ob/ob mice but not db/db mice. *Nat Genet* 14: 95-97, 1996.

256. **van den Oever IA, Raterman HG, Nurmohamed MT, and Simsek S**. Endothelial dysfunction, inflammation, and apoptosis in diabetes mellitus. *Mediators Inflamm* 2010: 792393.
257. **Van Gaal LF, Mertens IL, and De Block CE**. Mechanisms linking obesity with cardiovascular disease. *Nature* 444: 875-880, 2006.
258. **van Marken Lichtenbelt WD, Vanhommerig JW, Smulders NM, Drossaerts JM, Kemerink GJ, Bouvy ND, Schrauwen P, and Teule GJ**. Cold-activated brown adipose tissue in healthy men. *N Engl J Med* 360: 1500-1508, 2009.
259. **Velazquez L, Fellous M, Stark GR, and Pellegrini S**. A protein tyrosine kinase in the interferon alpha/beta signaling pathway. *Cell* 70: 313-322, 1992.
260. **Velazquez L, Mogensen KE, Barbieri G, Fellous M, Uze G, and Pellegrini S**. Distinct domains of the protein tyrosine kinase tyk2 required for binding of interferon-alpha/beta and for signal transduction. *J Biol Chem* 270: 3327-3334, 1995.
261. **Verbsky JW, Bach EA, Fang YF, Yang L, Randolph DA, and Fields LE**. Expression of Janus kinase 3 in human endothelial and other non-lymphoid and non-myeloid cells. *J Biol Chem* 271: 13976-13980, 1996.
262. **Vgontzas AN, Papanicolaou DA, Bixler EO, Kales A, Tyson K, and Chrousos GP**. Elevation of plasma cytokines in disorders of excessive daytime sleepiness: role of sleep disturbance and obesity. *J Clin Endocrinol Metab* 82: 1313-1316, 1997.
263. **Villarroya F, Iglesias R, and Giralt M**. PPARs in the Control of Uncoupling Proteins Gene Expression. *PPAR Res* 2007: 74364, 2007.
264. **Vinkemeier U**. Getting the message across, STAT! Design principles of a molecular signaling circuit. *J Cell Biol* 167: 197-201, 2004.
265. **Virtanen KA, Lidell ME, Orava J, Heglind M, Westergren R, Niemi T, Taittonen M, Laine J, Savisto NJ, Enerback S, and Nuutila P**. Functional brown adipose tissue in healthy adults. *N Engl J Med* 360: 1518-1525, 2009.
266. **Vondra K, Rath R, Bass A, Slabochova Z, Teisinger J, and Vitek V**. Enzyme activities in quadriceps femoris muscle of obese diabetic male patients. *Diabetologia* 13: 527-529, 1977.
267. **Wajchenberg BL**. beta-cell failure in diabetes and preservation by clinical treatment. *Endocr Rev* 28: 187-218, 2007.
268. **Wajchenberg BL**. Subcutaneous and visceral adipose tissue: their relation to the metabolic syndrome. *Endocr Rev* 21: 697-738, 2000.
269. **Walden TB, Timmons JA, Keller P, Nedergaard J, and Cannon B**. Distinct expression of muscle-specific microRNAs (myomirs) in brown adipocytes. *J Cell Physiol* 218: 444-449, 2009.
270. **Wang D, Stravopodis D, Teglund S, Kitazawa J, and Ihle JN**. Naturally occurring dominant negative variants of Stat5. *Mol Cell Biol* 16: 6141-6148, 1996.
271. **Wang ND, Finegold MJ, Bradley A, Ou CN, Abdelsayed SV, Wilde MD, Taylor LR, Wilson DR, and Darlington GJ**. Impaired energy homeostasis in C/EBP alpha knockout mice. *Science* 269: 1108-1112, 1995.
272. **Wassink AM, Olijhoek JK, and Visseren FL**. The metabolic syndrome: metabolic changes with vascular consequences. *Eur J Clin Invest* 37: 8-17, 2007.
273. **Watford WT, and O'Shea JJ**. Human tyk2 kinase deficiency: another primary immunodeficiency syndrome. *Immunity* 25: 695-697, 2006.

274. **Watling D, Guschin D, Muller M, Silvennoinen O, Witthuhn BA, Quelle FW, Rogers NC, Schindler C, Stark GR, Ihle JN, and et al.** Complementation by the protein tyrosine kinase JAK2 of a mutant cell line defective in the interferon-gamma signal transduction pathway. *Nature* 366: 166-170, 1993.
275. **Wen Z, Zhong Z, and Darnell JE, Jr.** Maximal activation of transcription by Stat1 and Stat3 requires both tyrosine and serine phosphorylation. *Cell* 82: 241-250, 1995.
276. **Westerberg R, Mansson JE, Golozoubova V, Shabalina IG, Backlund EC, Tvrdik P, Retterstol K, Capecchi MR, and Jacobsson A**. ELOVL3 is an important component for early onset of lipid recruitment in brown adipose tissue. *J Biol Chem* 281: 4958-4968, 2006.
277. **Wick KR, and Berton MT**. IL-4 induces serine phosphorylation of the STAT6 transactivation domain in B lymphocytes. *Mol Immunol* 37: 641-652, 2000.
278. **Wolf G**. Brown adipose tissue: the molecular mechanism of its formation. *Nutr Rev* 67: 167-171, 2009.
279. **Wu Z, Puigserver P, Andersson U, Zhang C, Adelmant G, Mootha V, Troy A, Cinti S, Lowell B, Scarpulla RC, and Spiegelman BM**. Mechanisms controlling mitochondrial biogenesis and respiration through the thermogenic coactivator PGC-1. *Cell* 98: 115-124, 1999.
280. **Wu Z, Puigserver P, and Spiegelman BM**. Transcriptional activation of adipogenesis. *Curr Opin Cell Biol* 11: 689-694, 1999.
281. **Xue B, Rim JS, Hogan JC, Coulter AA, Koza RA, and Kozak LP**. Genetic variability affects the development of brown adipocytes in white fat but not in interscapular brown fat. *J Lipid Res* 48: 41-51, 2007.
282. **Yamaoka K, Saharinen P, Pesu M, Holt VE, 3rd, Silvennoinen O, and O'Shea JJ**. The Janus kinases (Jaks). *Genome Biol* 5: 253, 2004.
283. **Yamauchi T, Kamon J, Minokoshi Y, Ito Y, Waki H, Uchida S, Yamashita S, Noda M, Kita S, Ueki K, Eto K, Akanuma Y, Froguel P, Foufelle F, Ferre P, Carling D, Kimura S, Nagai R, Kahn BB, and Kadowaki T**. Adiponectin stimulates glucose utilization and fatty-acid oxidation by activating AMP-activated protein kinase. *Nat Med* 8: 1288-1295, 2002.
284. **Yan SJ, Lim SJ, Shi S, Dutta P, and Li WX**. Unphosphorylated STAT and heterochromatin protect genome stability. *Faseb J*.
285. **Yang E, Wen Z, Haspel RL, Zhang JJ, and Darnell JE, Jr.** The linker domain of Stat1 is required for gamma interferon-driven transcription. *Mol Cell Biol* 19: 5106-5112, 1999.
286. **Yang J, Croniger CM, Lekstrom-Himes J, Zhang P, Fenyus M, Tenen DG, Darlington GJ, and Hanson RW**. Metabolic response of mice to a postnatal ablation of CCAAT/enhancer-binding protein alpha. *J Biol Chem* 280: 38689-38699, 2005.
287. **Yang J, Huang J, Dasgupta M, Sears N, Miyagi M, Wang B, Chance MR, Chen X, Du Y, Wang Y, An L, Wang Q, Lu T, Zhang X, Wang Z, and Stark GR**. Reversible methylation of promoter-bound STAT3 by histone-modifying enzymes. *Proc Natl Acad Sci U S A*.
288. **Yang J, Liao X, Agarwal MK, Barnes L, Auron PE, and Stark GR**. Unphosphorylated STAT3 accumulates in response to IL-6 and activates transcription by binding to NFkappaB. *Genes Dev* 21: 1396-1408, 2007.

289. **Yang J, and Stark GR**. Roles of unphosphorylated STATs in signaling. *Cell Res* 18: 443-451, 2008.
290. **Yeh TC, Dondi E, Uze G, and Pellegrini S**. A dual role for the kinase-like domain of the tyrosine kinase Tyk2 in interferon-alpha signaling. *Proc Natl Acad Sci U S A* 97: 8991-8996, 2000.
291. **Yu H, and Jove R**. The STATs of cancer--new molecular targets come of age. *Nat Rev Cancer* 4: 97-105, 2004.
292. **Yu HY, Wang BL, Zhao J, Yao XM, Gu Y, and Li Y**. Protective effect of bicyclol on tetracycline-induced fatty liver in mice. *Toxicology* 261: 112-118, 2009.
293. **Yuan ZL, Guan YJ, Chatterjee D, and Chin YE**. Stat3 dimerization regulated by reversible acetylation of a single lysine residue. *Science* 307: 269-273, 2005.
294. **Zeqiraj E, and van Aalten DM**. Pseudokinases-remnants of evolution or key allosteric regulators? *Curr Opin Struct Biol* 20: 772-781.
295. **Zhang D, Liu ZX, Choi CS, Tian L, Kibbey R, Dong J, Cline GW, Wood PA, and Shulman GI**. Mitochondrial dysfunction due to long-chain Acyl-CoA dehydrogenase deficiency causes hepatic steatosis and hepatic insulin resistance. *Proc Natl Acad Sci U S A* 104: 17075-17080, 2007.
296. **Zhang JJ, Vinkemeier U, Gu W, Chakravarti D, Horvath CM, and Darnell JE, Jr.** Two contact regions between Stat1 and CBP/p300 in interferon gamma signaling. *Proc Natl Acad Sci U S A* 93: 15092-15096, 1996.
297. **Zhang JJ, Zhao Y, Chait BT, Lathem WW, Ritzi M, Knippers R, and Darnell JE, Jr.** Ser727-dependent recruitment of MCM5 by Stat1alpha in IFN-gamma-induced transcriptional activation. *Embo J* 17: 6963-6971, 1998.
298. **Zhang T, Kee WH, Seow KT, Fung W, and Cao X**. The coiled-coil domain of Stat3 is essential for its SH2 domain-mediated receptor binding and subsequent activation induced by epidermal growth factor and interleukin-6. *Mol Cell Biol* 20: 7132-7139, 2000.
299. **Zhang X, Wrzeszczynska MH, Horvath CM, and Darnell JE, Jr.** Interacting regions in Stat3 and c-Jun that participate in cooperative transcriptional activation. *Mol Cell Biol* 19: 7138-7146, 1999.
300. **Zhao Y, Wagner F, Frank SJ, and Kraft AS**. The amino-terminal portion of the JAK2 protein kinase is necessary for binding and phosphorylation of the granulocyte-macrophage colony-stimulating factor receptor beta c chain. *J Biol Chem* 270: 13814-13818, 1995.
301. **Zhou YJ, Chen M, Cusack NA, Kimmel LH, Magnuson KS, Boyd JG, Lin W, Roberts JL, Lengi A, Buckley RH, Geahlen RL, Candotti F, Gadina M, Changelian PS, and O'Shea JJ**. Unexpected effects of FERM domain mutations on catalytic activity of Jak3: structural implication for Janus kinases. *Mol Cell* 8: 959-969, 2001.
302. **Zhou Z, Yon Toh S, Chen Z, Guo K, Ng CP, Ponniah S, Lin SC, Hong W, and Li P**. Cidea-deficient mice have lean phenotype and are resistant to obesity. *Nat Genet* 35: 49-56, 2003.
303. **Zhu M, John S, Berg M, and Leonard WJ**. Functional association of Nmi with Stat5 and Stat1 in IL-2- and IFNgamma-mediated signaling. *Cell* 96: 121-130, 1999.
304. **Zhu Y, Qi C, Korenberg JR, Chen XN, Noya D, Rao MS, and Reddy JK**. Structural organization of mouse peroxisome proliferator-activated receptor gamma

(mPPAR gamma) gene: alternative promoter use and different splicing yield two mPPAR gamma isoforms. *Proc Natl Acad Sci U S A* 92: 7921-7925, 1995.